COMPARISONS AND CORRECTIONS OF CLIMATE MODELS FOR WAVES AND WATER LEVELS ALONG THE FRENCH COASTS FOR AN APPLICATION TO OFFSHORE WIND

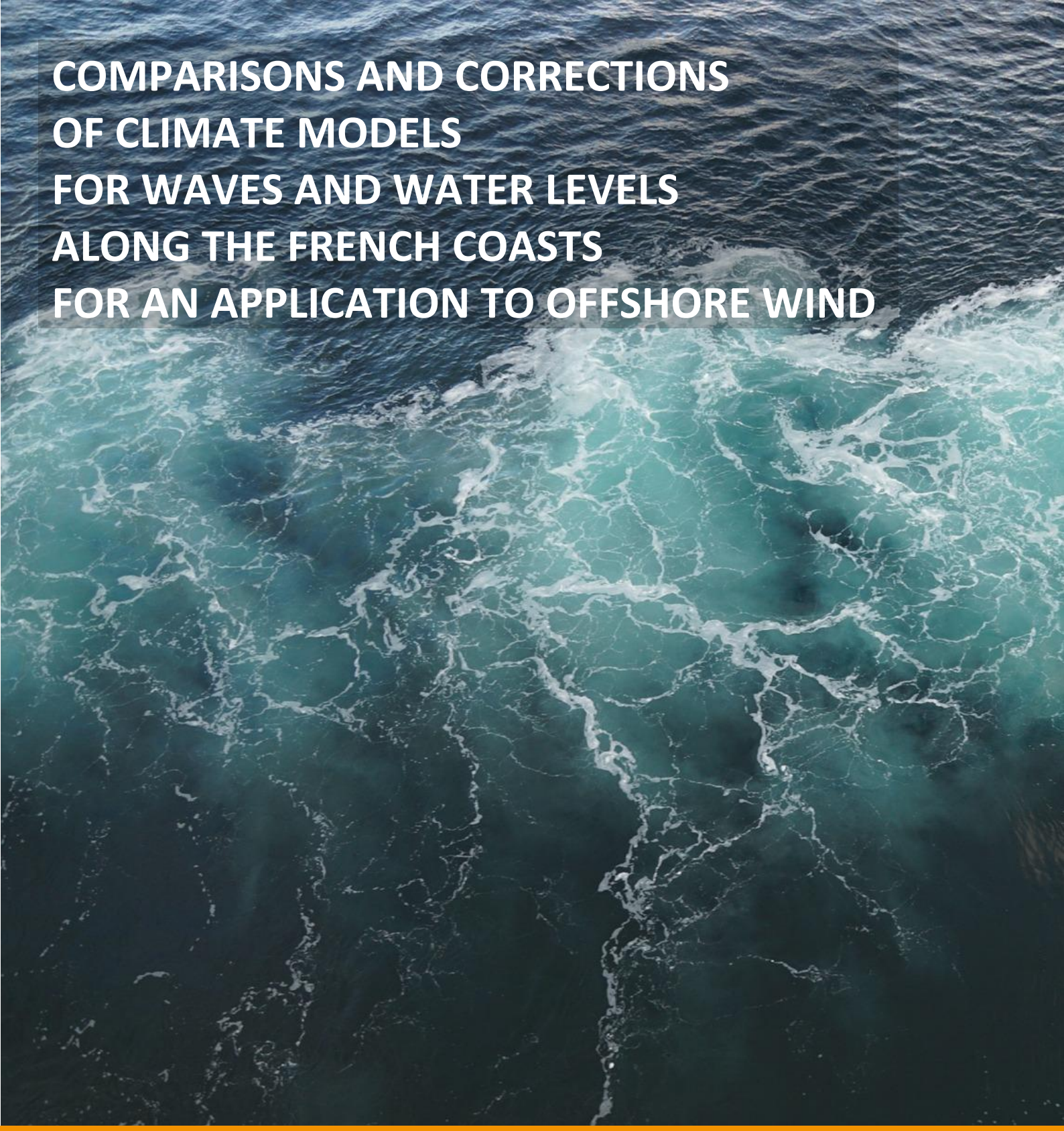

FRANCE ENERGIES MARINES

Le réseau de transport d'électricité

Ifremer

COMPARISONS AND CORRECTIONS OF CLIMATE MODELS FOR WAVES AND WATER LEVELS ALONG THE FRENCH COASTS FOR AN APPLICATION TO OFFSHORE WIND

AUTHORS:
Coline Poppeschi, Youen Kervella, and Tessa Chevallier, France Energies Marines
Nicolas Raillard, Ifremer
Laurent Dubus, RTE

Please cite this document as follows:
Poppeschi C.., Kervella Y., Chevallier T., Raillard N. & Dubus L. Comparisons and corrections of climate models for waves and water levels along the French coasts for an application to offshore wind farms. 2024, 65 pages.
Published: September 2024
Graphic design: halynea.com
Cover page photo credit: Strecoca/Pixabay

Table of contents

List of figures

List of tables

I. EXECUTIVE SUMMARY

This report presents the comparison and bias correction of wave and water level data, with applications to the Offshore Wind Industry (OWI), particularly in the context of wind farm design. The analysis focuses on both average and extreme wave and water level conditions, distinguishing between historical periods (used for method validation) and future climate projections (used to assess long-term changes). The geographical focus is on the French coastline, with particular attention to offshore wind farm locations.

Wave observations and reanalyses are compared using annual and seasonal cycles, as well as their statistical distributions, evaluated through standard performance metrics. The objective is to identify the most suitable reanalysis dataset along the French coast for downscaling General Circulation Models (GCMs). Wave comparisons are conducted between two reanalysis datasets—ResourceCode (RSCD) from IFREMER and HYWAT from SHOM—along the English Channel and Atlantic coasts. Both datasets show good agreement with buoy observations, with small biases and high correlations. HYWAT is selected as the most suitable reanalysis for these regions.

For the Mediterranean Sea, the MEDUG and MED-WAV reanalyses (provided by Copernicus) are evaluated against wave observations. MED-WAV demonstrates better performance and is therefore selected for the remainder of the study. Regarding water levels, comparisons are made between tide gauge observations and two reanalyses: GTSM-ERA5 and IBI-MFC. The good agreement observed supports the selection of GTSM-ERA5 for bias correction of climate model outputs along all three French coastlines.

Once the most appropriate reanalyses are selected, the CDF-t bias correction method is applied to reduce discrepancies between reanalyses and climate model projections. To validate the methodology, the correction is first applied to historical model simulations. The results show a significant improvement in the alignment of statistical distributions, confirming the robustness of the method and its suitability for application to future climate projections.

II. GLOSSARY

CD Chart Datum
CDF-t Cumulative Distribution Function transform
CMEMS Copernicus Marine Environment Monitoring Service
C3S Copernicus Climate Change Service
DP Peak direction
GCM General Circulation Model
GTSM Global Tidal and Surge Model
HS Significant Height Wave
HYWAT Hydrodynamics and Waves hindcast
MSL Mean Sea Level
RCM Regional Climatic Model
RMSE Root Mean Square Error
RSCD Resource Code
SI Scatter Index
SSP Shared Socio-economic Pathways
STD Standard Deviation
TAC Thematic Assembly Center
TP Wave period
WWIII WaveWatch3

III. INTRODUCTION

In the context of climate change, global temperatures are rising and CO_2 emissions must be reduced. However, global energy demand continues to grow. Offshore wind power offers a sustainable solution to reduce our carbon footprint. Given their multi-decade lifespan, offshore wind farms are, or will be, exposed to the impacts of climate change. The 2CNOW project investigates the effects of climate change on waves and water levels, which may influence the design and operation of offshore wind farms.

Changes in water levels can affect hydrodynamic conditions, foundation stability, and corrosion processes. Waves contribute to hydrodynamic loads on structures and influence weather windows for maintenance operations. Additionally, both waves and water level variations can drive morphological changes in landfall zones. This report presents comparisons and bias corrections between wave and water level observations and model projections, with a focus on future climate scenarios.

To explore future trends and their potential impacts on offshore wind farms, three types of datasets are compared: observations, reanalyses, and climate models. Observations consist of local time series measured at fixed points, often with discontinuities. Reanalyses are model-based datasets that assimilate observational data (satellite and in situ) to produce spatially and temporally consistent records over several decades (>30 years; Bartók et al., 2019). They offer broad spatial coverage and continuous temporal resolution, making them valuable for historical analysis and future projections. General Circulation Models (GCMs), on the other hand, simulate large-scale physical processes in the atmosphere and ocean. While they are powerful tools for climate projection, their coarse resolution limits their accuracy in coastal environments. Small-scale processes are often parameterized rather than explicitly resolved, introducing uncertainties. Moreover, GCM outputs can vary significantly depending on how these processes are represented.

Based on these datasets, the following methodology is applied:

1. **Processing of observational data**, ensuring the removal of spurious values and sufficient data coverage for reliable statistics.
2. **Comparison between reanalyses and observations**, using performance metrics to quantify consistency and select the most suitable reanalysis.
3. **Selection of the best reanalysis** to correct future climate model outputs, based on interannual variability and seasonal cycle comparisons (Eyring et al., 2021).
4. **Bias adjustment of climate models** during the historical period.
5. **Correction of climate model outputs** for future periods.
6. **Application of the methodology** to offshore wind farm locations.

This report presents Steps 1 to 4 of the methodology. It details the selection of the most appropriate reanalysis for waves and water levels based on comparisons with observations, and the subsequent use of this reanalysis to downscale climate model outputs. Each French coastline—the English Channel, the Atlantic coast, and the Mediterranean Sea—is analyzed separately, as literature (Poppeschi et al., 2024) shows that observed trends vary by region due to differing physical processes. For instance, the Atlantic coast is more sensitive to storm tracks than the other regions. The selection of the best reanalysis may therefore be made by maritime front, to account for local-scale processes.

This report serves as a foundation for validating the methodology used to compare and correct climate model outputs at regional scales. Once validated, the methodology will be applied to future climate projections under various Shared Socioeconomic Pathway (SSP) scenarios, which incorporate different greenhouse gas emission trajectories and societal developments. Finally, statistical analyses will be conducted to quantify the potential impacts of climate change on offshore wind farm design.

The first part of the report focuses on waves, including comparisons between reanalyses and observations, followed by bias correction of climate models using the selected reanalysis. The second part applies the same methodology to water levels.

IV. WAVE DATA

1 Observations

In-situ data are provided by the CMEMS (Copernicus Marine Environment Monitoring Service) in situ TAC (Thematic Assembly Center) for the Significant Wave Height (Hs) expressed in meters. Other parameters for waves are going to be explored in the next report such as the period (Tp) and the peak direction (Dp). Hs is measured by moored buoys, anchored at fixed locations. Even if the data are validated and qualified by CMEMS, some outliers may remain, thus the raw data is first analyzed. Outliers defined as Hs exceeding 20 m or lower than 0 m are detected and removed. Also, outliers are deleted if the data is superior to three times the standard deviation of timeseries (Bentamy & Croize-Fillon, 2014). Finally, timeseries with at least 10 continuous and recent years are kept, for periods when the reanalysis data is also available.

According to the treatment described above, 12 buoys are retained for this study and represented in Figure 1. More precisely, we selected 3 stations in the English Channel, 5 stations on the Atlantic coast and 4 stations in the Mediterranean Sea. A color code with green for the English Channel, blue for the Atlantic coast, and red for the Mediterranean Sea is chosen for the entire study as a reference. The selected stations are distributed along France's 3 coastlines, as close as possible to future offshore wind farms (orange squares on the map, Figure 1).

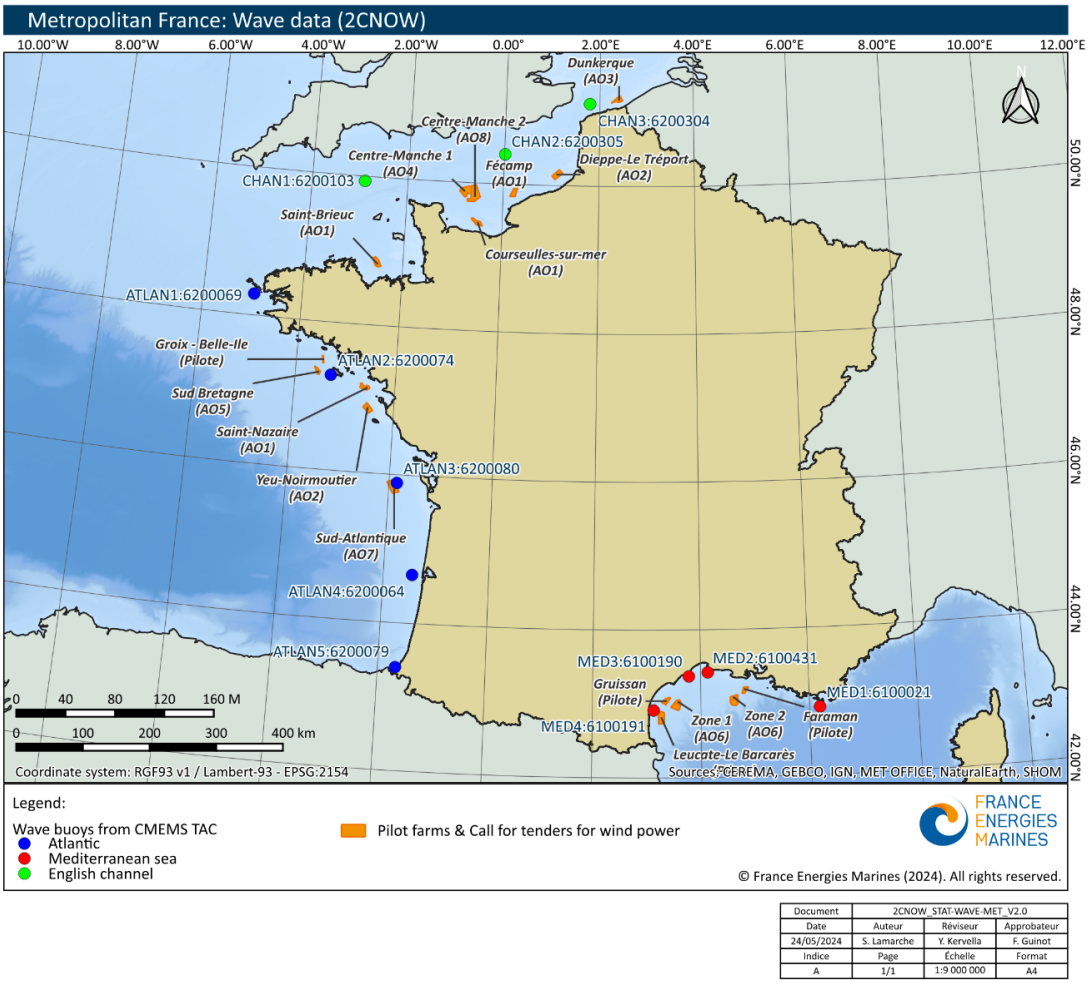

Figure 1. Map of the buoys measuring wave Hs selected for the study around France

2 Reanalysis data

Four reanalysis data sets are analysed in this study based on their high spatial resolution. For the English Channel and the Atlantic Ocean, two reanalyses are used: RESOURCECODE (RSCD, Accensi et al., 2022) and HYWAT (Hydrodynamics and Waves hindcast, Jourdan et al., 2020). Both reanalyses are available on an hourly basis. For the Mediterranean Sea, two other reanalyses are used: the MEDUG reanalysis (Faidherbe et al., 2024) and the MED-WAV (Korres et al., 2021). Other reanalysis can be found, as the one used by Laugel et al. (2014) for example, based on the ANEMOC database but the other reanalysis is either of lower spatial resolution or not free to access so they are not considered in this study.

2.1 Reanalyses used for the Atlantic Ocean and the English Channel

The **RSCD** reanalysis is operated by Ifremer (https://ressourcecode.ifremer.fr) and covers the period from 1994 to 2021 using hourly wind forcing from the ERA5 10m wind speed (ECMWF), and tidal currents and water levels that are recomposed from harmonic atlases from MARS and FES2014 (Lyard et al., 2021). Wet boundaries are forced by the global wave model of Alday et al. (2021) (https://archimer.ifremer.fr/doc/00709/82121/). The wave model is WW3 (WaveWatch III) with ST4 parametrization. This regional model covers Gibraltar to Faeroe Islands. The grid is unstructured and extends as far shoreward as a few kilometres from the coast.

The **HYWAT** reanalysis from 1979 to 2022 (44 years) is operated by the SHOM (https://doi.org/10.17183/REJEUX_HYWAT). The HYWAT reanalysis extends from latitudes between 43°N and 52°N and longitudes between 7°W and 5°E in a non-structured grid. The wave model used is Wavewatch III with TEST471 physical parameterization corresponding to the default ST4 parameterization in WW3 v6.07.1. (Ardhuin et al., 2010, Leckler et al., 2013, among others), and the outputs are provided with an hourly temporal resolution and a 30km spatial resolution. The HYWAT reanalysis is forced by the atmospheric reanalysis ERA5 (ECMWF), the currents are provided by HYCOM (Jourdan et al., 2020) and surface elevation by LEGOS 2011 NEA tidal atlas (Lyard et al., 2021).

2.2 Reanalyses used for the Mediterranean Sea

The **MEDUG** reanalysis is available from 2003 to 2022 (20 years) and provided by the SHOM (Faidherbe et al., 2024). The reanalysis covers the Mediterranean Sea, 40°45'N – 44°30'N and 3°E – 11°45'E. The grid used is unstructured like in the HYWAT reanalysis with the same bathymetry (Michaud et al., 2015). The resolution is high with 200 m close to the coast and 700 to 1000 m close to offshore wind farms. MEDUG is forced by ERA5 from ECMWF at 30 km spatial resolution and an hourly temporal resolution. The reanalysis uses the model WW3 v-6.07.1.

The **MED-WAV** reanalysis dataset (https://doi.org/10.25423/cmcc/medsea_multiyear_wav_006_012) is a multi-year wave reanalysis starting from January 1993, composed by hourly wave parameters at 1/24° horizontal resolution, covering the Mediterranean Sea and extending up to 18.125°W into the Atlantic Ocean. The MED-WAV modelling system is based on wave model WAM 4.6.2 and has been developed as a nested sequence of two computational grids (coarse and fine) to ensure that swell propagating from the North Atlantic (NA) towards the strait of Gibraltar is correctly entering the Mediterranean Sea. The coarse grid covers the North Atlantic Ocean from 75°W to 10°E and from 70° N to 10° S in 1/6° resolution while the nested fine grid covers the Mediterranean Sea from 18.125° W to 36.2917° E and from 30.1875° N to 45.9792° N with a 1/24° resolution. The modelling system resolves the prognostic part of the wave spectrum with 24 directional and 32 logarithmically distributed frequency bins. The wave system also includes an optimal interpolation assimilation scheme assimilating significant wave height along track satellite observations available through CMEMS and it is forced with daily averaged currents from Med-Physics and with 1-h, 0.25° horizontal-resolution ERA5 reanalysis 10m-above-sea-surface winds from ECMWF. The MED-WAV reanalysis is provided by Copernicus and was created by the HCMR (Greece).

3 Climate models

From the paper of Meucci et al. (2024), we evaluated eight climatic models forced by a 10m wind speed from CMIP6: ACCESS-CM2, AWI-CM-1-1-MR, CMCC-CM2-SR5, EC-EARTH3, IPSL-CM6A-LR, KIOST-ESM, MPI-ESM1-2-LR and MRI-ESM2-0. The historical period covers 1985 to 2014, and the future period is from 2071 to 2100 for all models, except for ACCESS-CM2 and EC-EARTH3 which cover the entire period from 1961 to 2100. The wave model used is WWIII with ST6 parametrization (Fernández et al., 2021). The resolution of these global models is 0.5°. Three scenarios are used: historical, SSP1-2.6 and SSP5-8.5. The model output time step is 3-hourly (Meucci et al., 2024).

V. COMPARISONS FOR WAVE DATA

To compare observations, reanalysis and models, we selected the closest point of reanalysis (example: RSCD) and models (example: GCM – General Circulation Models) to the observation (example: GL_TS_MO_6200074, called *ATLAN2* in the rest of this report) points as explained in Figure 2 (Maps for all stations are available in Appendix 1). Comparisons are made by analysing annual mean, annual maxima, seasonal cycles and cumulative distribution functions (Figure 3, Figure 4, Figure 5). The coherence between datasets using scatter plots is also provided in Appendix 2. To quantify these comparisons, statistical metrics, hereafter called scores, are presented in dedicated tables and described above. Since one of the objectives of the 2C NOW project is to evaluate the possible impacts of climate change on the design of offshore wind farms, both the mean and extreme conditions are considered.

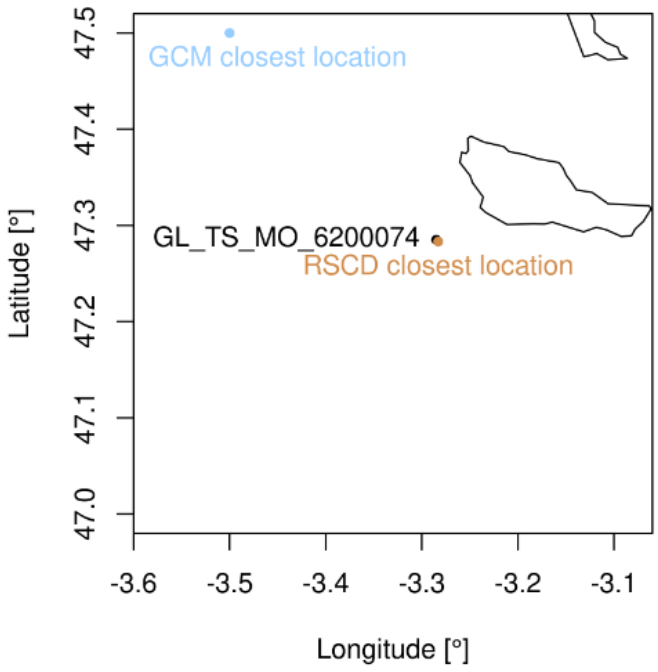

Figure 2. Representation of the selection of the closest points of models and reanalysis of observational data, at location ATLAN2

1 Definition of scores

Several statistical metrics were calculated for each station between the observations and the reanalyses: the correlation, the bias and the normalized root mean square error. These scores are calculated over the concurrent period of the observations and the 2 reanalyses so that the comparisons are fair. To complete these metrics computation, Taylor diagrams are also drawn to compare the reanalyses. A Taylor diagram is a mathematical representation to compare models and observations (Taylor, 2001).

In this study, scores are calculated for “mean” and “extreme” conditions: when we refer to "mean conditions" in the remainder of this report, we are referring to data under the 95th percentiles, this percentile being calculated from observations. When we refer to "extreme conditions", we are looking at data above the 95th percentile, calculated from observations, for waves (for water levels, extreme conditions concern both values above the 95th percentile and also values below the 5th percentile).

1.1 Correlation

Correlation is the measure of linear dependency between two datasets, ranging from 0 to 1, and a value of 1 indicates a perfect correlation between the 2 datasets (in our case, we compute a temporal correlation between the observations and the reanalyses).

1.2 Bias

The bias is the mean difference between the reanalysis and the observations. If both datasets are in coherence, the bias will be close to zero.

$$BIAS = \frac{\sum_{i=1}^{N} M_i - O_i}{N}$$

Here, *M* and *O* present reanalysis and reference measurements and *N* is the length of overlapped time.

1.3 Normalized root mean square error (NRMSE)

The NRMSE corresponds to the distance between the regression line and data points, divided by the range of the observations.

$$RMSE = \sqrt{\frac{\sum_{i=1}^{N}(M_i - O_i)^2}{N}} \qquad NRMSE = \frac{RMSE}{O_{max} - O_{min}}$$

2 Comparisons for stations located in the Channel

In the English Channel (Figure 3, Figure 4, Figure 5), both reanalyses show good agreement with the observations, despite a constant bias of around 0.5 m, and are close to each other. HYWAT always seems to be closer to the observations than RSCD, and this result is even more visible for extreme values, with a tendency of over-estimating the extremes for RSCD.

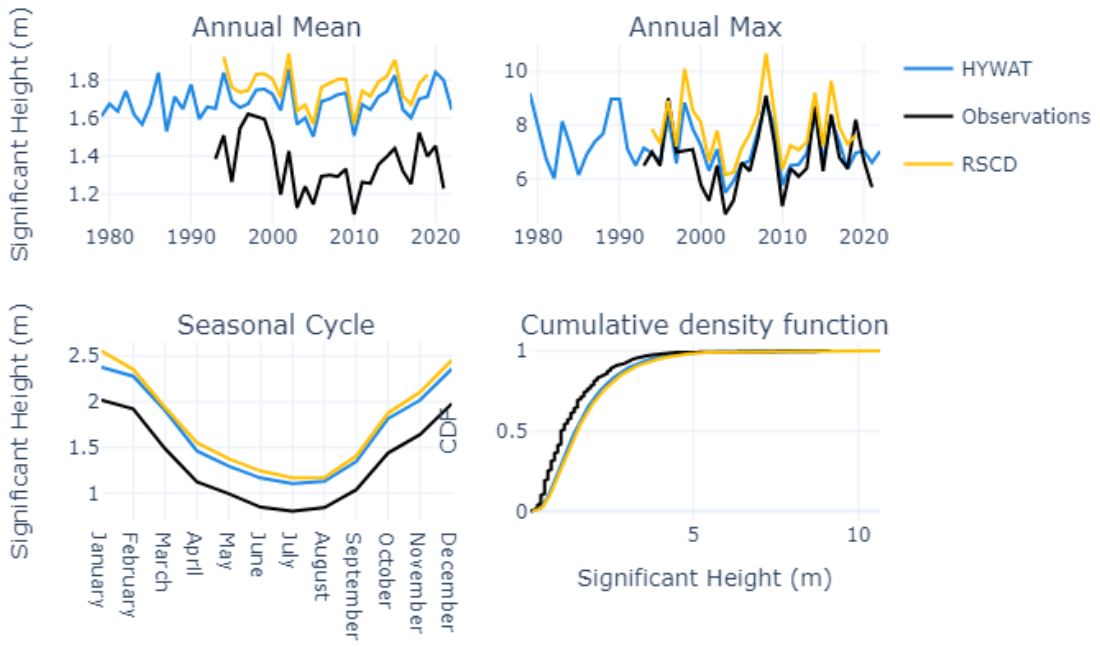

Figure 3. Comparisons between observations (black) and reanalyses: RSCD (yellow) and HYWAT (blue) at station CHAN1

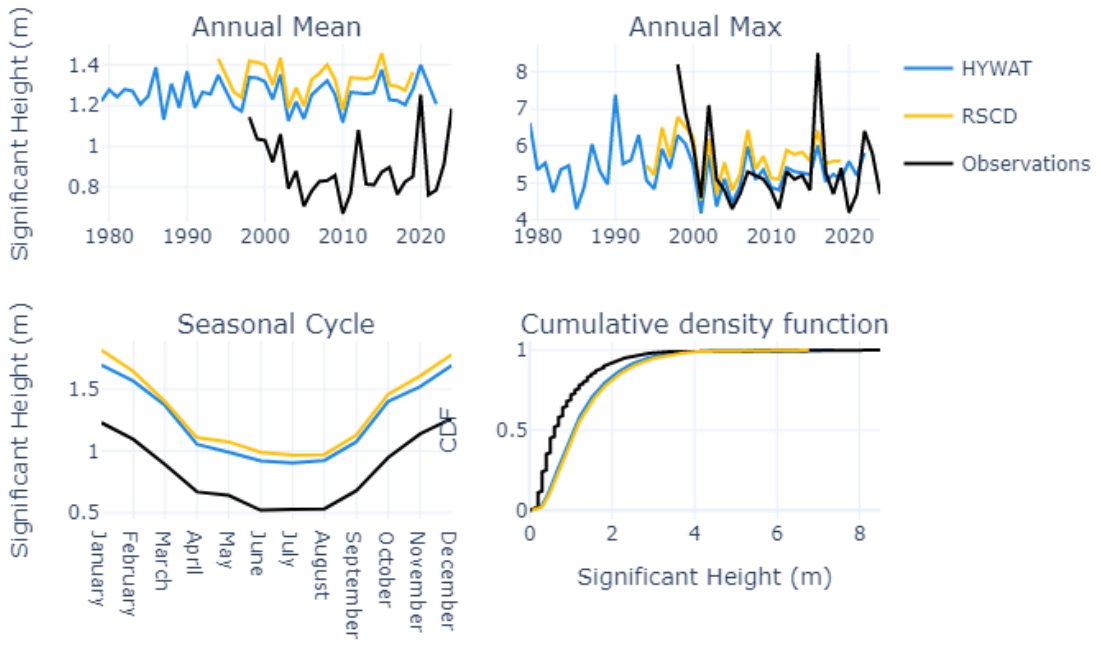

Figure 4. Comparisons between observations (black) and reanalyses: RSCD (yellow) and HYWAT (blue) at station CHAN2

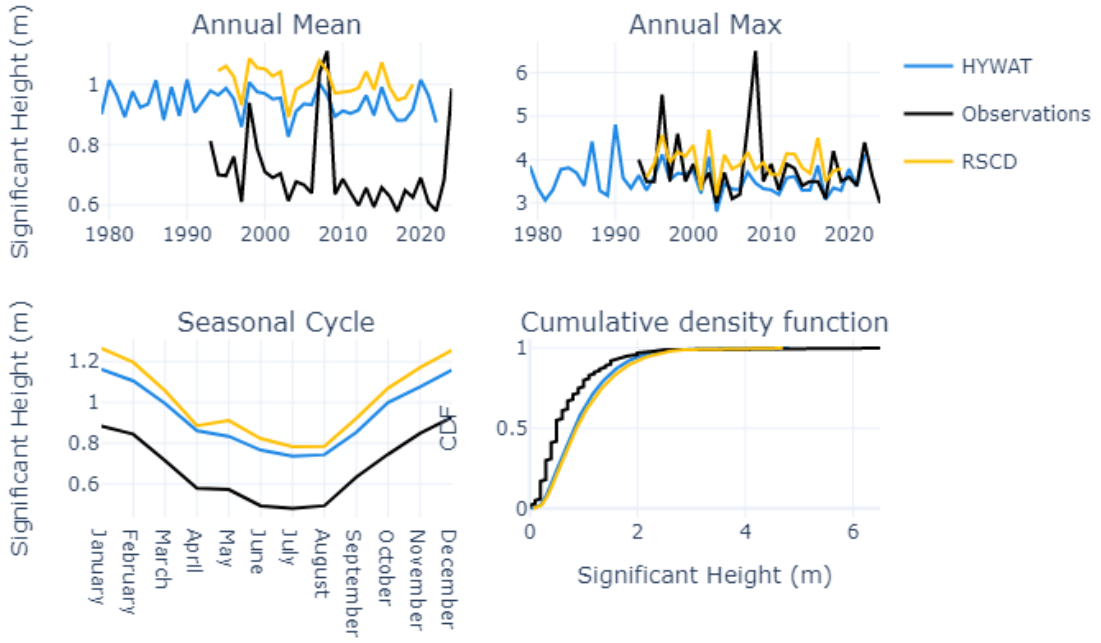

Figure 5. Comparisons between observations (black) and reanalyses: RSCD (yellow) and HYWAT (blue) at station CHAN3

In the following tables (Table 1, Table 2, Table 3), the scores are shown for both reanalyses at all the Channel stations and for mean and extreme conditions. The best reanalysis is each time highlighted by bold writing. For almost all scores and all stations, the HYWAT reanalysis shows better results, whether for mean conditions or for extreme conditions.

In detail:

- The correlation between HYWAT and observations is very good for normal conditions with values greater than 0.87, and weaker for extreme conditions with values between 0.4 and 0.77 (results nevertheless better than for the RSCD reanalysis).
- The bias between HYWAT and observations is around 0.3-0.4 m for normal and extreme conditions, and always a few centimetres below the RSCD bias. This is not a very good result given the range of values observed. This bias is even a little weaker at the CHAN3 station (East of the English Channel), especially for extreme conditions.
- The NRMSE between HYWAT and observations presents values from 15% to 23% for mean conditions and around 11% for extreme conditions. These poor results are notably due to the strong existing bias, as mentioned before. The results are even worse in terms of NRMSE for RSCD.

HYWAT is therefore considered as the best available reanalysis for the English Channel stations.

Table 1. Correlation for mean and extreme conditions at Channel stations

Correlation	Mean Conditions		Extreme Conditions	
[no units]	RSCD	HYWAT	RSCD	HYWAT
CHAN1	0.9	**0.93**	0.71	**0.77**
CHAN2	0.9	**0.91**	0.56	**0.59**
CHAN3	0.83	**0.87**	0.36	**0.4**

Table 2. Bias for mean and extreme conditions at Channel stations

Bias	Mean Conditions		Extreme Conditions	
[m]	RSCD	HYWAT	RSCD	HYWAT
CHAN1	0.41	**0.34**	0.61	**0.4**
CHAN2	0.48	**0.42**	0.51	**0.3**
CHAN3	0.34	**0.26**	**0.03**	-0.13

Table 3. NRMSE for mean and extreme conditions at Channel stations.

NRMSE	Mean Conditions		Extreme Conditions	
[%]	RSCD	HYWAT	RSCD	HYWAT
CHAN1	18.42	**15.09**	15.78	**11.55**
CHAN2	27.58	**23.61**	13.33	**10.72**
CHAN3	26.15	**20.55**	12.24	**11.13**

3 Comparisons for stations located in the Atlantic Ocean

Along the Atlantic coast (Figure 6, Figure 7, Figure 8, Figure 9 and Figure 10), both reanalyses show good agreement with the observations, with a lower bias than in the English Channel, and are close to each other. Seasonal cycles are well represented, with in most cases a slight underestimation of waves during winter, which is also found on the annual maxima graphs, and a slight overestimation during summer.

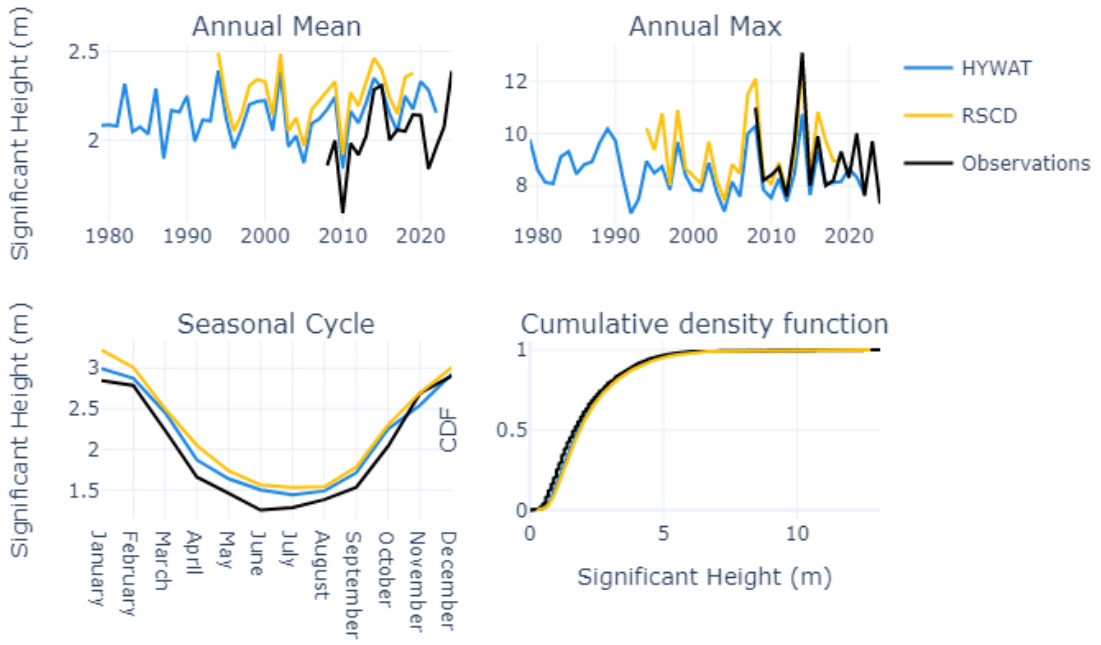

Figure 6. Comparisons between observations (black) and reanalyses: RSCD (yellow) and HYWAT (blue) at station ATLAN1

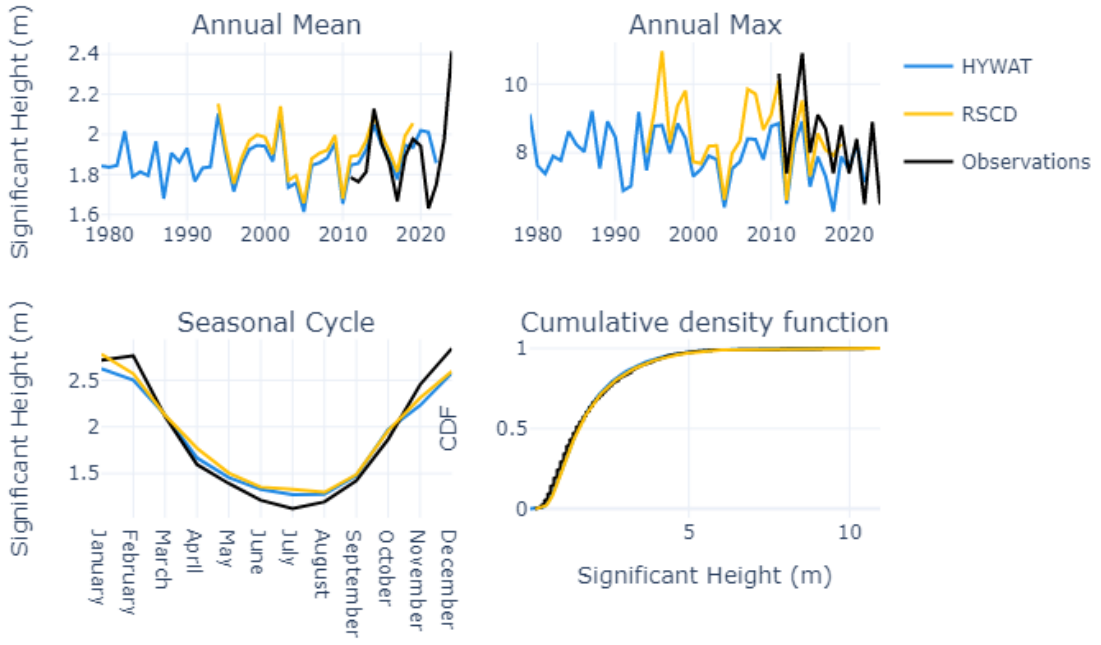

Figure 7. Comparisons between observations (black) and reanalyses: RSCD (yellow) and HYWAT (blue) at station ATLAN2

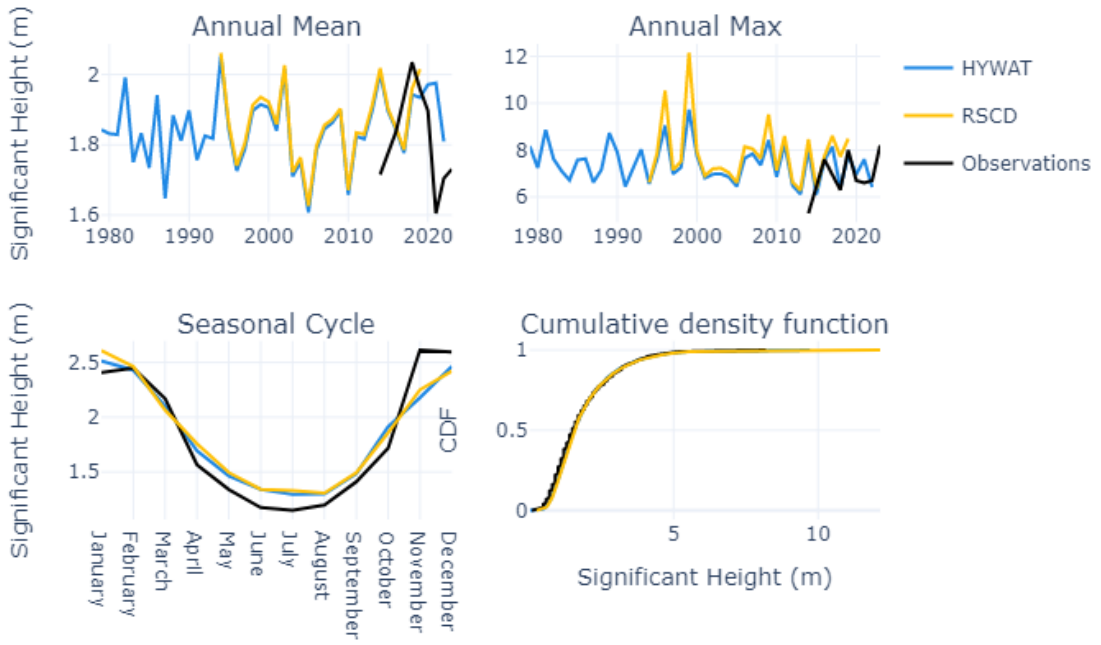

Figure 8. Comparisons between observations (black) and reanalyses: RSCD (yellow) and HYWAT (blue) at station ATLAN3

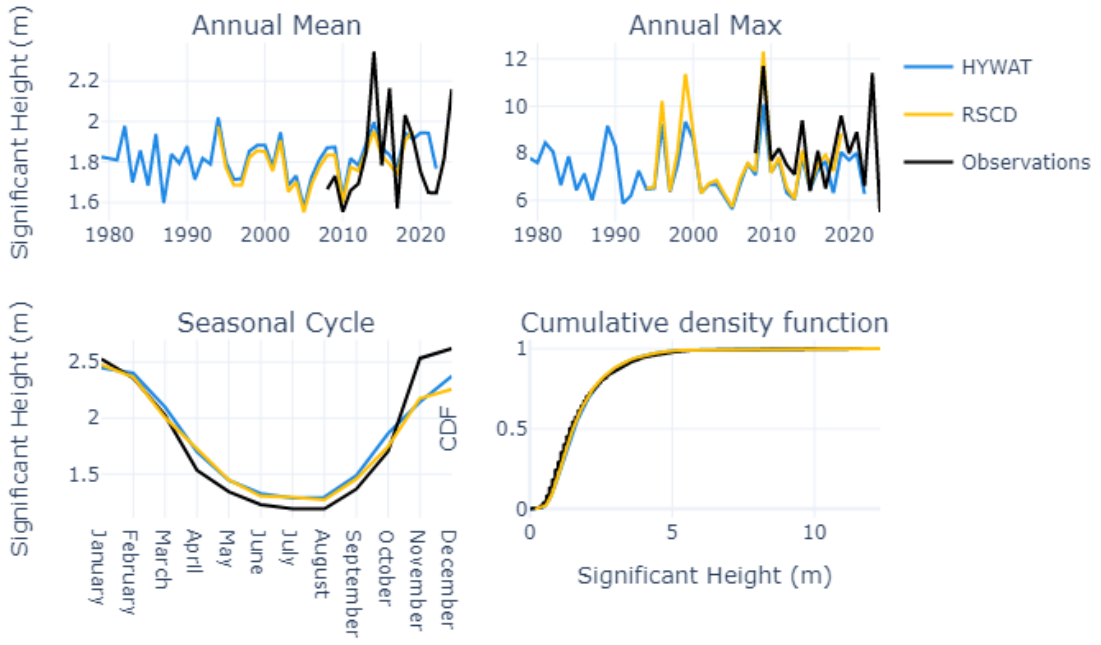

Figure 9. Comparisons between observations (black) and reanalyses: RSCD (yellow) and HYWAT (blue) at station ATLAN4

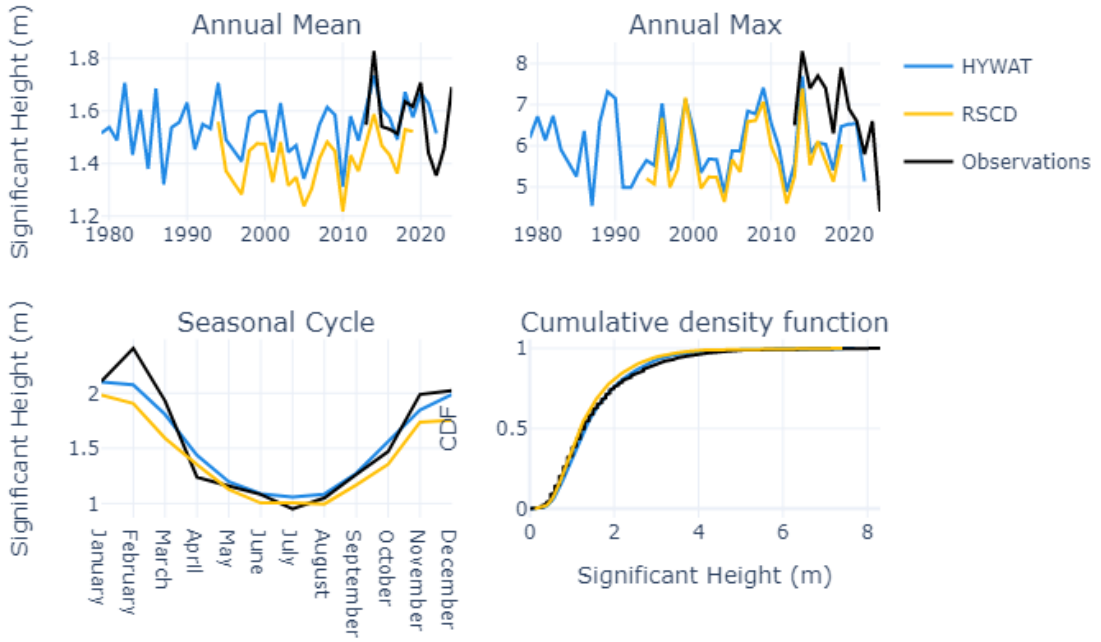

Figure 10. Comparisons between observations (black) and reanalyses: RSCD (yellow) and HYWAT (blue) at station ATLAN5

In the following tables (Table 4, Table 5, Table 6), the scores are shown for both reanalyses at all the Atlantic stations and for mean and extreme conditions. The best reanalysis is each time highlighted by bold writing. Both reanalyses present a good comparison for mean conditions with high correlations (> 0.90), small biases (< 10 cm) except at station ATLAN1 located near Brest, and a NRMSE lower than 9%.

For extreme conditions, the correlations are also very good with values generally above 0.7-0.8. The biases remain low overall, with higher values for the ATLAN4 and ATLAN5 stations located on the Basque coast. The NRMSE are between 8 and 12% except at the ATLAN5 station which has a value of more than 20% for the RSCD reanalysis.

Overall, on the Atlantic coast, the 2 reanalyses present good correlations with a slight advantage for the RSCD reanalysis, while the bias and the NRMSE present better results for the HYWAT reanalysis.

In view of these results and to maintain consistency between the 2 connected maritime facades (the English Channel and the Atlantic Ocean), the HYWAT reanalysis is retained.

Table 4. Correlation for mean and extreme conditions at Atlantic stations

Correlation	Mean Conditions		Extreme Conditions	
[no units]	RSCD	HYWAT	RSCD	HYWAT
ATLAN1	**0.96**	**0.96**	**0.86**	0.85
ATLAN2	**0.97**	**0.97**	**0.86**	**0.86**
ATLAN3	**0.97**	0.96	**0.88**	0.85
ATLAN4	**0.96**	**0.96**	0.83	**0.84**
ATLAN5	**0.94**	0.93	**0.77**	0.7

Table 5. Bias for mean and extreme conditions at Atlantic stations

Bias	Mean Conditions		Extreme Conditions	
[m]	RSCD	HYWAT	RSCD	HYWAT
ATLAN1	0.26	**0.15**	0.32	**0.02**
ATLAN2	0.08	**0.03**	**0.01**	-0.21
ATLAN3	0.05	**0.03**	**0.03**	-0.07
ATLAN4	**0.05**	0.08	-0.39	**-0.38**
ATLAN5	-0.09	**0.03**	-0.77	**-0.58**

Table 6. NRMSE for mean and extreme conditions at Atlantic stations

NRMSE	Mean Conditions		Extreme Conditions	
[%]	RSCD	HYWAT	RSCD	HYWAT
ATLAN1	8.65	**7.13**	7.59	**6.19**
ATLAN2	6.11	**5.87**	**8.14**	8.4
ATLAN3	**5.78**	6.0	**10.8**	11.84
ATLAN4	6.25	**6.21**	8.8	**8.54**
ATLAN5	8.03	**7.99**	20.53	**18.96**

4 Comparisons for stations located in the Mediterranean Sea

In the Mediterranean Sea (Figure 11, Figure 12, Figure 13, Figure 14), The MED-WAV reanalysis graphically presents less bias than the MED-UG reanalysis for the annual mean and seasonal cycles, at all stations except MED4, which is located west of the Gulf of Lion, near Leucate. The annual maxima seem well represented by the 2 reanalyses.

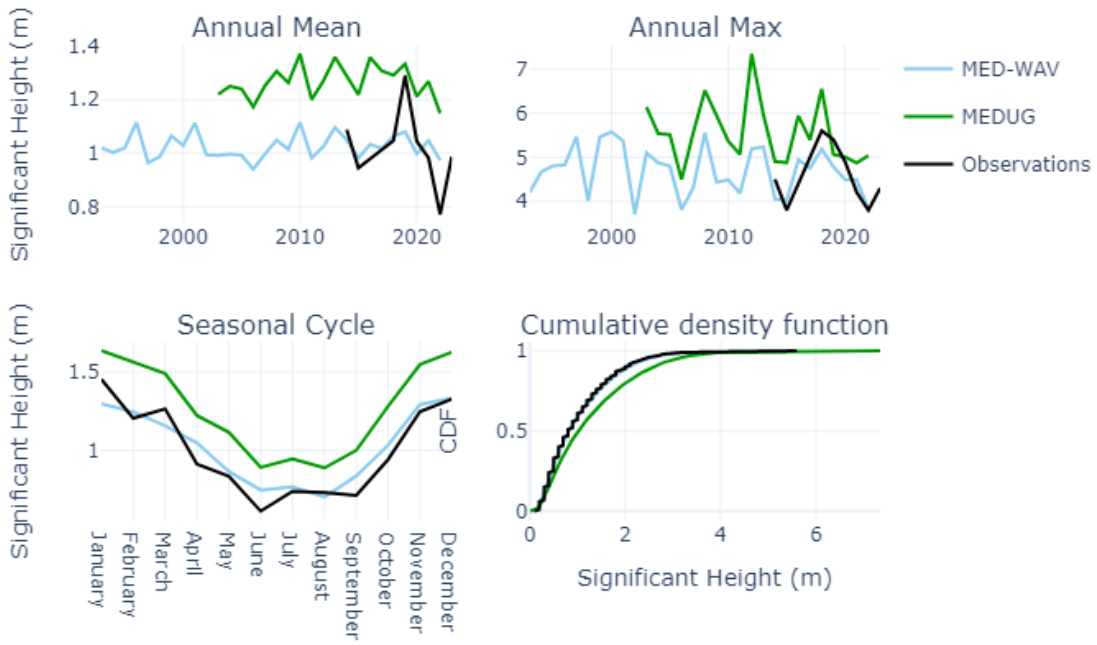

Figure 11. Comparisons between observations (black) and reanalyses: MED-WAV (blue) and MEDUG (green) at station MED1

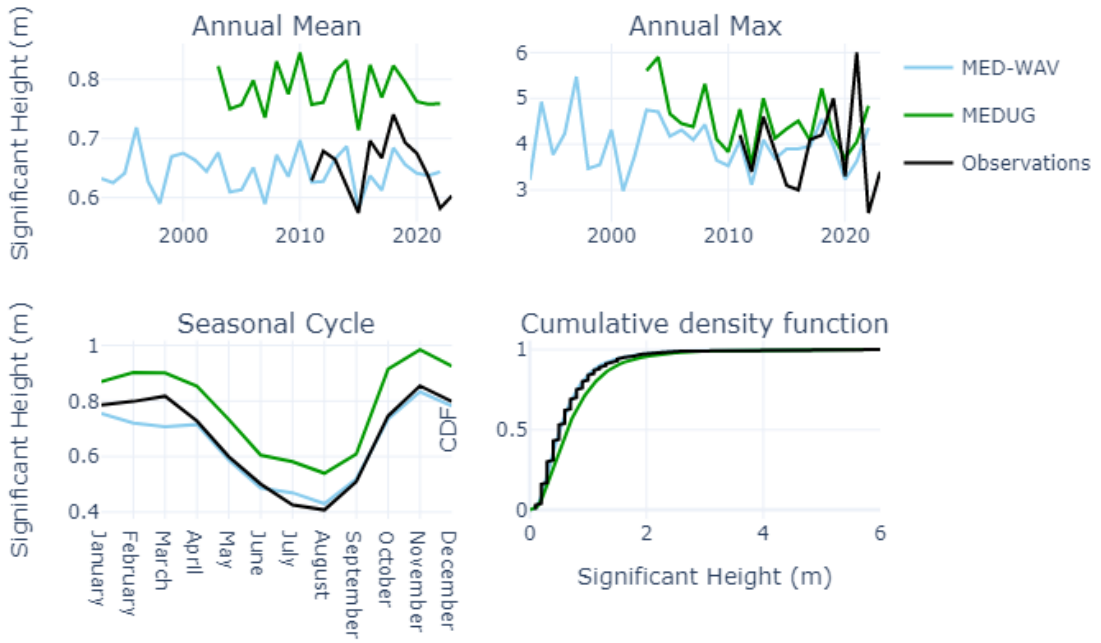

Figure 12. Comparisons between observations (black) and reanalyses: MED-WAV (purple) and MEDUG (green) at station MED2

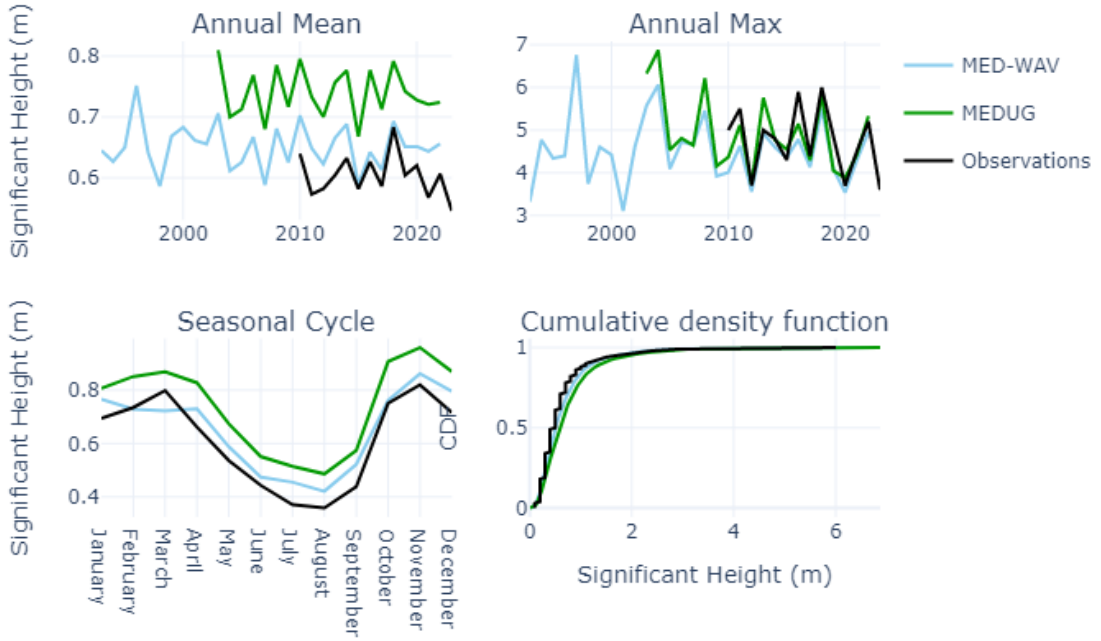

Figure 13. Comparisons between observations (black) and reanalyses: MED-WAV (purple) and MEDUG (green) at station MED3

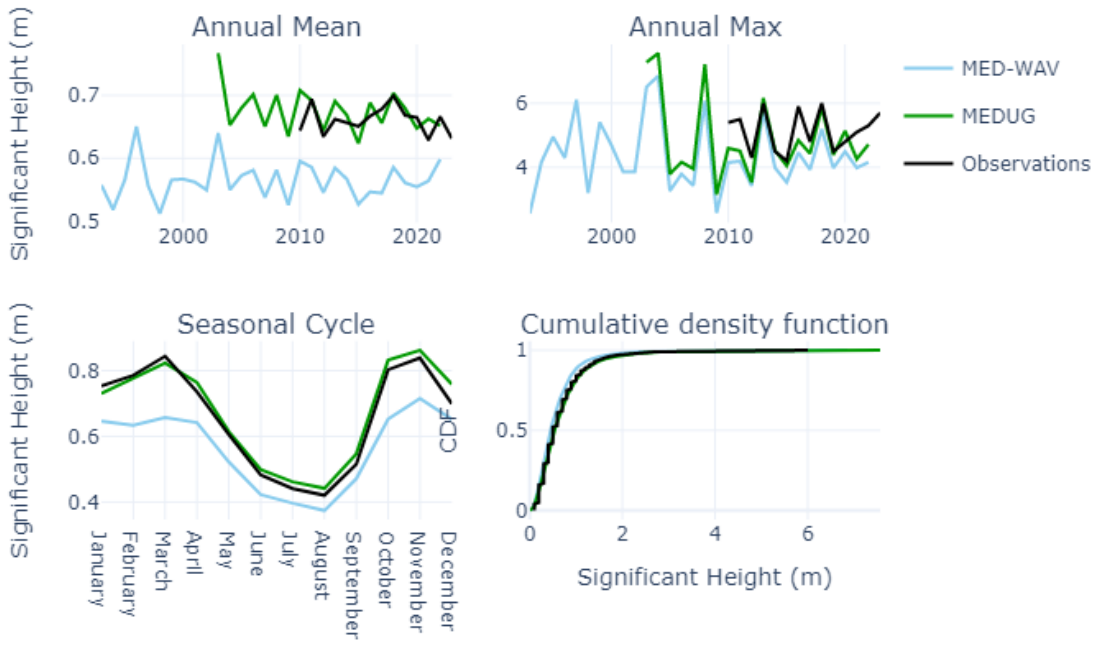

Figure 14. Comparisons between observations (black) and reanalyses: MED-WAV (purple) and MEDUG (green) at station MED4

In the following tables (Table 7, Table 8, Table 9), the scores are shown for both reanalyses at all the Mediterranean stations and for mean and extreme conditions. The best reanalysis is each time highlighted by bold writing. For almost all scores and all stations, the MED-WAV reanalysis shows better results for mean conditions. For extreme conditions, the results are less clear: MED-WAV is better for correlation, MED-UG is better for bias, and the scores are split for NRMSE.

In detail:

- The correlation between MED-WAV and observations is very good for normal conditions with values greater than 0.86, and weaker only for extreme conditions at stations MED1 and MED2, with values equal to 0.67 and 0.49 respectively (results nevertheless better than for the MEDUG reanalysis).
- The bias between MED-WAV and observations is very good for mean conditions with values lower than 0.1 m. For extreme conditions, MED-WAV is better at station MED1 and MEDUG is better at station MED2. The biases at the other 2 stations are comparable.
- The NRMSE between MED-WAV and observations is satisfactory for average conditions with values between 9 and 12%. For extreme conditions, the results are also good except at station MED1 with values of 15% and 25% for the MED-WAV and MEDUG reanalyses respectively.

The MED-WAV reanalysis therefore presents overall better scores than the MEDUG reanalysis and is therefore retained for the correction of climate models in the Mediterranean.

Table 7. Correlation for mean and extreme conditions at Mediterranean stations

Correlation	Mean Conditions		Extreme Conditions	
[no units]	MEDUG	MED-WAV	MEDUG	MED-WAV
MED1	0.9	**0.93**	0.55	**0.67**
MED2	0.87	**0.9**	0.66	**0.71**
MED3	0.85	**0.87**	0.83	**0.86**
MED4	0.83	**0.87**	0.86	**0.88**

Table 8. Bias for mean and extreme conditions at Mediterranean stations

Bias	Mean Conditions		Extreme Conditions	
[m]	MEDUG	MED-WAV	MEDUG	MED-WAV
MED1	0.23	**0.01**	0.45	**-0.11**
MED2	0.1	**-0.03**	**0.02**	-0.31
MED3	0.13	**0.05**	**0.12**	-0.14
MED4	**0.01**	-0.09	**-0.04**	-0.4

Table 9. NRMSE for mean and extreme conditions at Mediterranean stations

NRMSE	Mean Conditions		Extreme Conditions	
[%]	MEDUG	MED-WAV	MEDUG	MED-WAV
MED1	18.04	**9.6**	25.58	**15.49**
MED2	14.25	**10.11**	**12.24**	12.78
MED3	15.73	**11.0**	10.0	**8.8**
MED4	13.61	**12.33**	**9.55**	12.56

5 Conclusion of waves comparisons

The following table presents the numerical reanalyses which were retained for each French maritime seafront, in order to correct the waves climate models (see section VI).

Table 10. Best reanalyses for each French maritime seafront in terms of waves

Maritime seafront	Best reanalysis
English Channel	**HYWAT**
Atlantic Ocean	**HYWAT**
Mediterranean Sea	**MED-WAV**

VI. CORRECTIONS FOR WAVE DATA

Due to their coarse resolution and physical parameterizations, GCMs have bias compared to observations and reanalysis. A bias correction is applied to correct the differences between the distributions of the reanalysis and the models. Different approaches exist, based on a correction of the mean values, or a correction of the full distribution. Here we choose a method of the second kind, the CDF-t (Cumulative Distribution Function transform) method (Michelangeli et al., 2009). Also, the CDF-t method corrects all quantiles compared to the usual quantile-matching method for example (Kokic et al., 2013). The CDF-t method assumes that the transformation from the historical GCM to the local scale is unchanged in the future climate.

This can be translated as:

$$F_{o,f}(x) = F_{o,h}\left(F_{m\ h}^{-1}(F_{m,f}(x))\right)$$

where *Fo,h* is the CDF of observations in the historical period, *Fo,f* is the CDF of observations in the future period, *Fm,h* the CDF of one of the models in the historical period and *Fm,f* the CDF of the same model in the future period.

Finally, the CDF-t method is applied on raw and monthly data to avoid seasonality effect. A first result is shown in Figure 15 for one station in the Atlantic Ocean (buoy 6200069, offshore Brest). The CDF-t is applied at each station in the full common timeseries (between reanalyses and climate models) so from 1985-2014 for the English Channel and the Atlantic coast and over 1993-2014 for the Mediterranean Sea.

In Figure 17, we see from top to bottom, the annual mean, the cumulative density function and the seasonal cycle, before the CDFt (left) and after the CDFt (right). We can see that the downscaling works well on the whole distribution (the cumulative density functions of the climate models follow that of the reanalysis) and that the seasonal cycles are also perfectly in phase.

The next step, which will be the subject of a future 2C NOW report, will be to perform the CDF-t at the locations of offshore wind farms projects and analyze the future wave climate in the projections until 2100.

In the next chapter of this report, the same analysis is performed on water level data.

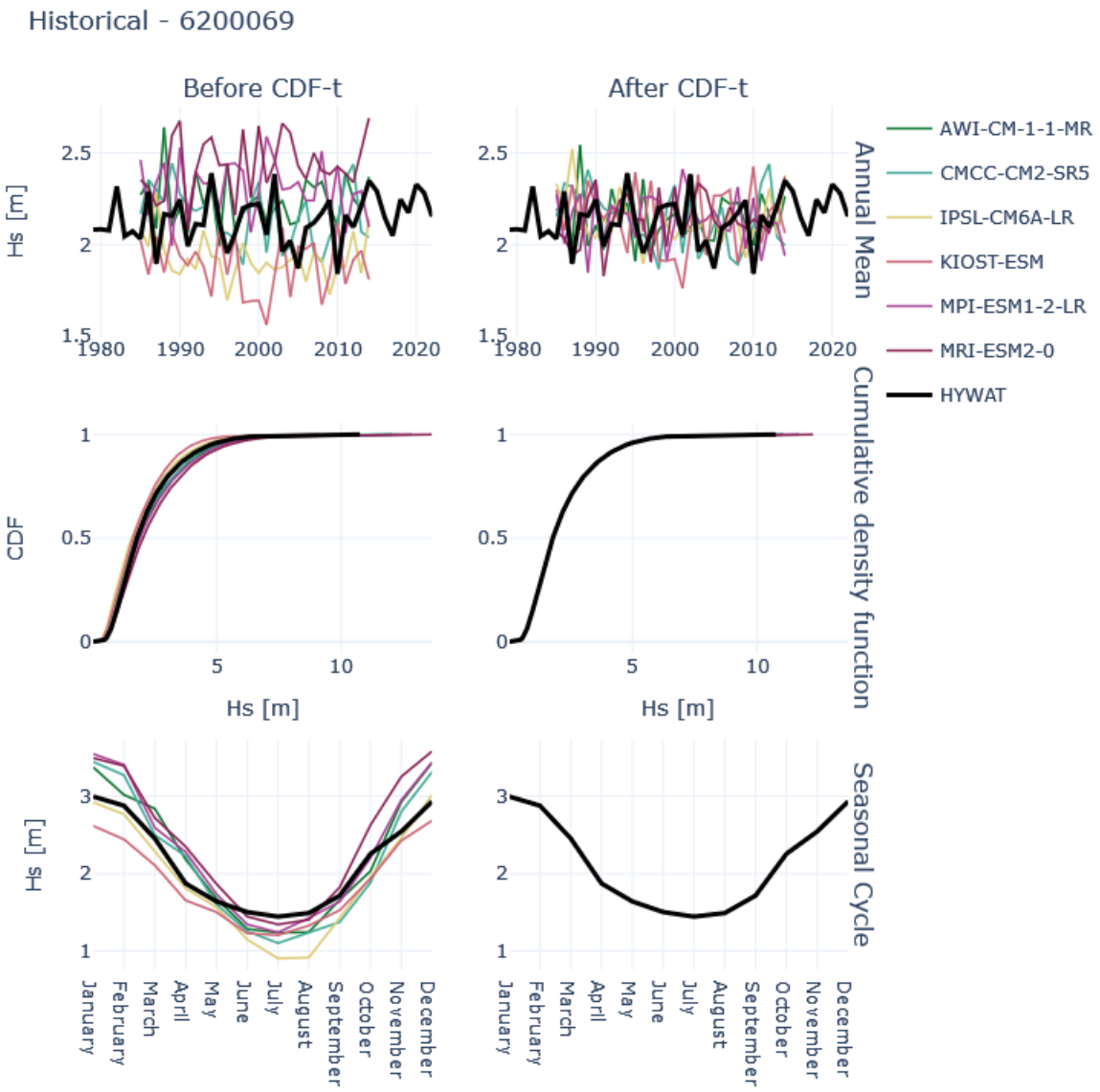

Figure 15. Representation of the best reanalysis HYWAT (bold black) at buoy 6200069 (offshore Brest) and the climatic models for the historical period, before the CDF-t is applied (left panel) and after the CDF-t is applied (right panel)

VII. WATER LEVEL DATA

The methodology used in the previous chapter for waves is used here for water levels. Comparisons are made on "total water levels", which include a tidal component (periodic phenomenon of astronomical origin), a slowly varying mean water level component, and a residual component also called "storm surge" linked in particular to atmospheric variations (winds, pressures). Only the last 2 components (mean water level, surge) can be impacted by climate change.

1 Observations

Water levels data are provided by the RONIM network operated by the SHOM in France through multiple tide gauge stations giving sea level data in meter. Data measured by French tide gauges are referenced vertically to chart datum (CD). Numerical reanalyses, on the other hand, have water level values based on their own mean sea level (their equilibrium position). To compare the reanalyses to the observations, their overall means are therefore removed in order to obtain oscillations around zero; the bias scores between the reanalyses and the observations will therefore not be presented in this part of the report.

The objective of the quality check on the water level observations is to keep as much information as possible. We describe water level outliers, as values that are twice as large than the 99th percentile (obs > 2*p99), or that are below the 1st percentile subtracted by twice its absolute value (obs < p1 - 2*|p1|). Any values fitting this description were deleted. Only the stations number 250 (Sète) and 710 (Solenzara) were impacted, erasing a handful of outliers. For the figures including the annual average only, we removed any year presenting more than 25% missing values (i.e. less than 2190 values a year). This prevents most bias while retaining enough information. After applying this quality control, there are 23 tide gauge stations left in total, with 7 stations in the English Channel, 11 stations along the Atlantic coast, and 7 stations in the Mediterranean Sea (Figure 16).

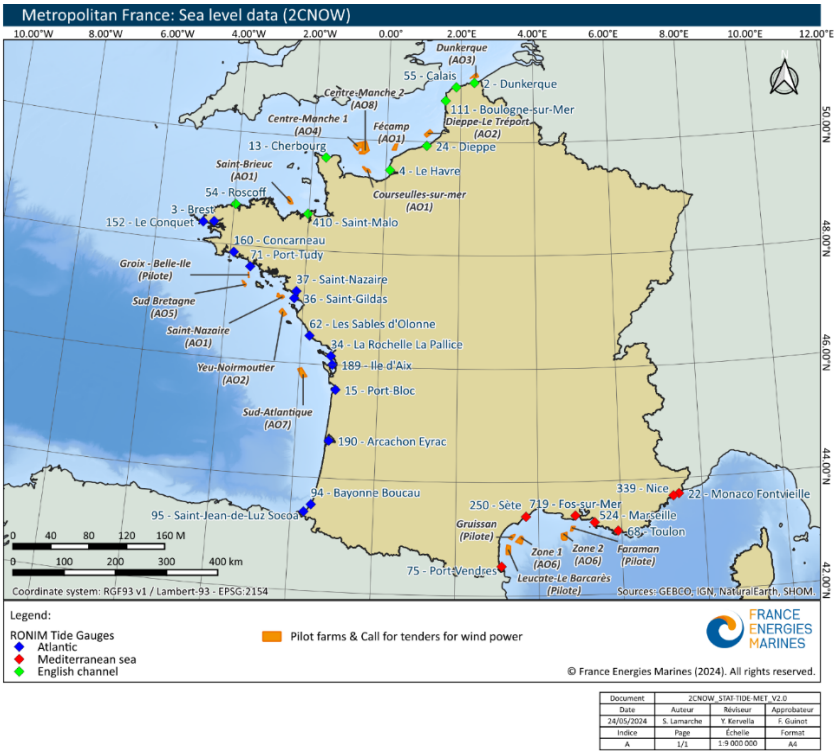

Figure 16. Map of the tide gauge stations selected for the study on water level

2 Reanalysis data

2.1 Reanalyses used for the Atlantic Ocean and the English Channel

The **GTSM-ERA5** reanalysis dataset, from Copernicus Climate Change Service (C3S), is used in this study to compare to the stations located on the Atlantic and Channel coasts. This reanalysis is available from 1979 to 2018 (https://doi.org/10.24381/cds.a6d42d60). The dataset provides data of mean sea level, storm surge residual, tidal elevation and total water level and is forced by ERA5 wind for the reanalysis component. This dataset is also forced by CMIP6 winds (see section Climate models). Data are available every 10 minutes at coastal grid points with a resolution of 0.1° (https://cds.climate.copernicus.eu/cdsapp#!/dataset/sis-water-level-change-timeseries-cmip6?tab=overview). Time series are computing using the Deltares Global Tidal and Surge Model (GTSM) version 3.0. More information about this dataset is provided by Table 11 below.

Table 11. Description of the Copernicus dataset used for water level analysis (Please note that this dataset is subject to change; up-to-date information: https://doi.org/10.24381/cds.a6d42d60)

DATA DESCRIPTION	
Data type	Gridded with variable grid step
Projection	Latitude-longitude grid
Horizontal coverage	Global
Horizontal resolution	Coastal grid points: 0.1° Ocean grid points: 0.25°, 0.5°, and 1° within 100 km, 500 km, and >500 km of the coastline, respectively
Vertical coverage	Surface
Vertical resolution	Single level
Temporal coverage	ERA5 reanalysis: 1979 to 2018 Climate projections historical: 1950 to 2014 Climate projections future: 2015 to 2050
Temporal resolution	Reanalysis: 10-minute, hourly and daily maximum Climate projections historical and future: 10-minute, annual
File format	NetCDF-4
Conventions	Climate and Forecast (CF) Metadata Convention v1.6, Attribute Convention for Dataset Discovery (ACDD) v1.3
Versions	Dataset version 1.0
Update frequency	No updates expected

The **IBI-MFC** reanalysis dataset (https://doi.org/10.48670/moi-00029), from Copernicus Marine Service, is also used in this study to compare to the stations located on the Atlantic and Channel coasts. The IBI-MFC provides an ocean physical reanalysis product for the Iberia-Biscay-Ireland (IBI) from 1993 to 2021, with an hourly timestep. The model system is run by Mercator-Ocean, within a numerical core based on the NEMO v3.6 ocean general circulation model run at 1/12° horizontal resolution. Altimeter data, in situ temperature and salinity vertical profiles and satellite sea surface temperature are assimilated.

2.2 Reanalyses used for the Mediterranean Sea

The **GTSM-ERA5** reanalysis dataset, described in previous paragraph, is also used in this study to compare to the stations located in the Mediterranean Sea.

The other reanalysis used in the Mediterranean is the **MED-MFC**, available on Copernicus Marine Service (https://doi.org/10.25423/CMCC/MEDSEA_MULTIYEAR_PHY_006_004_E3R1). This dataset is generated by a numerical system composed of an hydrodynamic model, supplied by the Nucleus for European Modelling of the Ocean (NEMO) and a variational data assimilation scheme (OceanVAR) for temperature and salinity vertical profiles and satellite Sea Level Anomaly along track data. The model horizontal grid resolution is 1/24˚ (ca. 4-5 km) and the unevenly spaced vertical levels are 141. The reanalysis dataset covers the period from 1987 to 2024, with an hourly timestep.

3 Climate models

At the climate model level, the **GTSM** dataset is also used (https://cds.climate.copernicus.eu/cdsapp#!/dataset/10.24381/cds.a6d42d60?tab=overview), and is forced this time, in terms of climate forcing, with 5 Atmospheric General Circulation Models (AGCMs) of the high resolution Coupled Model Intercomparison Project Phase 6 (**CMIP6**) experiment: CMCC-CM2-VHR4, EC-Earth3P-HR, GFDL-CM4C192-SST, HadGEM3-GC31-HM and HadGEM3-GC31-HM-SST. Only one future scenario is available in addition to the historical part, and it is the high-emissions scenario SSP5-8.5, proposed by IPCC. The historical period covers 1950 to 2014 and the future period starts in 2015 until 2050.

VIII. COMPARISONS FOR WATER LEVEL DATA

To compare total water levels, the first approach is to do some scatter plots between observations and the reanalyses (Appendix 2.2). For each station the linear regression line on all the data points is also plotted. The good fitting indicates that observations and the reanalysis are matching for every station. Note that some papers already validated the GTSM-ERA5 reanalysis with tide gauge stations and confirm the similarities (Muis et al., 2020; Dullaart et al., 2020). Comparisons are then made by analysing annual mean, annual maxima and cumulative distributions. To quantify these comparisons, statistical metrics (scores, described in section 1) are presented in dedicated tables.

Since one of the objectives of the 2C NOW project is to evaluate the possible impacts of climate change on the design of offshore wind farms, both the mean and extreme conditions are considered: when we refer to "mean conditions" in the remainder of this report, we are referring to data between the 5th and 95th percentiles, these percentiles being calculated from observations. When we refer to "extreme conditions", we are looking at both values above the 95th percentile and values below the 5th percentile, calculated from observations.

1 Comparisons for stations located in the English Channel

The following figures (Figure 17 to Figure 24) show the comparisons between observations and reanalyses for the Channel stations. We can see that the trends are generally rather well represented for the annual mean, and that there is more bias for the annual max, even if these annual maximums seem to be well correlated temporally. Visually, the GTSM-ERA5 reanalysis seems to perform slightly better than the IBI-MFC reanalysis.

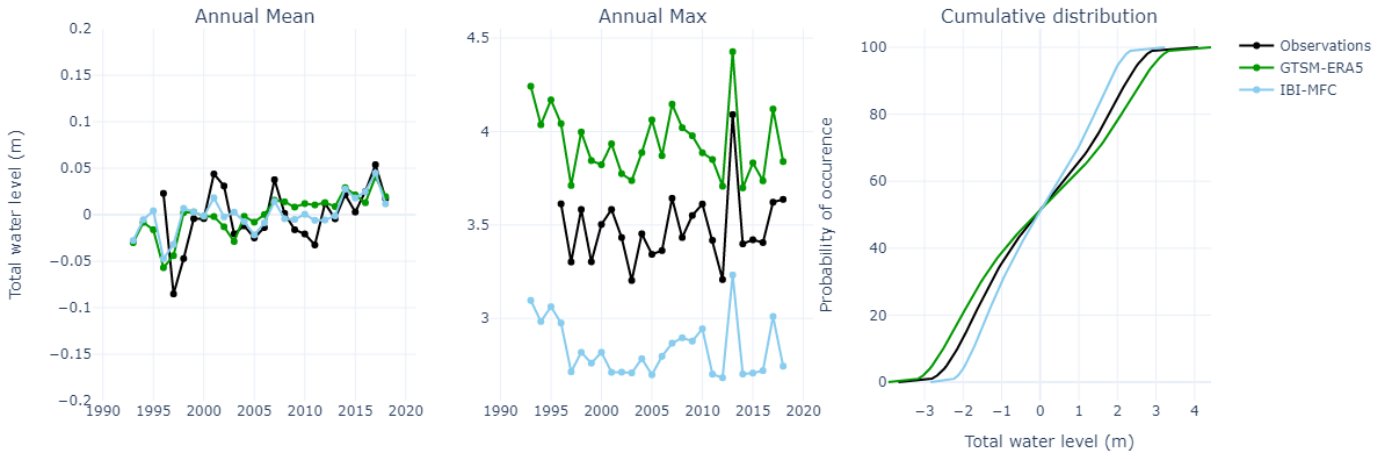

Figure 17. Comparisons between observations (black) and reanalyses: GTSM-ERA5 (green) and IBI-MFC (blue) at station 2 (Dunkerque)

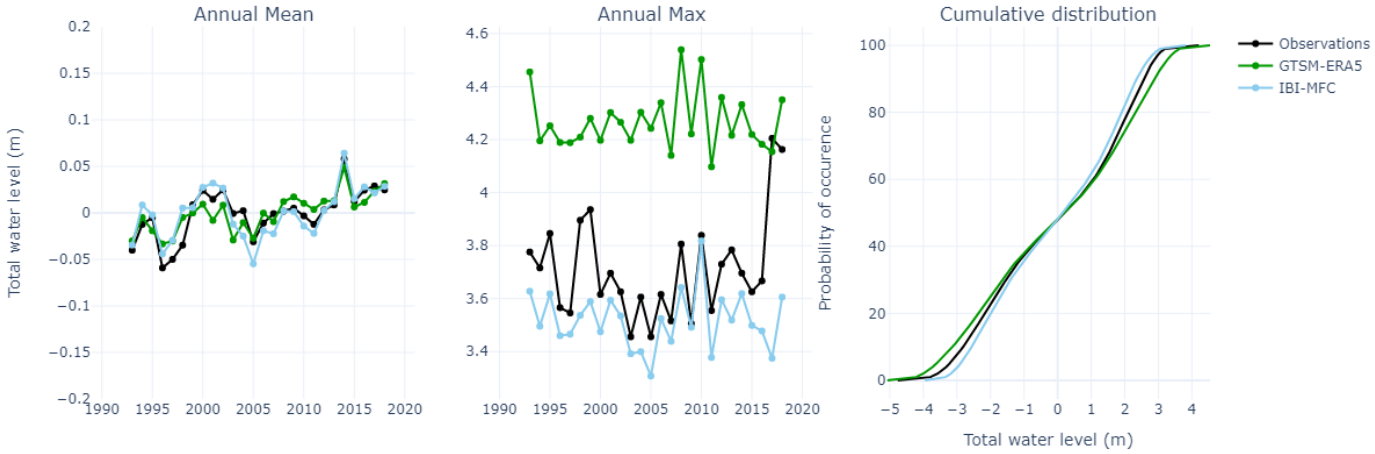

Figure 18. Comparisons between observations (black) and reanalyses: GTSM-ERA5 (green) and IBI-MFC (blue) at station 4 (Le Havre)

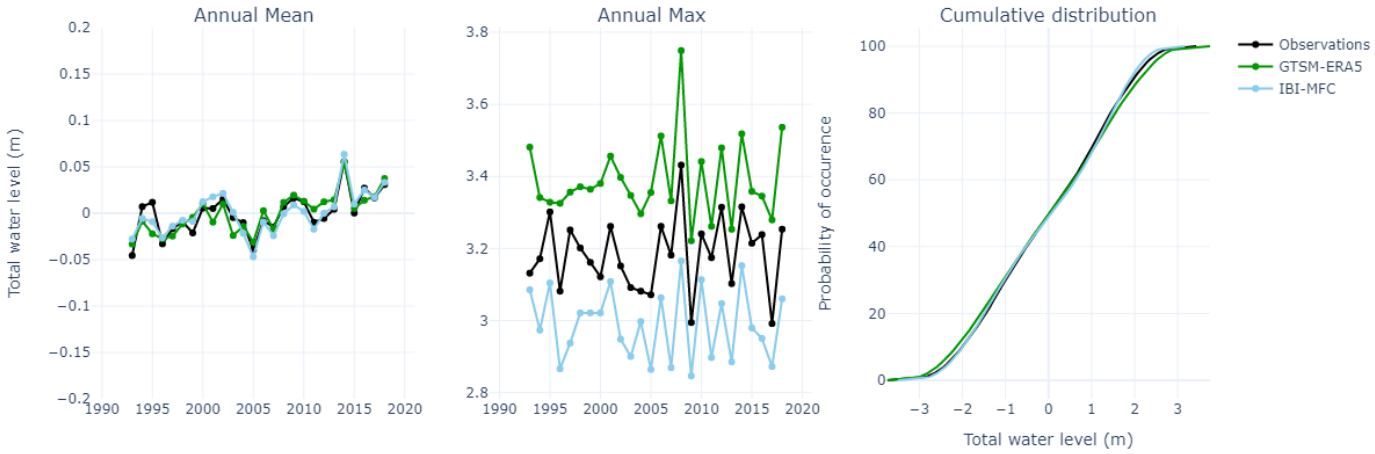

Figure 19. Comparisons between observations (black) and reanalyses: GTSM-ERA5 (green) and IBI-MFC (blue) at station 13 (Cherbourg)

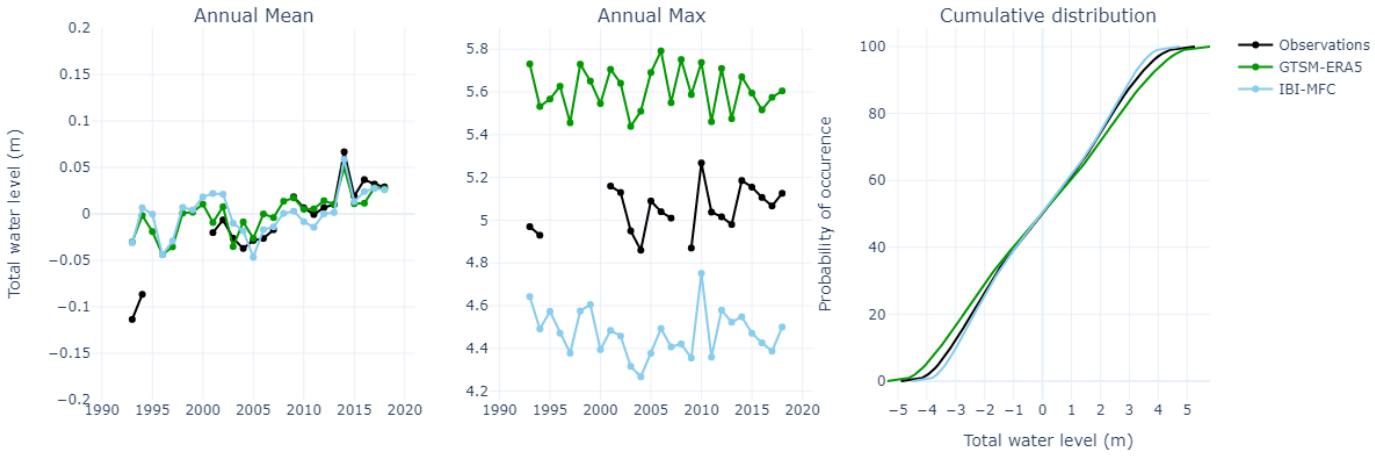

Figure 20. Comparisons between observations (black) and reanalyses: GTSM-ERA5 (green) and IBI-MFC (blue) at station 24 (Dieppe)

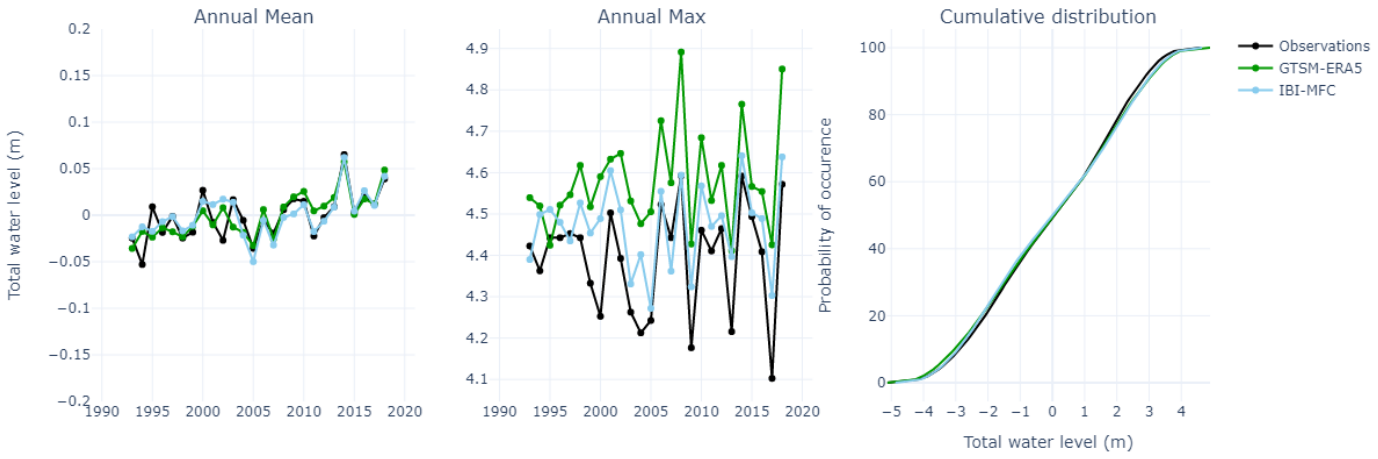

Figure 21. Comparisons between observations (black) and reanalyses: GTSM-ERA5 (green) and IBI-MFC (blue) at station 54 (Roscoff)

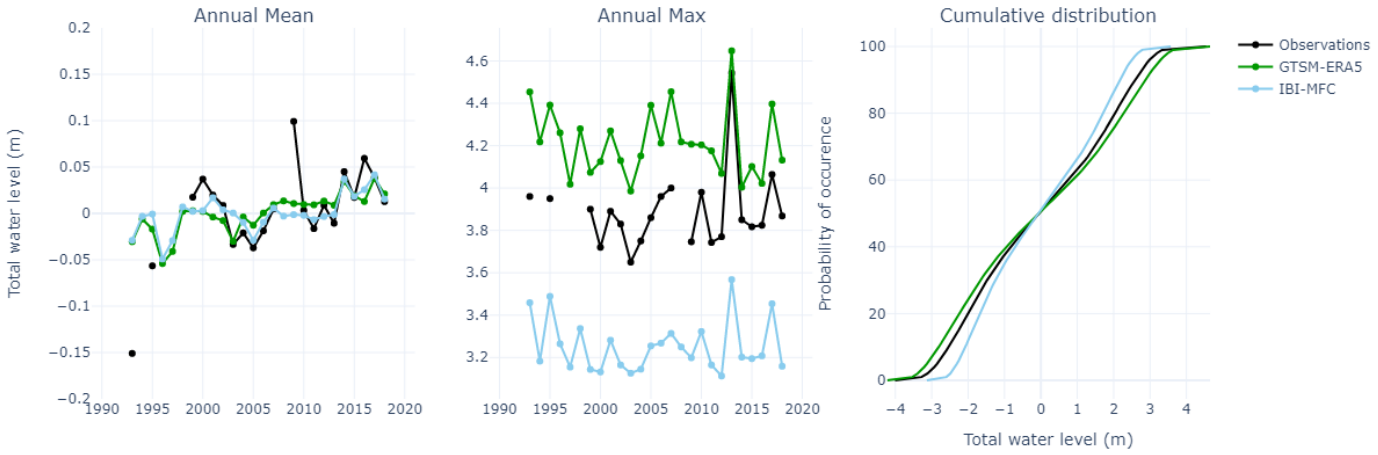

Figure 22. Comparisons between observations (black) and reanalyses: GTSM-ERA5 (green) and IBI-MFC (blue) at station 55 (Calais)

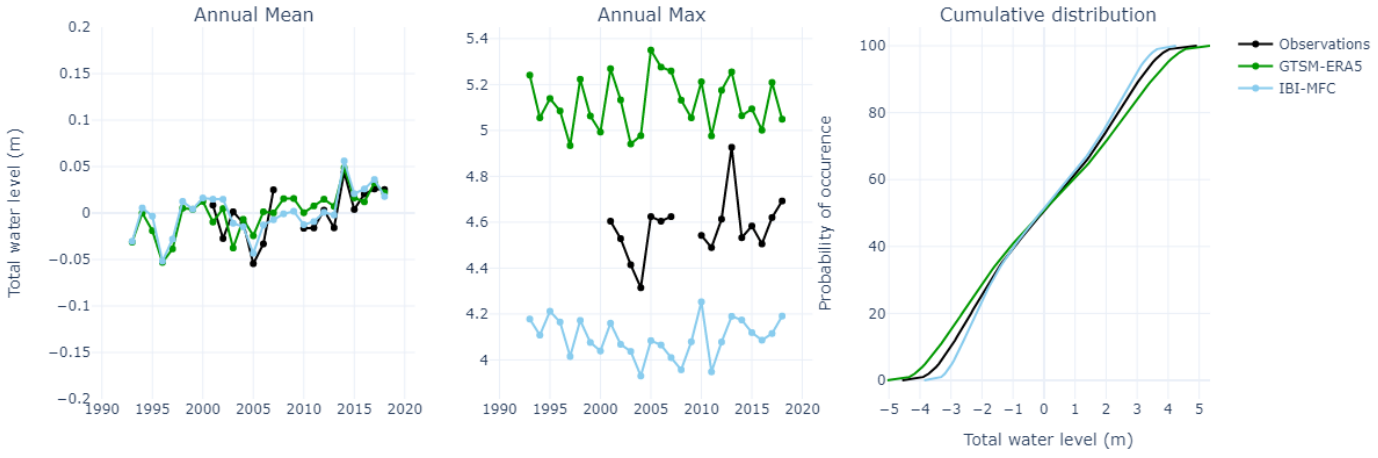

Figure 23. Comparisons between observations (black) and reanalyses: GTSM-ERA5 (green) and IBI-MFC (blue) at station 111 (Boulogne-sur-Mer)

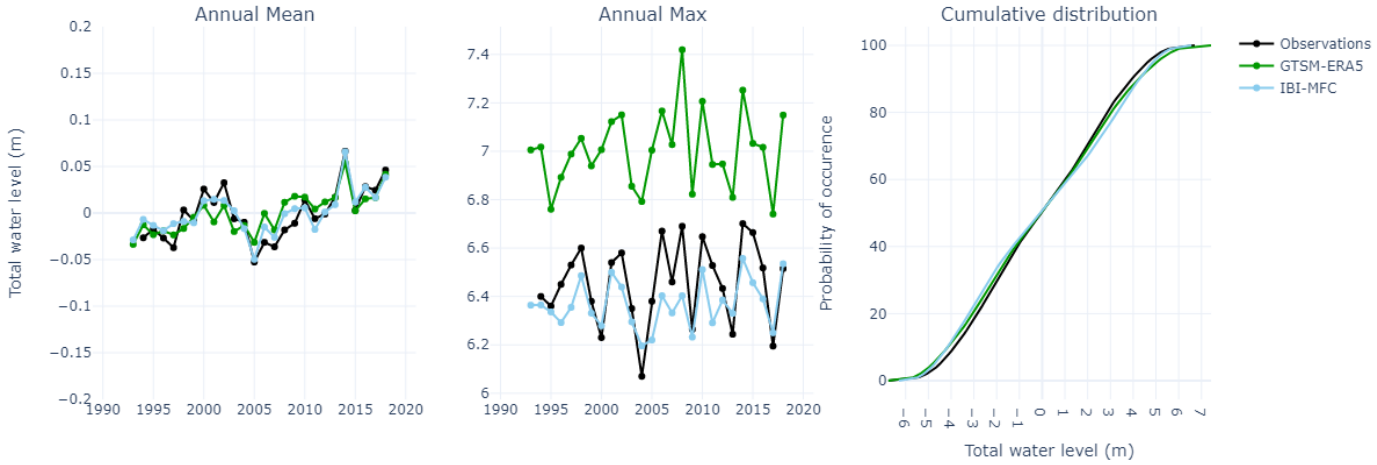

Figure 24. Comparisons between observations (black) and reanalyses: GTSM-ERA5 (green) and IBI-MFC (blue) at station 410 (Saint-Malo)

In the following tables (Table 12 and Table 13), the scores are shown for both reanalyses at all the Channel stations and for mean and extreme conditions. The best reanalysis is each time highlighted by bold writing. For almost all scores and all stations, the GTSM-ERA5 reanalysis shows better results, whether for mean conditions or for extreme conditions.

In detail:

- The correlation between GTSM-ERA5 and observations is very good for normal conditions with values greater than 0.99, and a bit weaker for extreme conditions with values between 0.61 and 0.88 (results nevertheless better than for the IBI-MFC reanalysis).
- The NRMSE between GTSM-ERA5 and observations presents values from 2% to 5% for mean conditions and from 15% to 35% for extreme conditions. The difference in results between the mean conditions and the extreme conditions is notably due to the biases observed in the previous figures (and therefore also to the bias correction which was carried out). The results are worse in terms of NRMSE for IBI-MFC, except at station 4 (Le Havre).

GTSM-ERA5 is therefore the best reanalysis for the English Channel stations.

Table 12. Correlation for mean and extreme conditions at Channel stations

Correlation	Mean Conditions		Extreme Conditions	
[no units]	IBI-MFC	GTSM-ERA5	IBI-MFC	GTSM-ERA5
BOULOGNE-SUR-MER	0.96	**1.0**	0.44	**0.86**
CALAIS	0.98	**0.99**	0.48	**0.85**
CHERBOURG	0.97	**0.99**	0.77	**0.83**
DIEPPE	0.97	**1.0**	0.63	**0.88**
DUNKERQUE	0.98	**0.99**	0.54	**0.86**
LE_HAVRE	**0.99**	**0.99**	0.5	**0.61**
ROSCOFF	0.97	**0.99**	0.67	**0.86**
SAINT-MALO	0.97	**0.99**	0.41	**0.85**

Table 13. NRMSE for mean and extreme conditions at Channel stations

NRMSE	Mean Conditions		Extreme Conditions	
[%]	IBI-MFC	GTSM-ERA5	IBI-MFC	GTSM-ERA5
BOULOGNE-SUR-MER	7.1	**4.2**	47.27	**34.67**
CALAIS	6.49	**4.08**	42.72	**18.54**
CHERBOURG	5.36	**3.14**	19.65	**16.72**
DIEPPE	6.04	**3.91**	38.89	**30.2**
DUNKERQUE	6.42	**5.24**	42.33	**27.14**
LE_HAVRE	**3.72**	4.14	**24.94**	30.35
ROSCOFF	5.89	**2.87**	20.25	**15.83**
SAINT-MALO	6.47	**3.53**	32.16	**22.66**

2 Comparisons for stations located in the Atlantic Ocean

The following figures (Figure 25 to Figure 37) show the comparisons between observations and reanalyses for the Atlantic stations. Like in the English Channel, we can see that the trends are generally rather well represented for the annual mean and for the annual max, and that there is more bias for the annual maximums than for the annual mean, even if these annual maximums seem to be well correlated temporally (between reanalyses and observations).

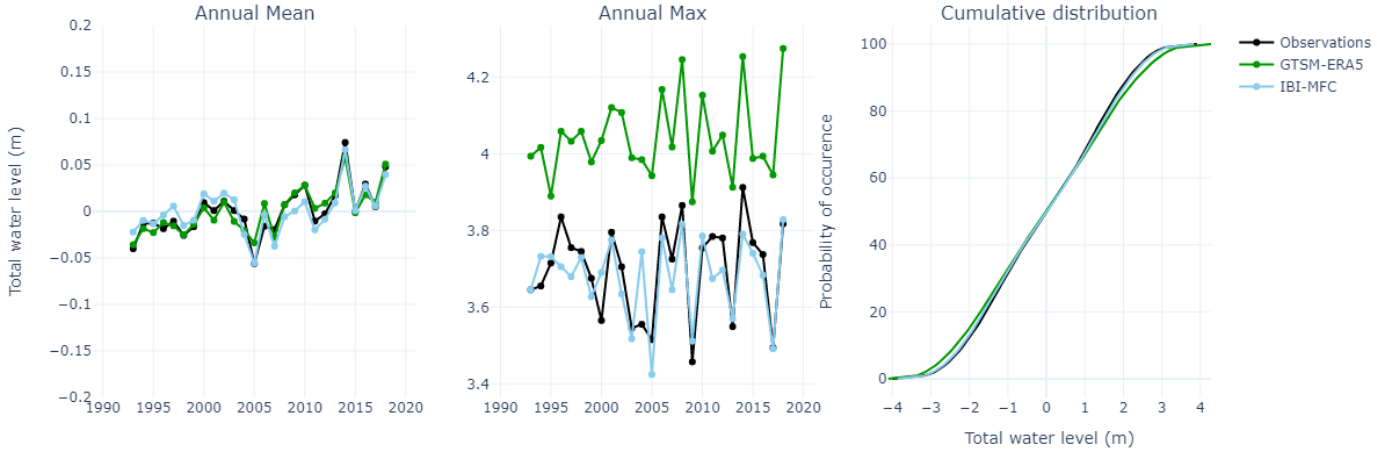

Figure 25. Comparisons between observations (black) and reanalyses: GTSM-ERA5 (green) and IBI-MFC (blue) at station 3 (Brest)

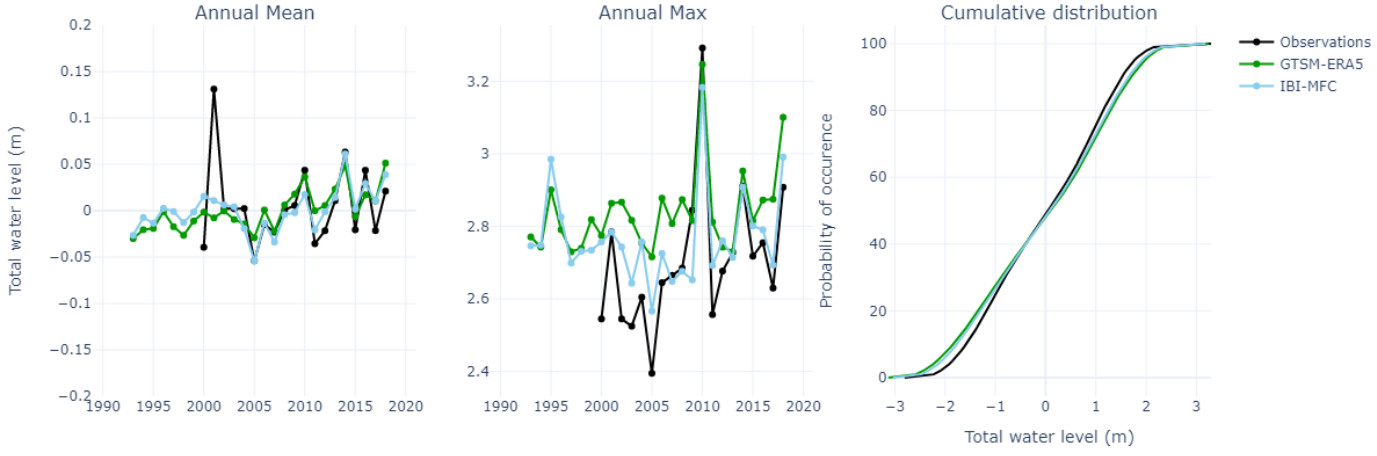

Figure 26. Comparisons between observations (black) and reanalyses: GTSM-ERA5 (green) and IBI-MFC (blue) at station 15 (Port-Bloc)

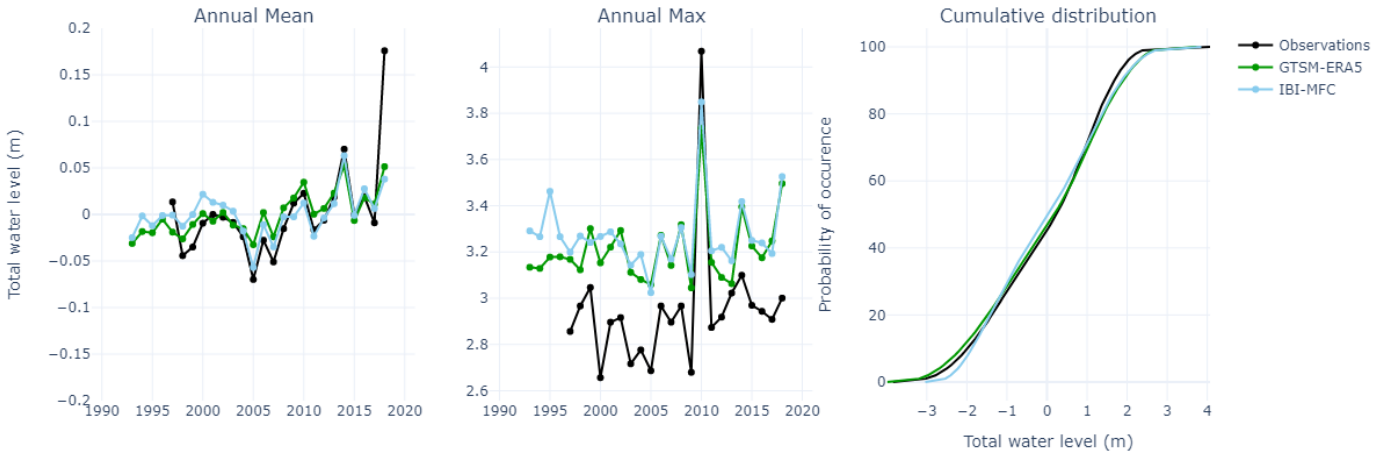

Figure 27. Comparisons between observations (black) and reanalyses: GTSM-ERA5 (green) and IBI-MFC (blue) at station 34 (La Rochelle)

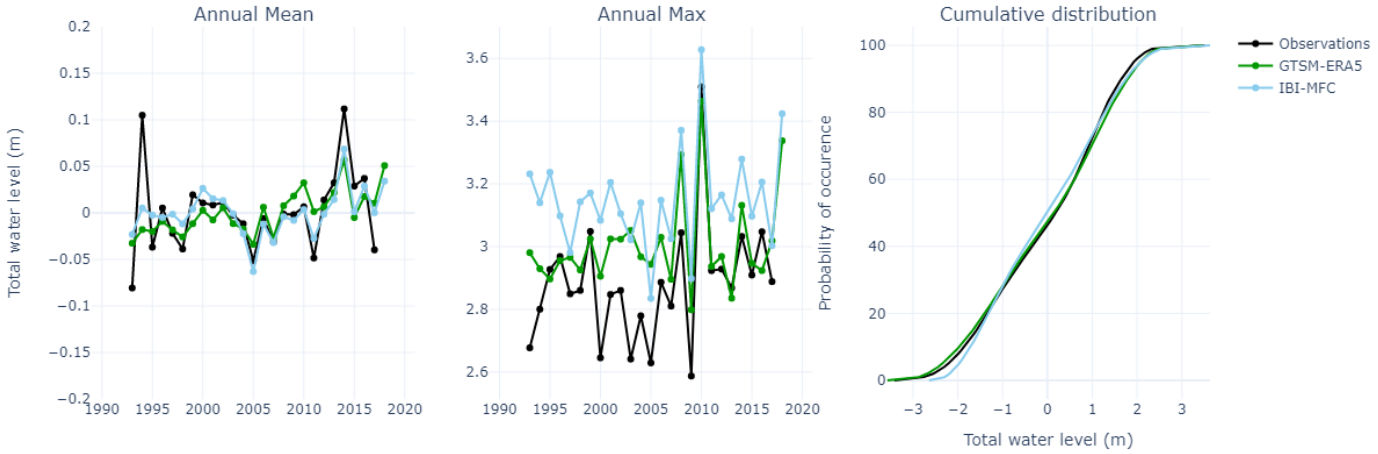

Figure 28. Comparisons between observations (black) and reanalyses: GTSM-ERA5 (green) and IBI-MFC (blue) at station 36 (Saint-Gildas)

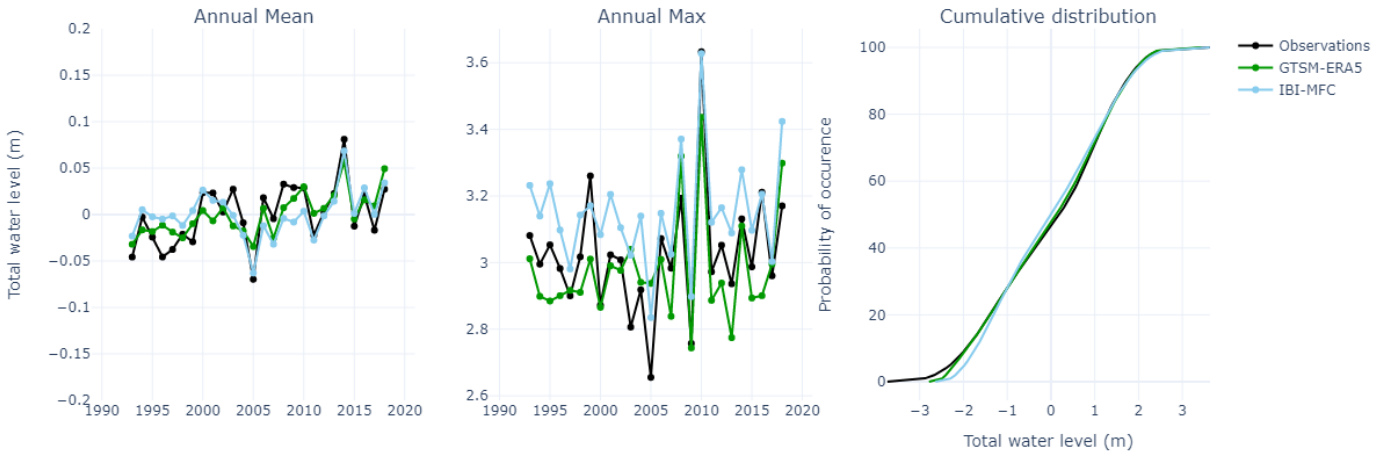

Figure 29. Comparisons between observations (black) and reanalyses: GTSM-ERA5 (green) and IBI-MFC (blue) at station 37 (Saint-Nazaire)

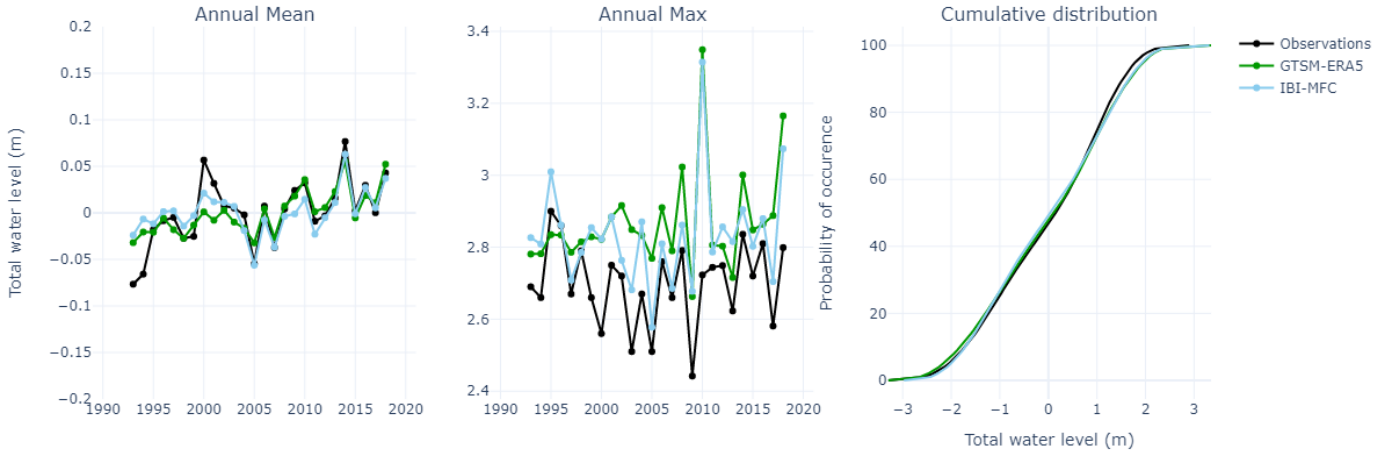

Figure 30. Comparisons between observations (black) and reanalyses GTSM-ERA5 (green) and IBI-MFC (blue) at station 62 (Les Sables d'Olonne)

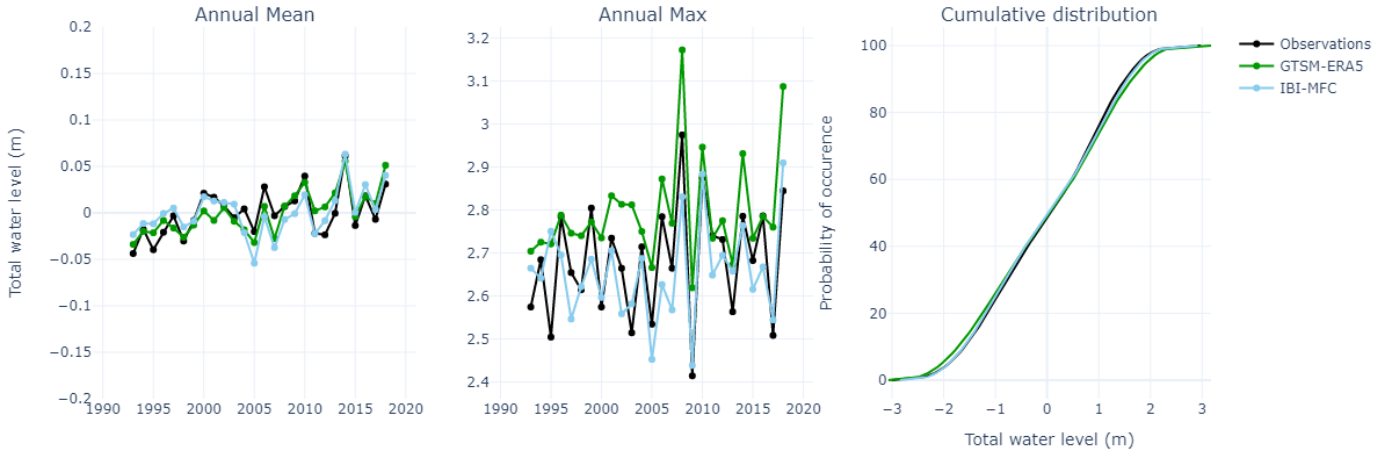

Figure 31. Comparisons between observations (black) and reanalyses: GTSM-ERA5 (green) and IBI-MFC (blue) at station 71 (Port-Tudy)

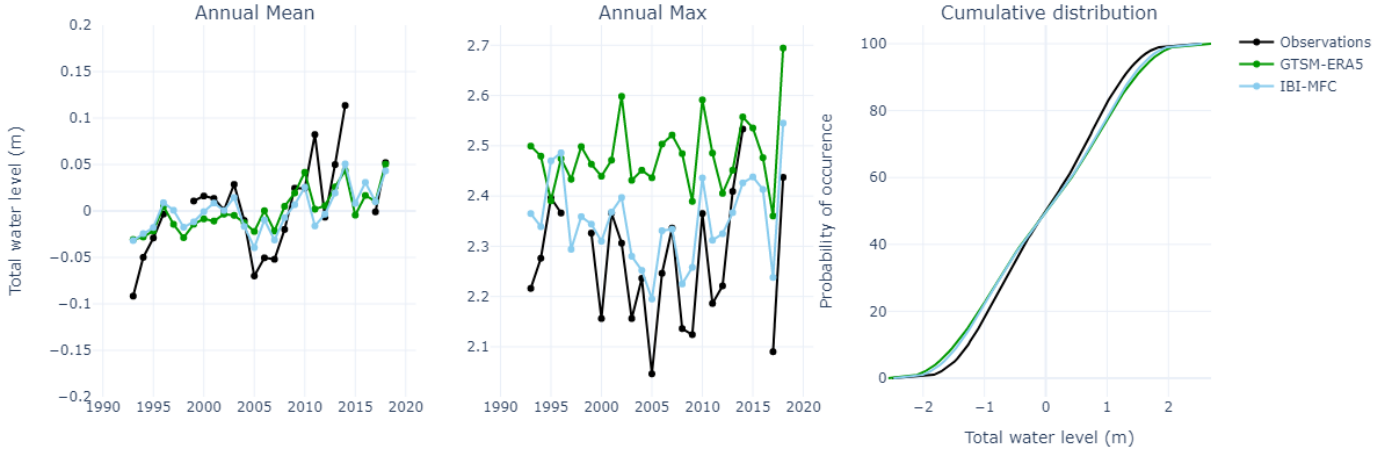

Figure 32. Comparisons between observations (black) and reanalyses: GTSM-ERA5 (green) and IBI-MFC (blue) at station 94 (Bayonne Boucau)

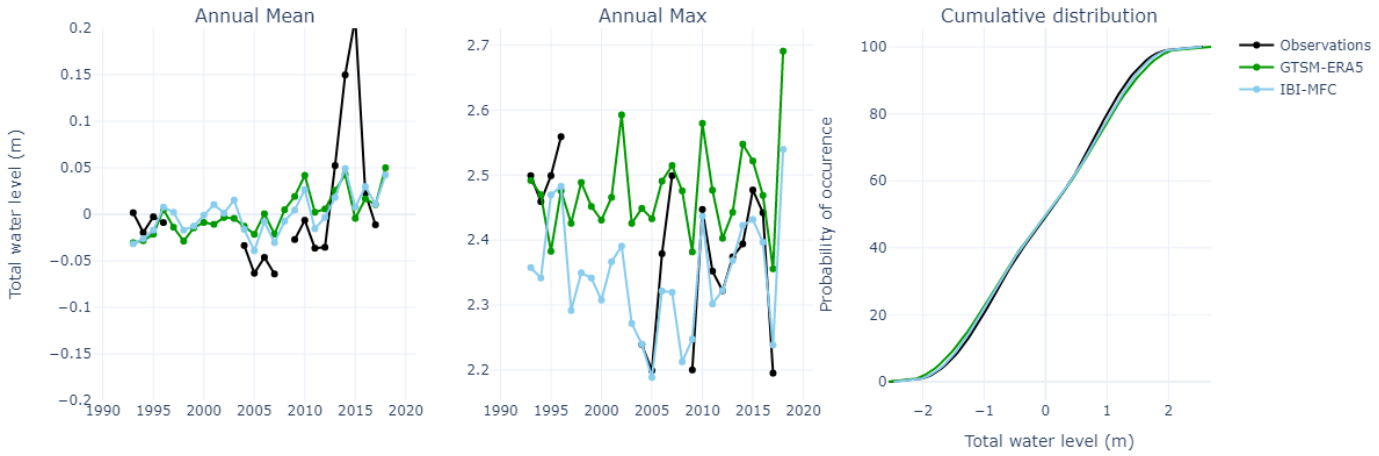

Figure 33. Comparisons between observations (black) and reanalyses: GTSM-ERA5 (green) and IBI-MFC (blue) at station 95 (Saint-Jean de Luz)

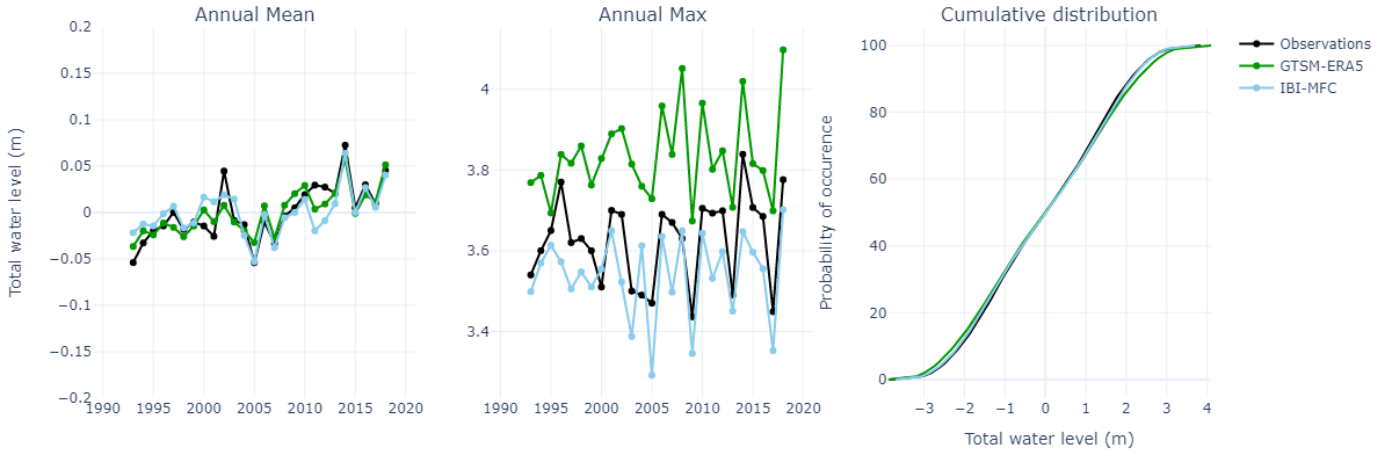

Figure 34. Comparisons between observations (black) and reanalyses: GTSM-ERA5 (green) and IBI-MFC (blue) at station 152 (Le Conquet)

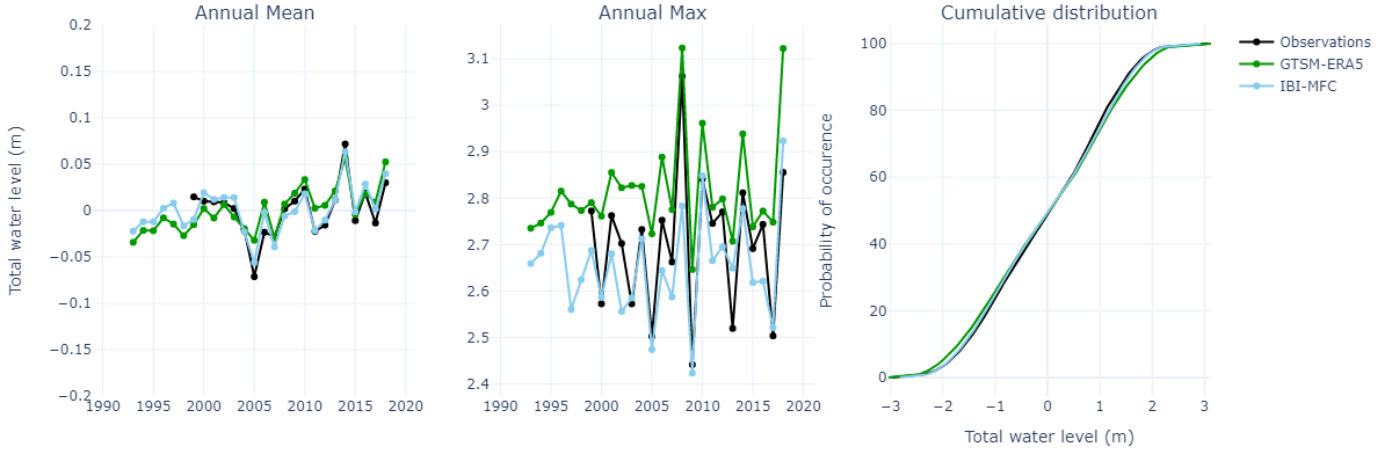

Figure 35. Comparisons between observations (black) and reanalyses: GTSM-ERA5 (green) and IBI-MFC (blue) at station 160 (Concarneau)

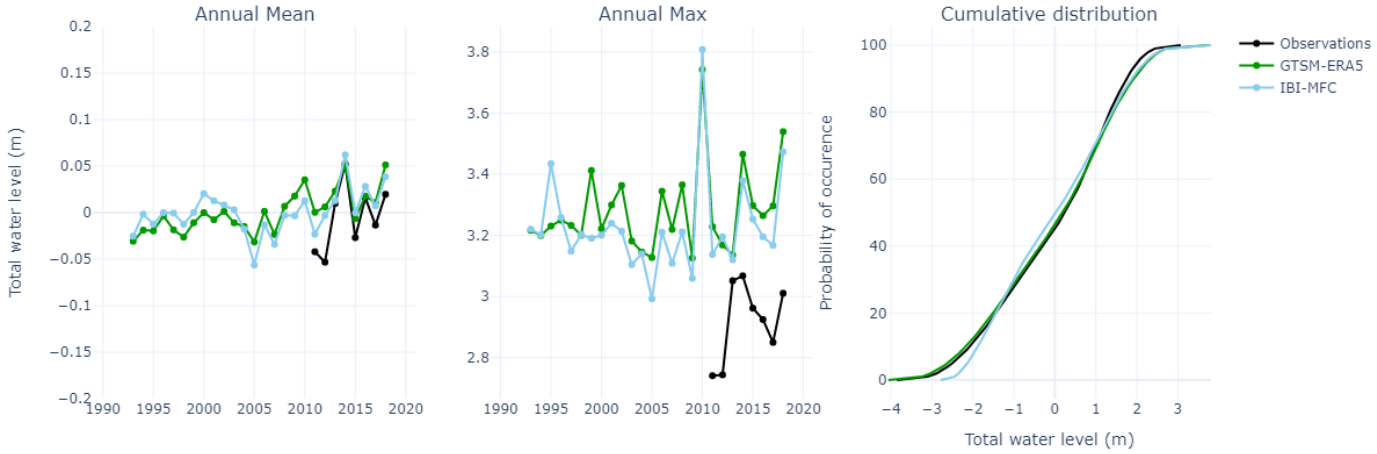

Figure 36. Comparisons between observations (black) and reanalyses: GTSM-ERA5 (green) and IBI-MFC (blue) at station 189 (Île d'Aix)

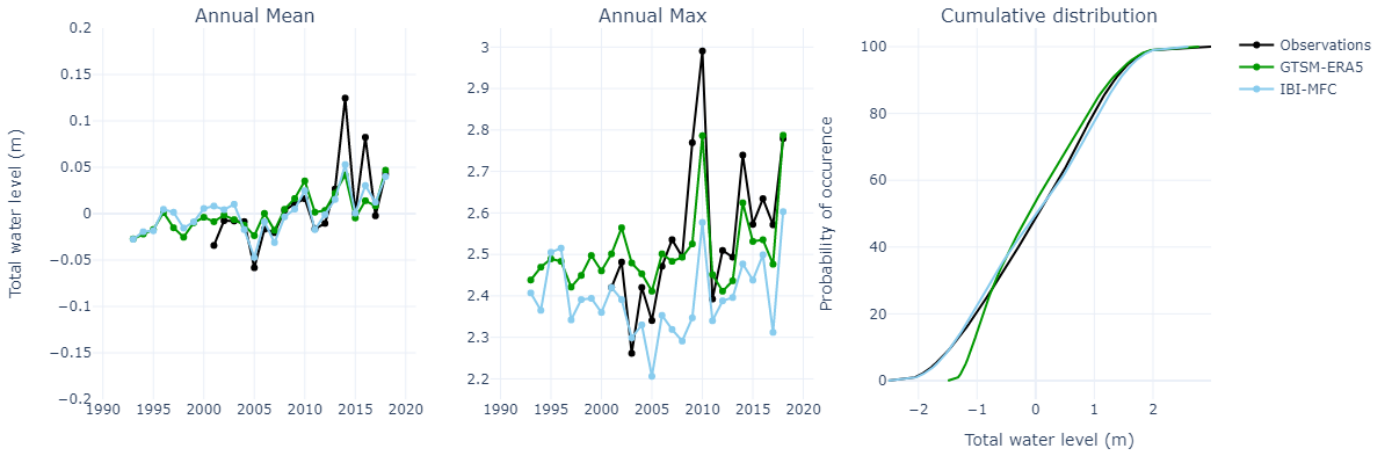

Figure 37. Comparisons between observations (black) and reanalyses: GTSM-ERA5 (green) and IBI-MFC (blue) at station 190 (Arcachon)

In the following tables (Table 14 and Table 15), the scores are shown for both reanalyses at all the Atlantic stations and for mean and extreme conditions. The best reanalysis is each time highlighted by bold writing. For almost all scores and all stations, the GTSM-ERA5 reanalysis shows better results, whether for mean conditions or for extreme conditions.

In detail:

- The correlation between GTSM-ERA5 and observations is very good for normal conditions with values greater than 0.94, and a bit weaker for extreme conditions with values between 0.68 and 0.85 (results nevertheless better than for the IBI-MFC reanalysis).
- The NRMSE between GTSM-ERA5 and observations presents values from 2% to 7% for mean conditions and from 9% to 25% for extreme conditions. The difference in results between the mean conditions and the extreme conditions is notably due to the biases observed in the previous figures (and therefore also to the bias correction which was carried out). At some stations, the NRMSE results are better with the IBI-MFC reanalysis, but this is not the majority (GTSM-ERA5 presents better results at 9 stations out of 13).

GTSM-ERA5 is therefore the best reanalysis for the Atlantic stations.

Table 14. Correlation for mean and extreme conditions at Atlantic stations

Correlation	Mean Conditions		Extreme Conditions	
[no units]	IBI-MFC	GTSM-ERA5	IBI-MFC	GTSM-ERA5
ARCACHON_EYRAC	0.74	**0.94**	0.25	**0.68**
BAYONNE_BOUCAU	0.94	**0.99**	0.58	**0.74**
BREST	0.95	**0.99**	0.53	**0.85**
CONCARNEAU	0.96	**0.99**	0.74	**0.84**
ILE_D_AIX	0.98	**0.99**	0.67	**0.75**
LA_ROCHELLE_LA_PALLICE	0.98	**0.99**	0.69	**0.76**
LES_SABLES_D_OLONNE	0.97	**0.99**	0.78	**0.8**
LE_CONQUET	0.94	**0.99**	0.64	**0.85**
PORT-BLOC	0.89	**0.98**	0.41	**0.72**
PORT-TUDY	0.96	**0.99**	0.76	**0.83**
SAINT-GILDAS	0.98	**0.99**	0.78	**0.79**
SAINT-JEAN-DE-LUZ_SOCOA	0.96	**0.99**	0.68	**0.81**
SAINT-NAZAIRE	0.98	**0.99**	**0.8**	0.78

Table 15. NRMSE for mean and extreme conditions at Atlantic stations

NRMSE	Mean Conditions		Extreme Conditions	
[%]	IBI-MFC	GTSM-ERA5	IBI-MFC	GTSM-ERA5
ARCACHON_EYRAC	15.59	**7.29**	45.18	**15.37**
BAYONNE_BOUCAU	8.32	**5.25**	**20.1**	21.71
BREST	7.4	**3.42**	25.85	**22.98**
CONCARNEAU	6.04	**3.18**	**12.27**	13.47
ILE_D_AIX	5.16	**3.64**	27.85	**25.45**
LA_ROCHELLE_LA_PALLICE	4.03	**3.34**	14.82	**13.02**
LES_SABLES_D_OLONNE	6.12	**3.35**	**15.88**	16.3
LE_CONQUET	8.14	**3.36**	21.01	**16.2**
PORT-BLOC	10.67	**4.94**	23.41	**14.9**
PORT-TUDY	6.17	**3.27**	**12.23**	14.02
SAINT-GILDAS	3.92	**3.14**	13.14	**10.37**
SAINT-JEAN-DE-LUZ_SOCOA	6.41	**3.24**	17.43	**14.04**
SAINT-NAZAIRE	4.7	**2.88**	10.37	**9.29**

3 Comparisons for stations located in the Mediterranean Sea

The following figures (Figure 38 to Figure 44) show the comparisons between observations and reanalyses for the Mediterranean stations. Like in the English Channel and in on the Atlantic coast, we can see that the trends are generally rather well represented for the annual mean and for the annual max, and that there is more bias for the annual max, even if these annual maximums seem to be well correlated temporally.

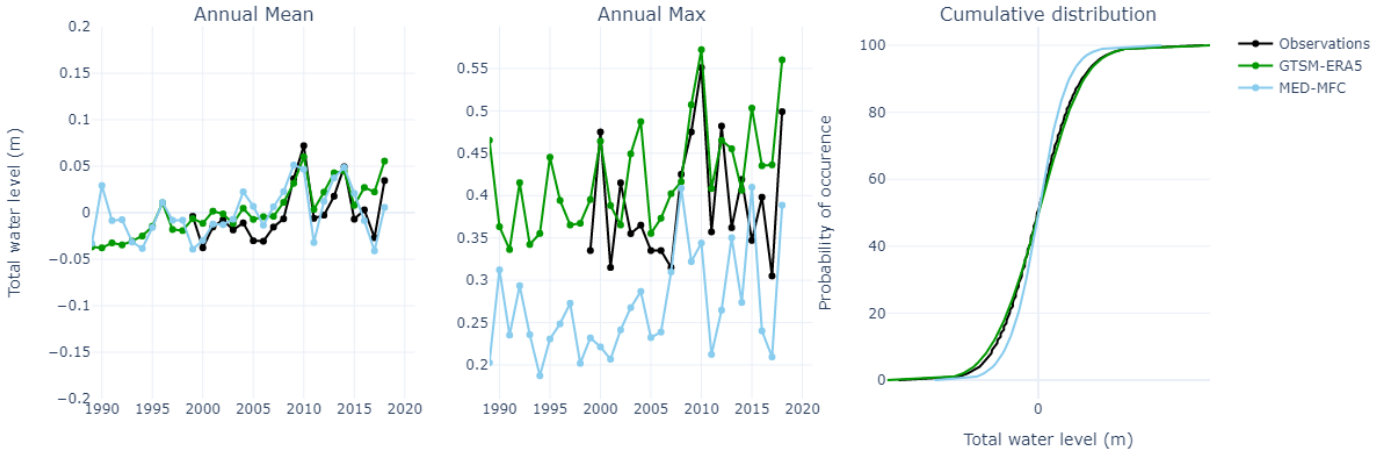

Figure 38. Comparisons between observations (black) and reanalyses: GTSM-ERA5 (green) and IBI-MFC (blue) at station 22 (Monaco)

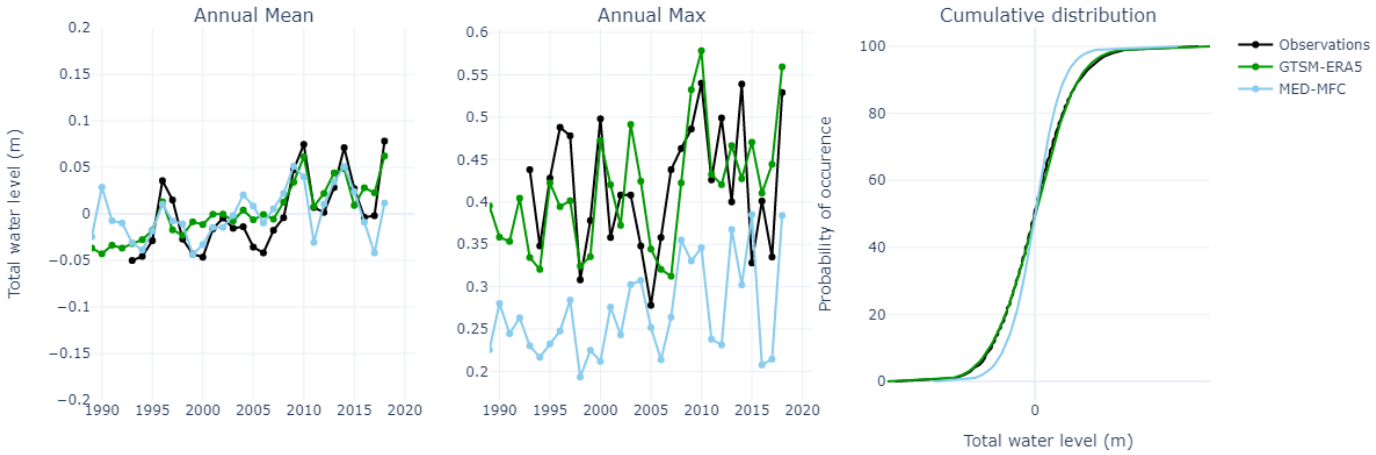

Figure 39. Comparisons between observations (black) and reanalyses: GTSM-ERA5 (green) and IBI-MFC (blue) at station 68 (Toulon)

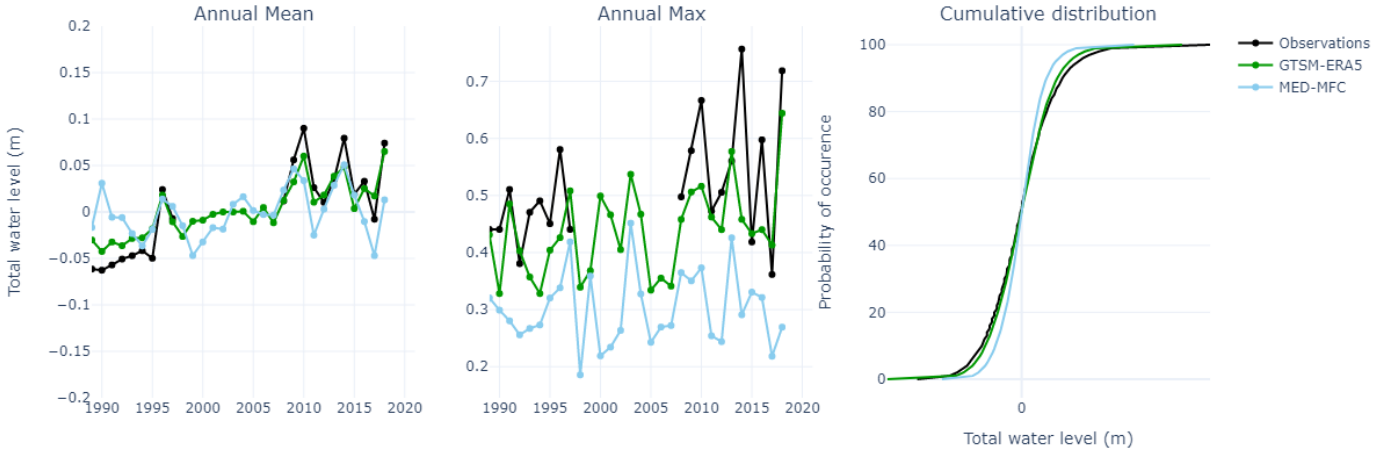

Figure 40. Comparisons between observations (black) and reanalyses: GTSM-ERA5 (green) and IBI-MFC (blue) at station 75 (Port-Vendres)

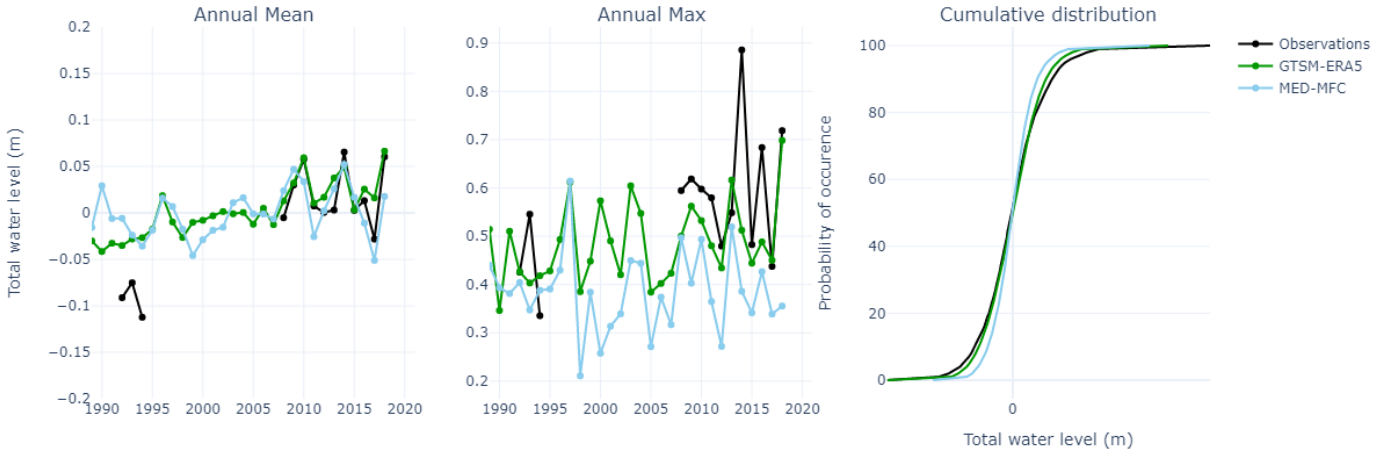

Figure 41. Comparisons between observations (black) and reanalyses: GTSM-ERA5 (green) and IBI-MFC (blue) at station 250 (Sète)

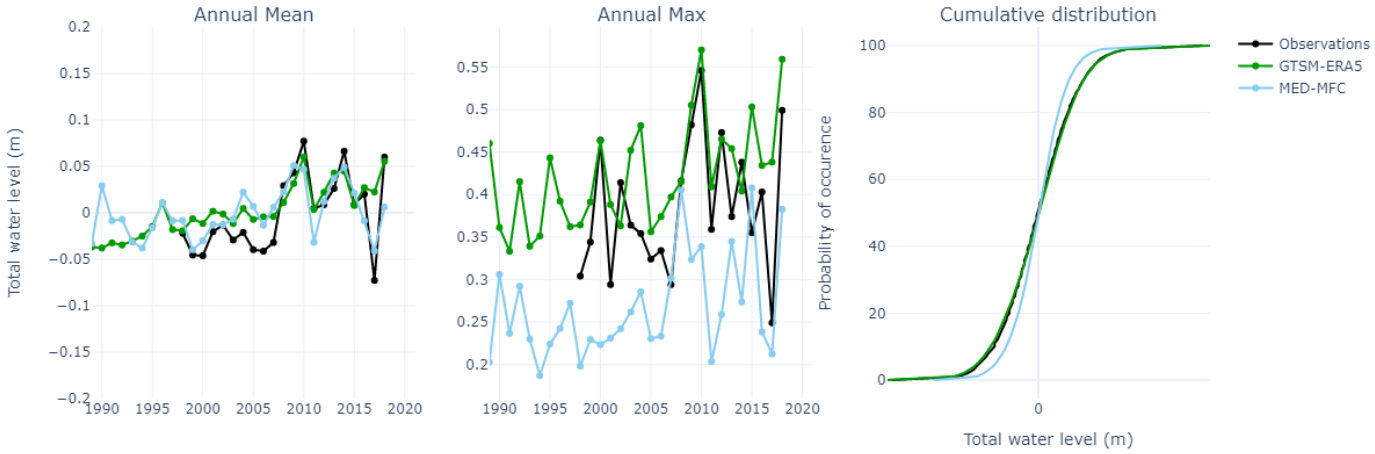

Figure 42. Comparisons between observations (black) and reanalyses: GTSM-ERA5 (green) and IBI-MFC (blue) at station 339 (Nice)

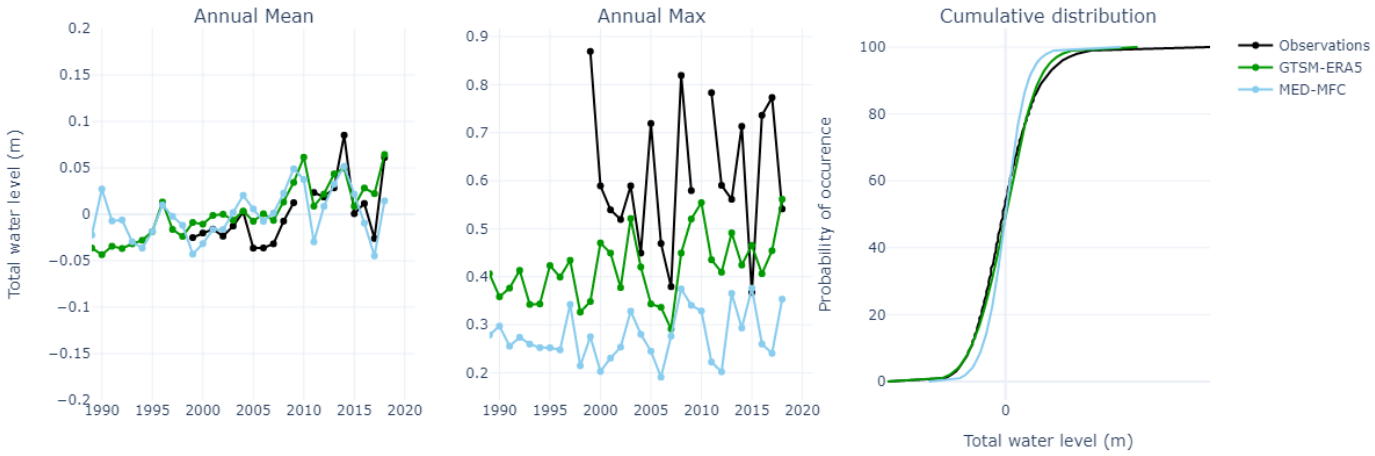

Figure 43. Comparisons between observations (black) and reanalyses: GTSM-ERA5 (green) and IBI-MFC (blue) at station 524 (Marseille)

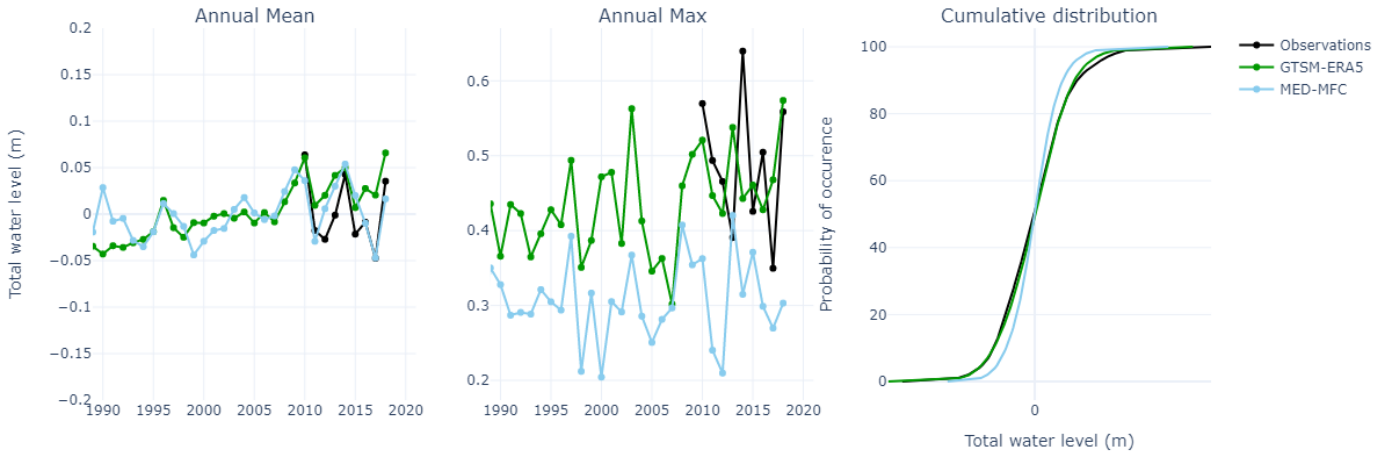

Figure 44. Comparisons between observations (black) and reanalyses: GTSM-ERA5 (green) and IBI-MFC (blue) at station 719 (Fos-sur-Mer)

In the following tables (Table 16 and Table 17), the scores are shown for both reanalyses at all the Mediterranean stations and for mean and extreme conditions. The best reanalysis is each time highlighted by bold writing. For both scores and all stations, the GTSM-ERA5 reanalysis shows better results, whether for mean conditions or for extreme conditions.

In detail:

- The correlation between GTSM-ERA5 and observations is very good for normal conditions with values greater than 0.76, and weaker for extreme conditions with values between 0.31 and 0.55 (results nevertheless better than for the IBI-MFC reanalysis). Note that the scores are lower than on the other seafronts because the concomitant time series (observations + reanalyses) are generally shorter.
- The NRMSE between GTSM-ERA5 and observations presents values from 2% to 7% for mean conditions and from 20% to 31% for extreme conditions. The difference in results between the mean conditions and the extreme conditions is notably due to the biases observed in the previous figures (and therefore also to the bias correction which was carried out). The results are worse in terms of NRMSE for IBI-MFC at all the stations.

GTSM-ERA5 is therefore the best reanalysis for the Mediterranean stations.

Table 16. Correlation for mean and extreme conditions at Mediterranean stations

Correlation	Mean Conditions		Extreme Conditions	
[no units]	MED-MFC	GTSM-ERA5	MED-MFC	GTSM-ERA5
FOS-SUR-MER	0.63	**0.78**	0.37	**0.42**
MARSEILLE	0.6	**0.76**	0.27	**0.31**
MONACO_FONTVIEILLE	0.55	**0.82**	0.35	**0.52**
NICE	0.56	**0.81**	0.34	**0.53**
PORT-VENDRES	0.64	**0.81**	0.45	**0.55**
SETE	0.7	**0.81**	0.53	**0.55**
TOULON	0.57	**0.78**	0.37	**0.53**

Table 17. NRMSE for mean and extreme conditions at Mediterranean stations

NRMSE	Mean Conditions		Extreme Conditions	
[%]	MED-MFC	GTSM-ERA5	MED-MFC	GTSM-ERA5
FOS-SUR-MER	10.74	**8.9**	40.2	**30.88**
MARSEILLE	9.19	**7.56**	34.17	**26.64**
MONACO_FONTVIEILLE	12.29	**8.99**	42.58	**22.75**
NICE	12.35	**9.28**	43.61	**23.73**
PORT-VENDRES	9.59	**7.41**	34.56	**22.53**
SETE	8.21	**6.87**	27.16	**20.52**
TOULON	12.23	**9.68**	45.98	**26.54**

4 Conclusion of water levels comparisons

The following table presents the numerical reanalyses which were retained for each French maritime seafront, in order to correct the water level climate models (see section VI).

Table 18. Best reanalyses for each French maritime seafront in terms of water levels

Maritime seafront	Best reanalysis
English Channel	**GTSM-ERA5**
Atlantic Ocean	**GTSM-ERA5**
Mediterranean Sea	**GTSM-ERA5**

IX. CORRECTIONS FOR TOTAL WATER LEVEL DATA

Like for the wave data in the first part of this report, the CDF-t method is used to downscale the climate models for water level. The CDFt is applied to the surges monthly in order to respect the seasonal cycles, and annually on the average level (no higher frequency variation of this level available in the datasets). This correction is not applied to the component linked to the tide as explained previously in this report.

In Figure 45, we see from top to bottom, the annual mean, the cumulative density function and the seasonal cycle, before the CDFt (left) and after the CDFt (right). We see that the cumulative density function was already well represented by climate models before the CDFt, in particular because the water level signal is largely dominated by the tidal component, and that this distribution is preserved after the CDFt. We also see that the CDFt acts on the seasonal cycles of climate models which correspond after the CDFt to that of the reanalysis. The next step, which will be the subject of a future 2C NOW report, will be to perform the CDF-t at the locations of offshore wind farms projects and analyse the future water level evolution in the projections until 2100.

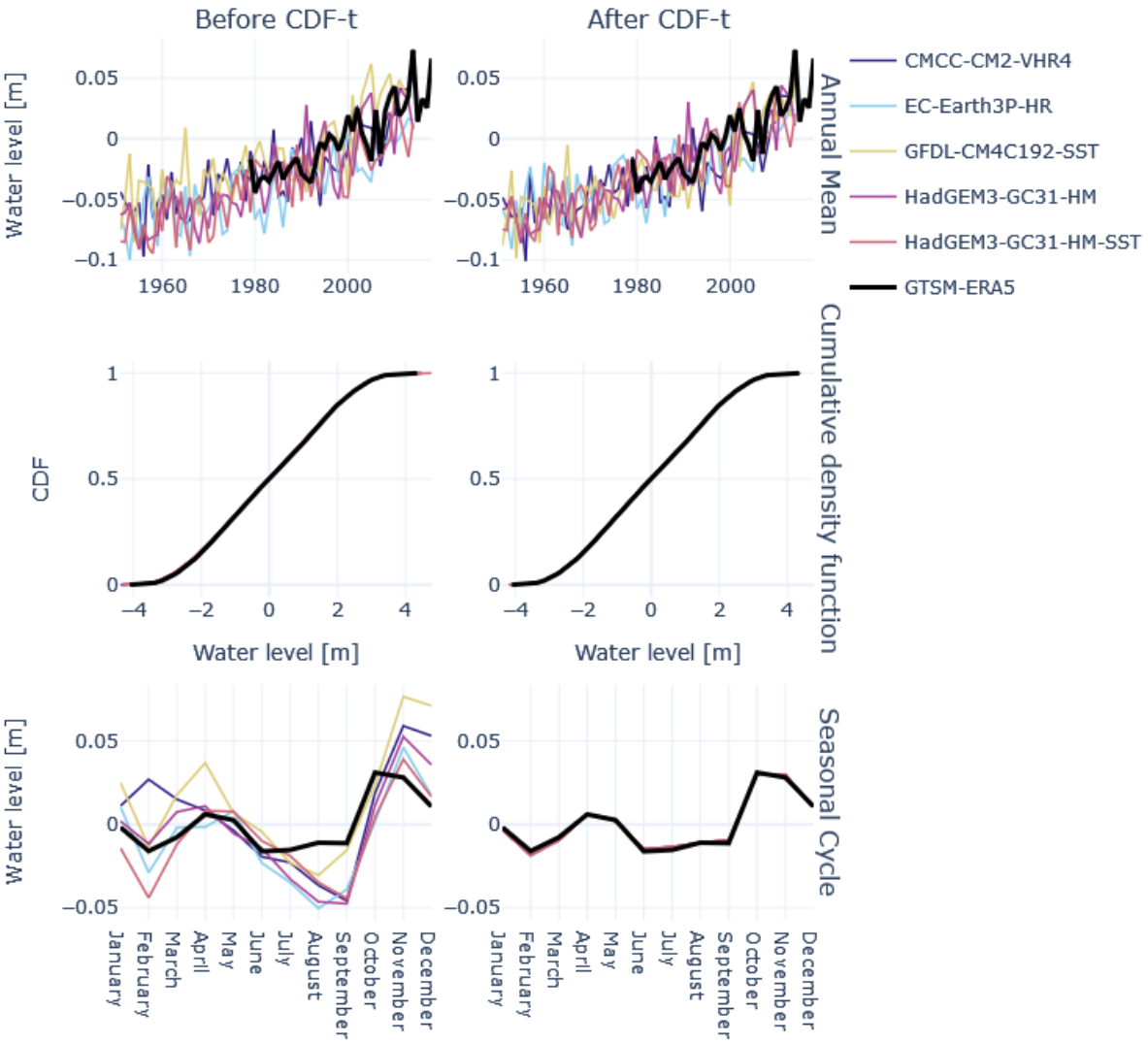

Figure 45. Representation of the best reanalysis GTSM-ERA5 (bold black) at station 3 (in Brest) and the climatic models for the historical period, before the CDF-t is applied (left panel) and after the CDF-t is applied (right panel)

X. CONCLUSION

To assess future changes in wave conditions and water levels at offshore wind farm sites, this report proposes a methodology to correct climate model projections using observational data and reanalyses. Since direct observations are not available at the offshore wind farm locations, a reanalysis or hindcast dataset with broader spatial coverage is required.

As a first step, comparisons between available observations and reanalysis datasets were conducted to identify the most suitable products for wave and water level variables along each French coastline. For wave data, the HYWAT reanalysis was selected for the English Channel and Atlantic coasts, while the MED-WAV reanalysis was chosen for the Mediterranean Sea. For water levels, the GTSM-ERA5 hindcast was selected for all three coastal regions (Table 19).

Table 19. Summary of best reanalyses for each seafront

Seafront	Waves	Water Levels
English Channel	HYWAT	GTSM-ERA5
Atlantic Ocean		
Mediterranean Sea	MED-WAV	

Using these selected reanalyses, the climate model outputs were bias-corrected at each offshore location of interest using the CDF-t method. This correction was applied to both historical and future projection periods. The results of the CDF-t correction are presented in this report.

XI. REFERENCES

Accensi, M., Alday, F., & Maisondieu, C. (2022). RESOURCECODE - Resource Characterization to Reduce the Cost of Energy through Coordinated Data Enterprise. Database user manual. Ref. WP3| Database development. ResourceCode Marine Data Toolbox. https://doi.org/10.13155/86306.

Alday, M., Accensi, M., Ardhuin, F., Dodet, G. (2021). A global wave parameter database for geophysical applications. Part 3: Improved forcing and spectral resolution. Ocean Modelling (1463-5003) (Elsevier BV), 2021-10, Vol. 166, P. 101848 (19p.). https://doi.org/10.1016/j.ocemod.2021.101848

Ardhuin, F., Rogers, E., Babanin, A. V., Filipot, J.-F., Magne, R., Rolan, A., van der Westhuysen, A., Queffeulou, P., Lefevre, J.-M., Aouf, L., Collard, F. (2010). Semiempirical Dissipation Source Functions for Ocean Waves. Part I: Definition, Calibration, and Validation. Journal of Physical Oceanography, 2010, 40 (9), pp.1917-1941. ⟨10.1175/2010JPO4324.1⟩. ⟨hal-04498822⟩

Bartók, B., Tobin, I., Vautard, R., Vrac, M., Jin, X., Levavasseur, G., Denvil, S., Dubus, L., Parey, S., Michelangeli, P.-A., Troccoli, A., Saint-Drenan, Y. M. (2019). A climate projection dataset tailored for the European energy sector. Climate services, 16, 100138. https://doi.org/10.1016/j.cliser.2019.100138.

Bentamy, A., & Croize-Fillon, D. (2014). Spatial and temporal characteristics of wind and wind power off the coasts of Brittany. Renewable Energy, 66, 670-679. http://dx.doi.org/10.1016/j.renene.2014.01.012.

Dullaart, J. C., Muis, S., Bloemendaal, N., & Aerts, J. C. (2020). Advancing global storm surge modelling using the new ERA5 climate reanalysis. *Climate Dynamics*, *54*, 1007-1021. https://doi.org/10.1007/s00382-019-05044-0.

Eyring, V., N.P. Gillett, K.M. Achuta Rao, R. Barimalala, M. Barreiro Parrillo, N. Bellouin, C. Cassou, P.J. Durack, Y. Kosaka, S. McGregor, S. Min, O. Morgenstern, and Y. Sun. (202). Human Influence on the Climate System. In Climate Change 2021: The Physical Science Basis. Contribution of Working Group I to the Sixth Assessment Report of the Intergovernmental Panel on Climate Change [Masson-Delmotte, V., P. Zhai, A. Pirani, S.L. Connors, C. Péan, S. Berger, N. Caud, Y. Chen, L. Goldfarb, M.I. Gomis, M. Huang, K. Leitzell, E. Lonnoy, J.B.R. Matthews, T.K. Maycock, T. Waterfield, O. Yelekçi, R. Yu, and B. Zhou (eds.)]. Cambridge University Press, Cambridge, United Kingdom and New York, NY, USA, pp. 423–552, https://doi.org/10.1017/9781009157896.005.

Faidherbe, T., Lopez, G., Leballeur, L., Michaud, H., Pezerat, M. (2024). 20 ans de rejeux d'états de mer à haute résolution sur les côtes méditerranéennes françaises. XVIII èmes journées nationales génie côtier – génie civil, Anglet. doi :105150/jngcgc.2024.005.

Fernández, L., Calvino, C., & Dias, F. (2021). Sensitivity analysis of wind input parametrizations in the WAVEWATCH III spectral wave model using the ST6 source term package for Ireland. *Applied Ocean Research*, *115*, 102826. https://doi.org/10.1016/j.apor.2021.102826.

Jourdan D., Paradis P., Pasquet A., Michaud H., Baraille R., Biscara L., Dalphinet A., Ohl P. (2020). La phase-3 du projet HOMONIM : définition et contenu. Actes des XVIèmes Journées Nationales Génie Côtier-Génie, (pp 779-788) - doi:10.5150/jngcgc.2020.087.

Kokic, P., Jin, H., & Crimp, S. (2013). Improved point scale climate projections using a block bootstrap simulation and quantile matching method. *Climate dynamics*, *41*, 853-866. https://doi.org/10.1007/s00382-013-1791-z.

Korres, G., Ravdas, M., Denaxa, D., & Sotiropoulou, M. (2021). Mediterranean Sea Waves Reanalysis INTERIM (CMEMS Med-Waves, MedWAM3I system) (Version 1) [Data set]. Copernicus Monitoring Environment Marine Service (CMEMS). https://doi.org/10.25423/CMCC/MEDSEA_MULTIYEAR_WAV_006_012_MEDWAM3I

Laugel, A., Menendez, M., Benoit, M., Mattarolo, G., & Méndez, F. (2014). Wave climate projections along the French coastline: dynamical versus statistical downscaling methods. Ocean Modelling, 84, 35-50. https://doi.org/10.1016/j.ocemod.2014.09.002.

Leckler, F., Ardhuin, F., Filipot, J.-F., Mironov, A. (2013). Dissipation source terms and whitecap statistics, Ocean Modelling, 2013, https://doi.org/10.1016/j.ocemod.2013.03.007

Lyard, F. H., Allain, D. J., Cancet, M., Carrère, L., & Picot, N. (2021). FES2014 global ocean tide atlas: design and performance. *Ocean Science*, *17*(3), 615-649. https://doi.org/10.5194/os-17-615-2021.

Meucci, A., Young, I. R., Trenham, C., & Hemer, M. (2024). An 8-model ensemble of CMIP6-derived ocean surface wave climate. Scientific Data, 11(1), 100. https://doi.org/10.1038/s41597-024-02932-x.

Michaud, H., Pasquet, A., Baraille, R., Leckler, F., Aouf, L., Dalphinet, A., ... & Filipot, J. F. (2015). Implementation of the new French operational coastal wave forecasting system and application to a wave-current interaction study. In 14th International Workshop on Wave Hindcasting and Forecasting and 5th Coastal Hazard Symposium.

Michelangeli, P. A., Vrac, M., & Loukos, H. (2009). Probabilistic downscaling approaches: Application to wind cumulative distribution functions. Geophysical Research Letters, 36(11). doi:10.1029/2009GL038401.

Muis, S., Apecechea, M. I., Dullaart, J., de Lima Rego, J., Madsen, K. S., Su, J., Yan, K., Verlaan, M. (2020). A high-resolution global dataset of extreme sea levels, tides, and storm surges, including future projections. *Frontiers in Marine Science*, *7*, 263. https://doi.org/10.3389/fmars.2020.00263.

Poppeschi, C., Patra, A., Kervella, Y., Pimoult M., Dubus L. (2024) State of the Art of Climate Change Impact on Offshore Wind. 71 p.

Taylor, K. E. (2001). Summarizing multiple aspects of model performance in a single diagram. Journal of geophysical research: atmospheres, 106(D7), 7183-7192. https://doi.org/10.1029/2000JD900719.

XII. APPENDICES

1 Appendix 1: Datapoint selection maps

Legend: Observations (black square), reanalysis MEDUG (green circle), reanalysis HYWAT (blue circle) and reanalysis RSCD (red star).

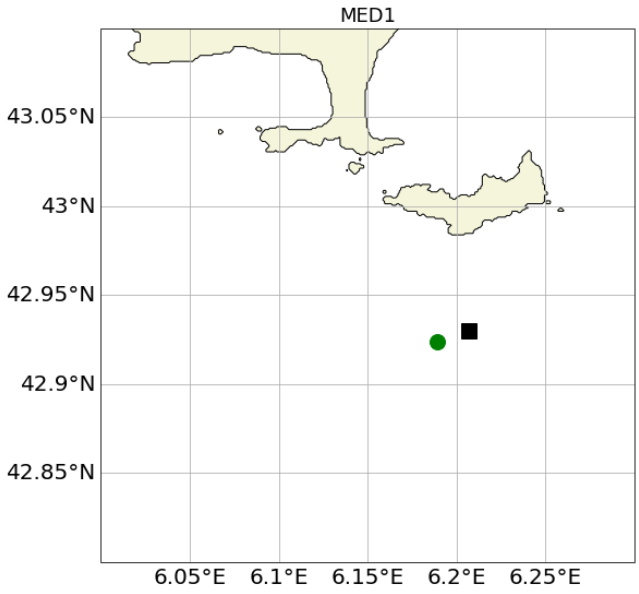

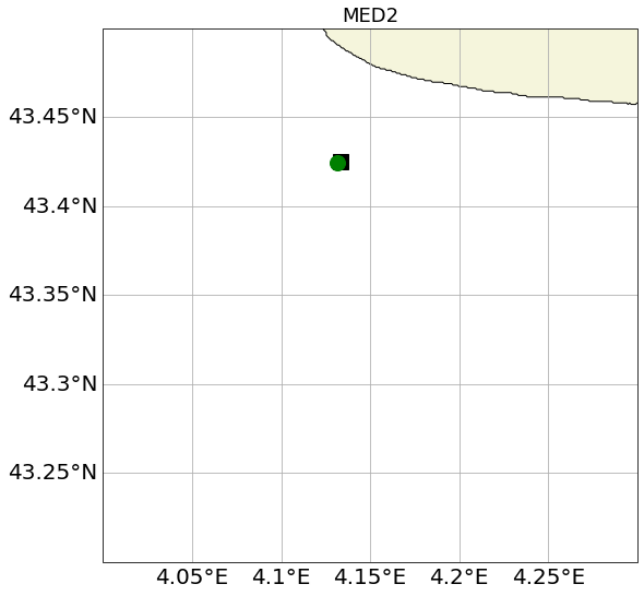

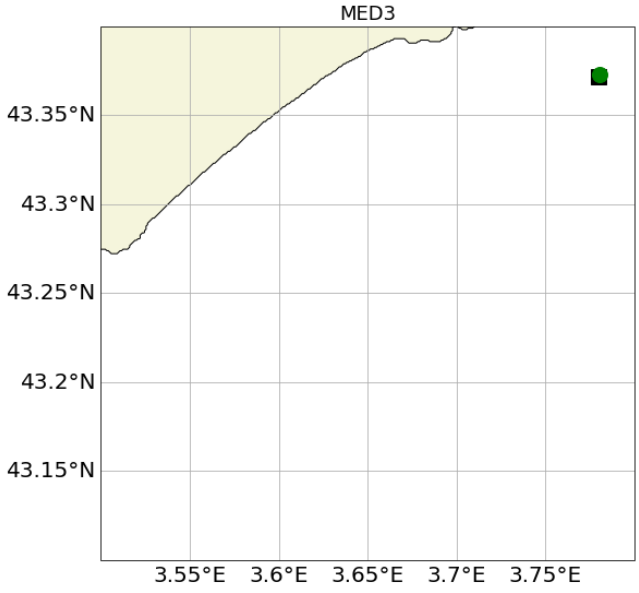

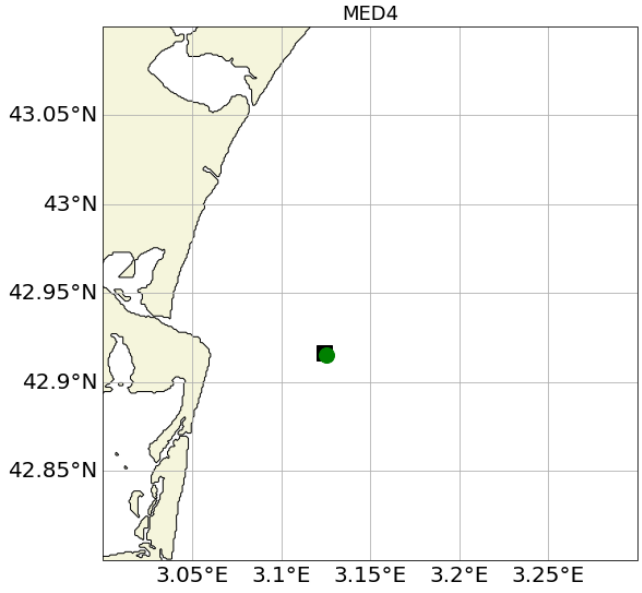

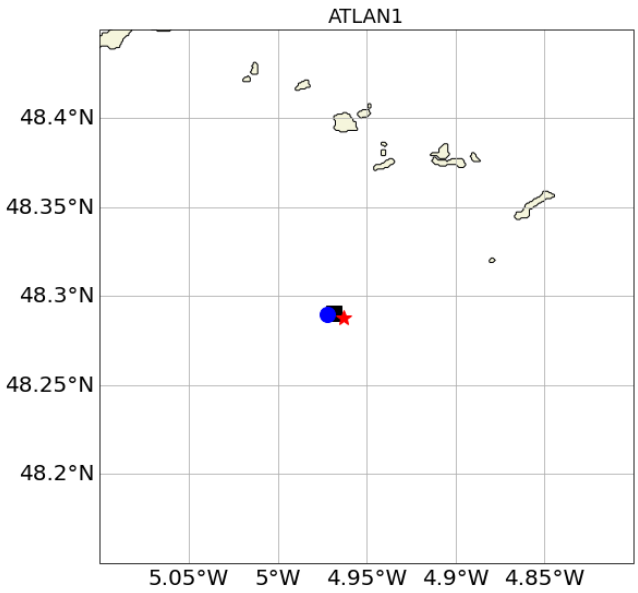
ATLAN1
48.4°N
48.35°N
48.3°N
48.25°N
48.2°N
5.05°W
5°W
4.95°W
4.9°W
4.85°W

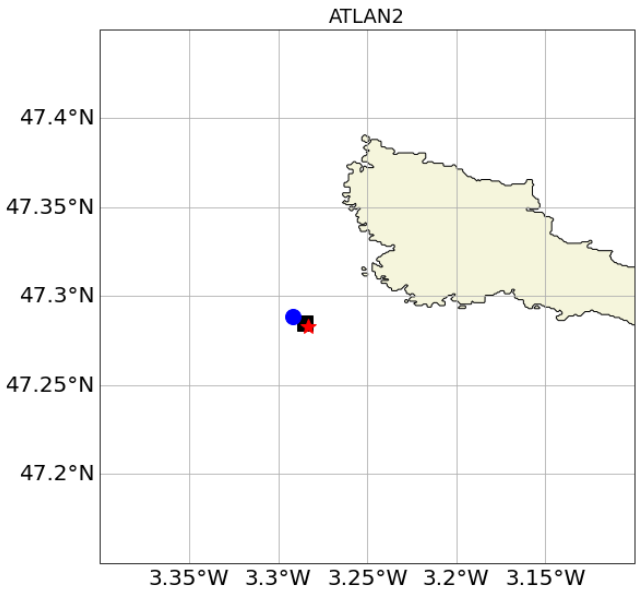
ATLAN2
47.4°N
47.35°N
47.3°N
47.25°N
47.2°N
3.35°W
3.3°W
3.25°W
3.2°W
3.15°W

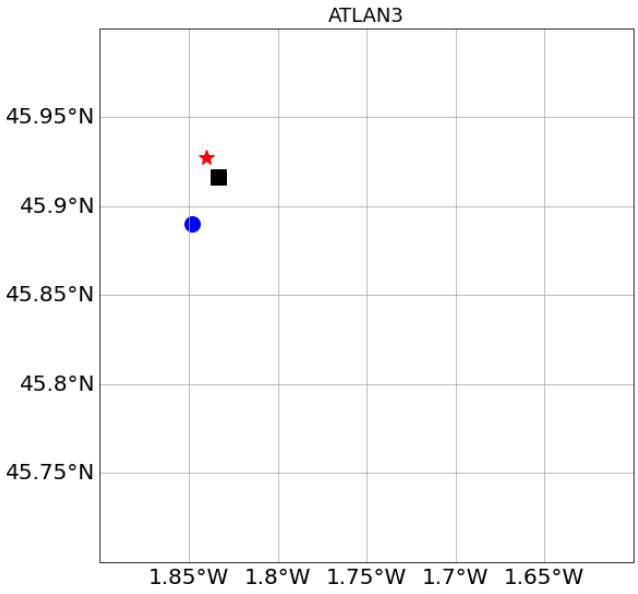
ATLAN3
45.95°N
45.9°N
45.85°N
45.8°N
45.75°N
1.85°W
1.8°W
1.75°W
1.7°W
1.65°W

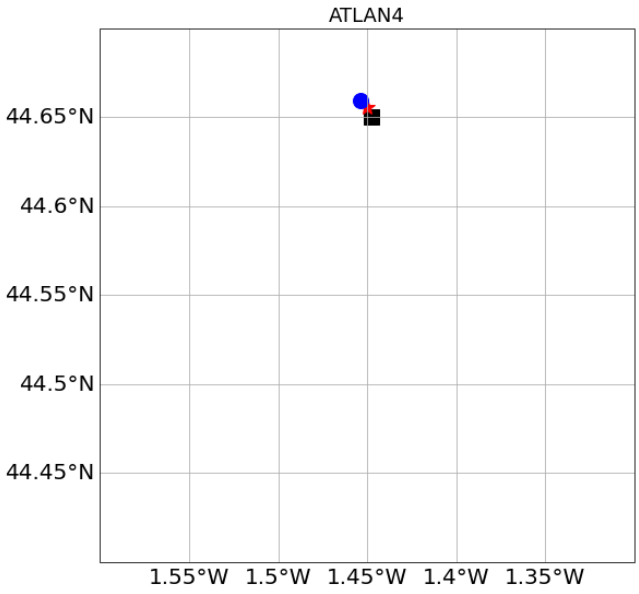
ATLAN4
44.65°N
44.6°N
44.55°N
44.5°N
44.45°N
1.55°W
1.5°W
1.45°W
1.4°W
1.35°W

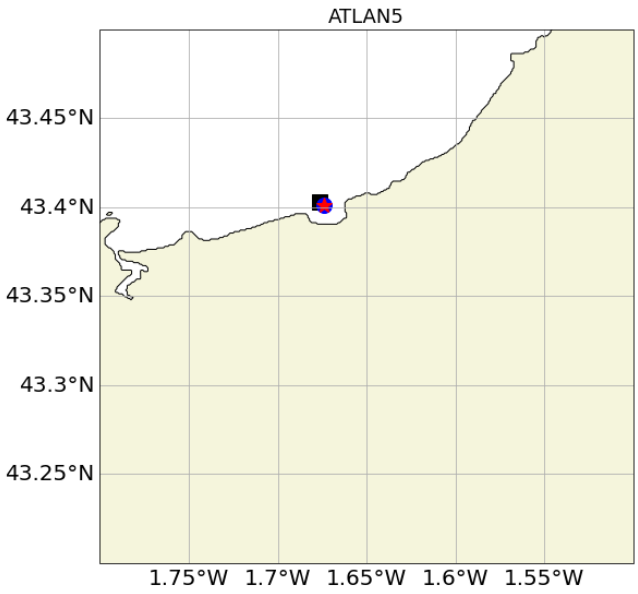
ATLAN5
43.45°N
43.4°N
43.35°N
43.3°N
43.25°N
1.75°W
1.7°W
1.65°W
1.6°W
1.55°W

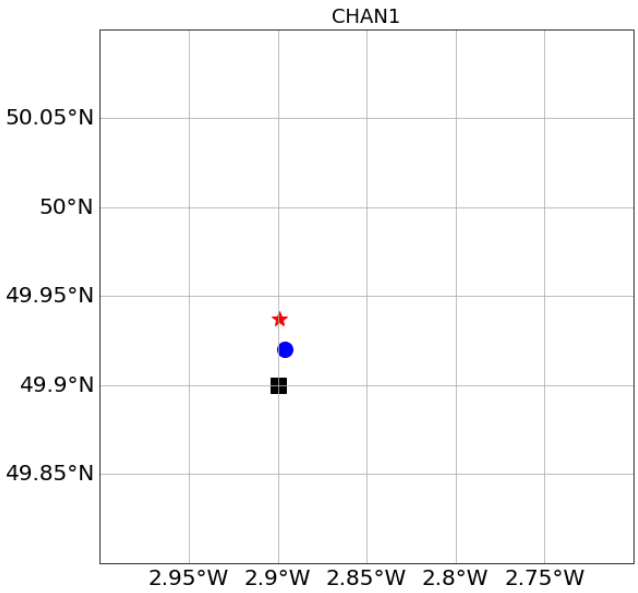
CHAN1
50.05°N
50°N
49.95°N
49.9°N
49.85°N
2.95°W
2.9°W
2.85°W
2.8°W
2.75°W

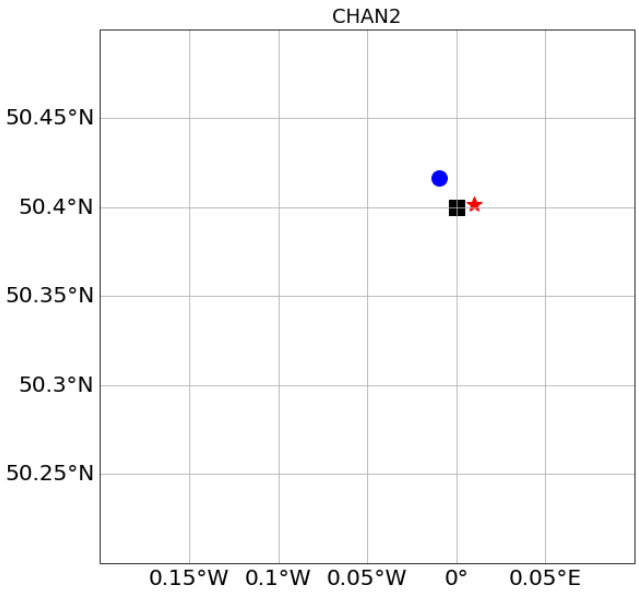
CHAN2
50.45°N
50.4°N
50.35°N
50.3°N
50.25°N
0.15°W
0.1°W
0.05°W
0°
0.05°E

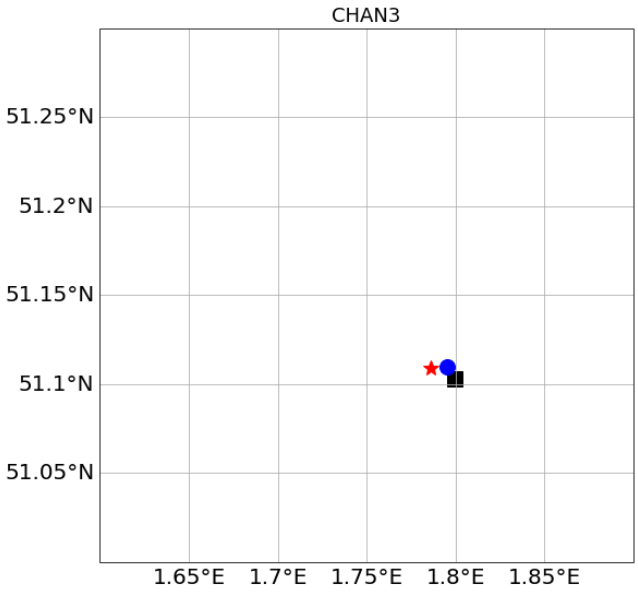
CHAN3
51.25°N
51.2°N
51.15°N
51.1°N
51.05°N
1.65°E
1.7°E
1.75°E
1.8°E
1.85°E

2 Appendix 2: Scatter plots

2.1 Waves

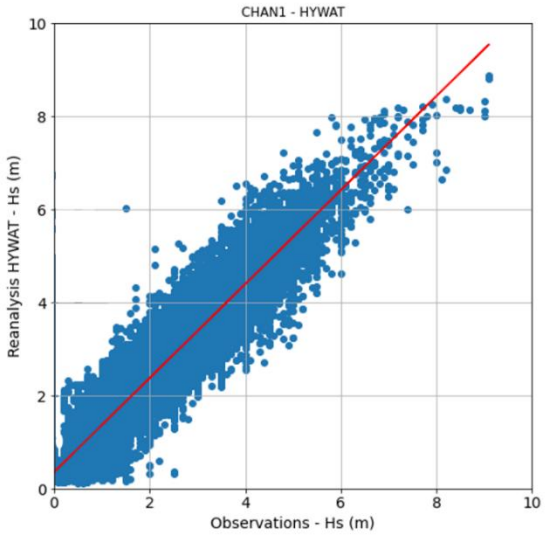

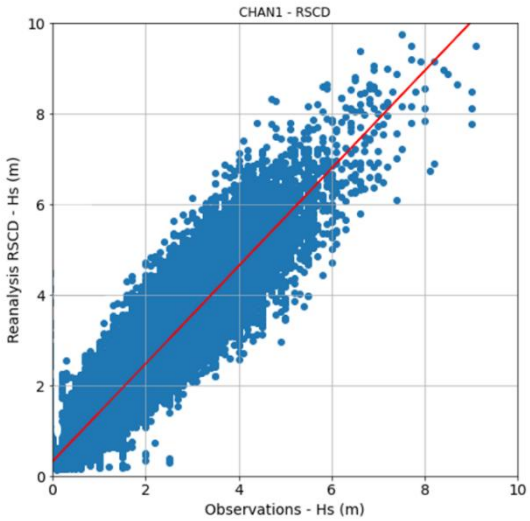

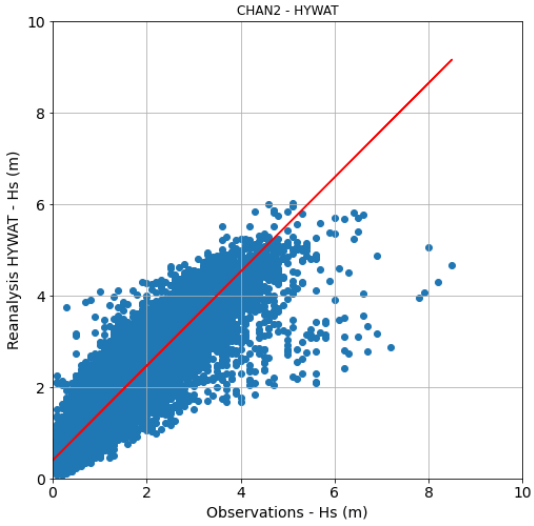

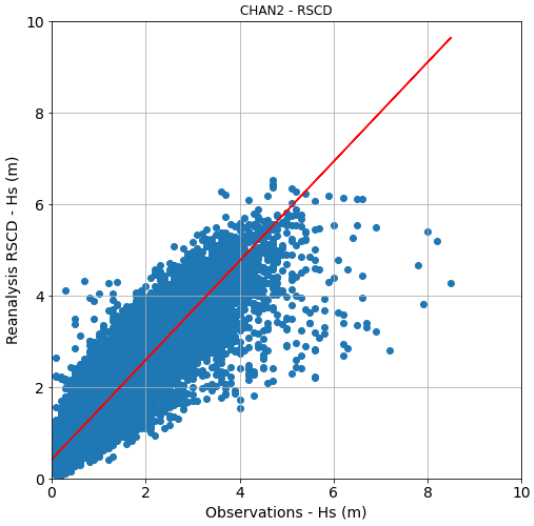

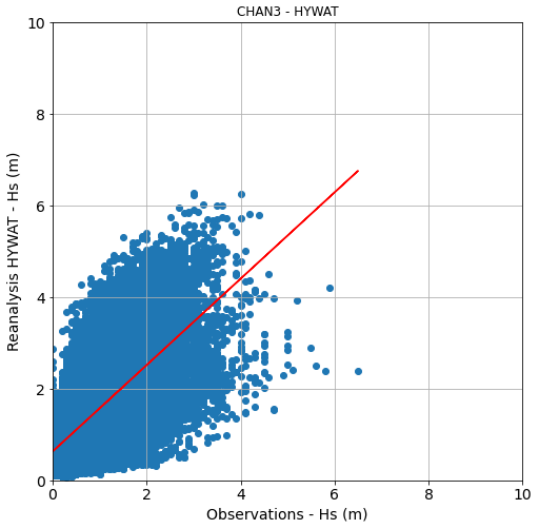

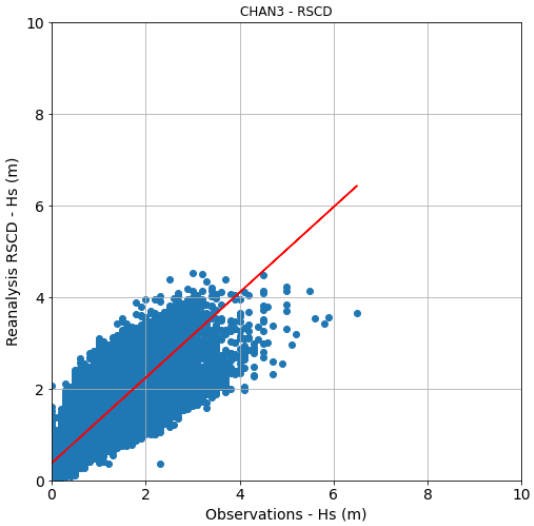

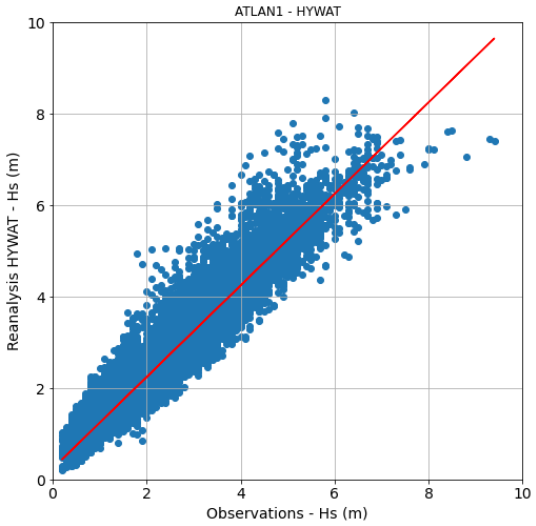
ATLAN1 - HYWAT
Reanalysis HYWAT - Hs (m)
Observations - Hs (m)

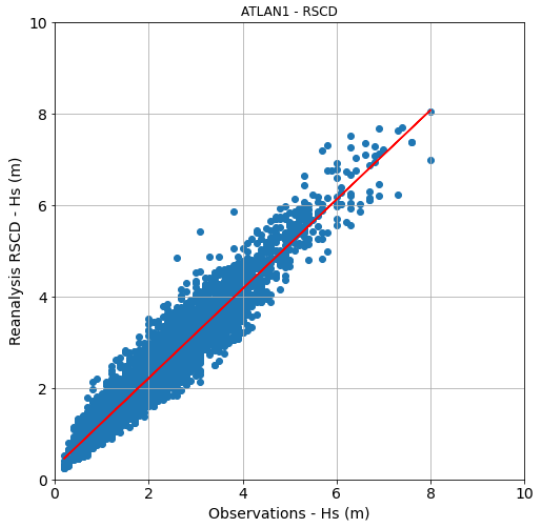
ATLAN1 - RSCD
Reanalysis RSCD - Hs (m)
Observations - Hs (m)

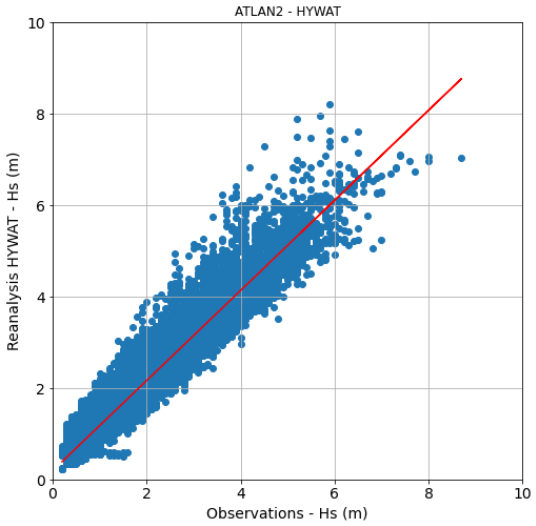
ATLAN2 - HYWAT
Reanalysis HYWAT - Hs (m)
Observations - Hs (m)

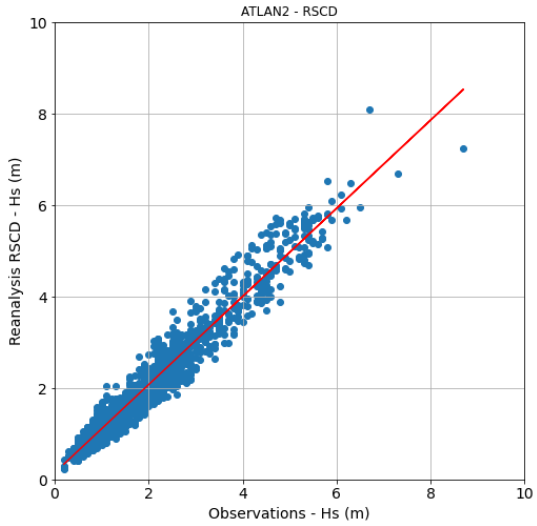
ATLAN2 - RSCD
Reanalysis RSCD - Hs (m)
Observations - Hs (m)

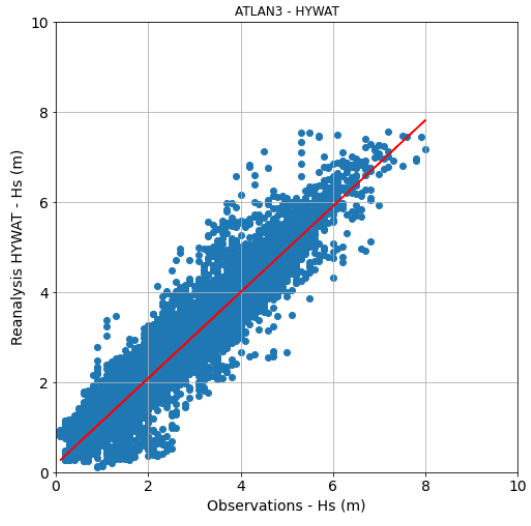
ATLAN3 - HYWAT
Reanalysis HYWAT - Hs (m)
Observations - Hs (m)

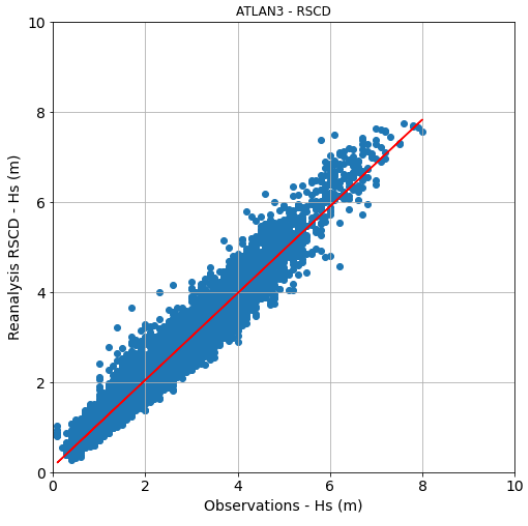
ATLAN3 - RSCD
Reanalysis RSCD - Hs (m)
Observations - Hs (m)

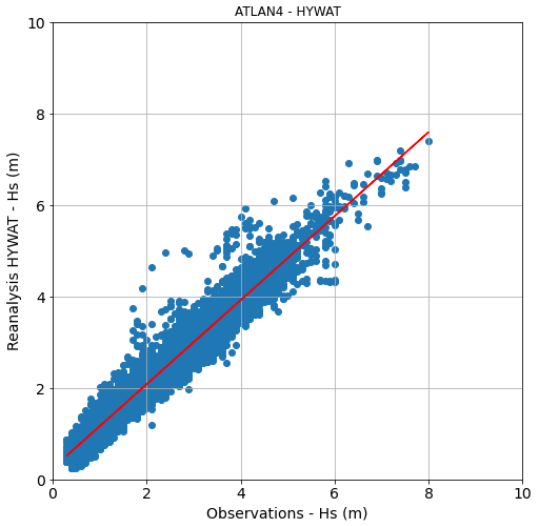
ATLAN4 - HYWAT
Reanalysis HYWAT - Hs (m)
Observations - Hs (m)
0
2
4
6
8
10

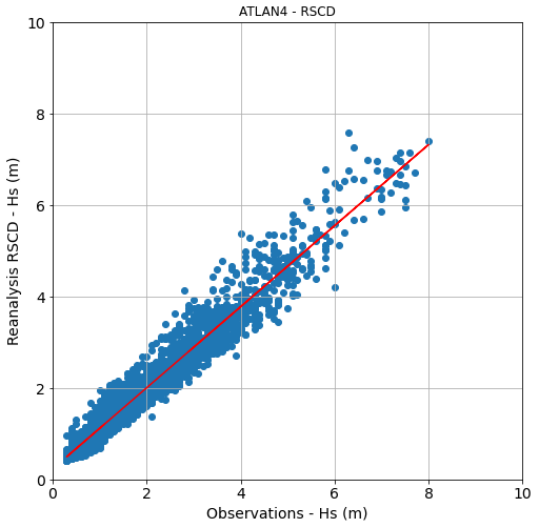
ATLAN4 - RSCD
Reanalysis RSCD - Hs (m)
Observations - Hs (m)
0
2
4
6
8
10

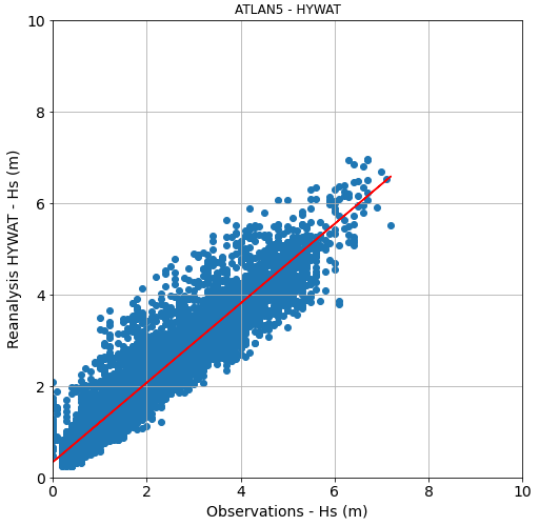
ATLAN5 - HYWAT
Reanalysis HYWAT - Hs (m)
Observations - Hs (m)
0
2
4
6
8
10

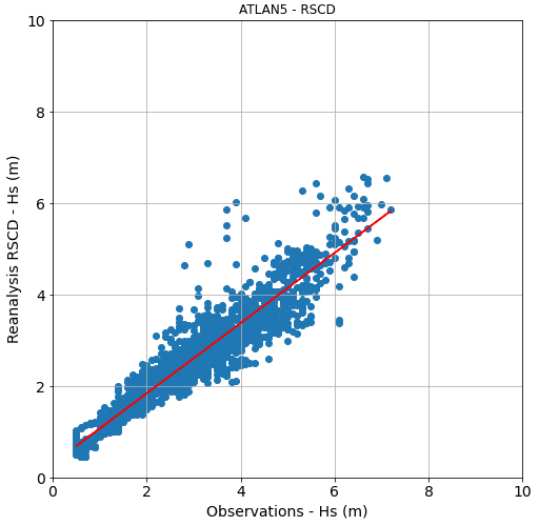
ATLAN5 - RSCD
Reanalysis RSCD - Hs (m)
Observations - Hs (m)
0
2
4
6
8
10

MED1 - n

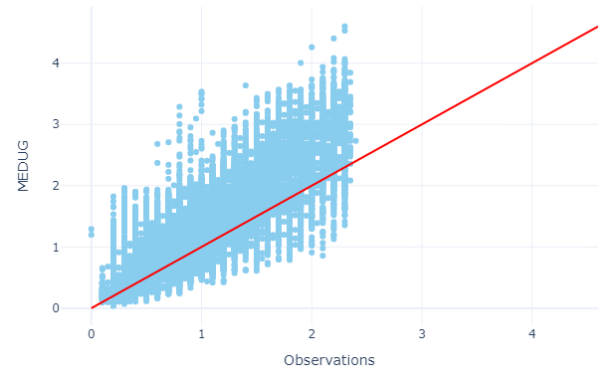

MED1 - n

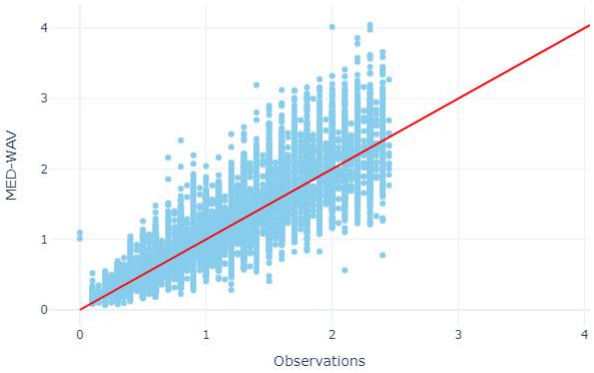

MED2 - n

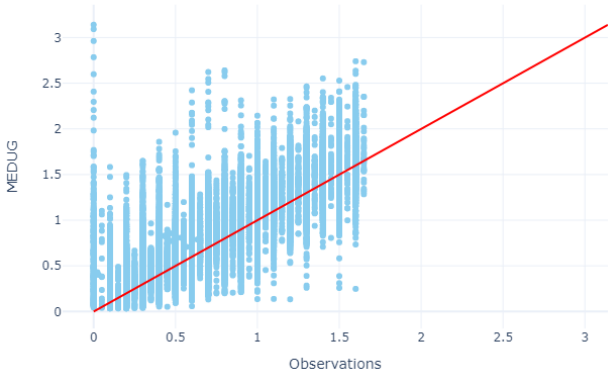

MED2 - n

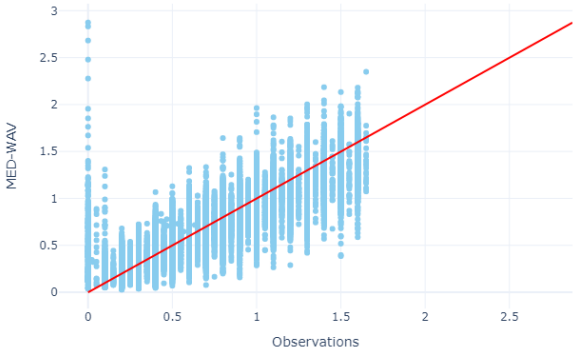

MED3 - n

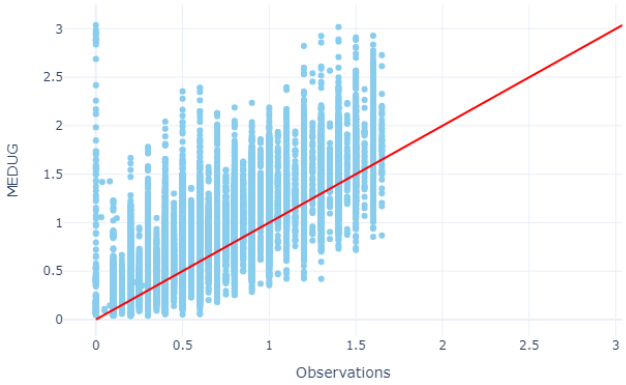

MED3 - n

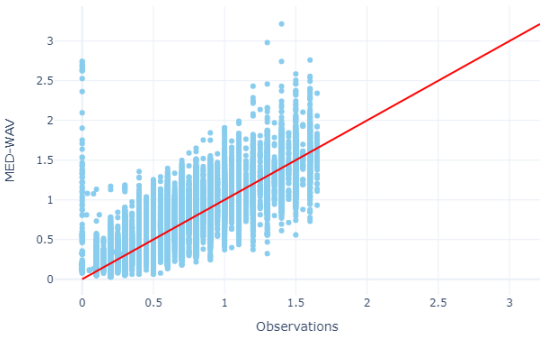

MED4 - n

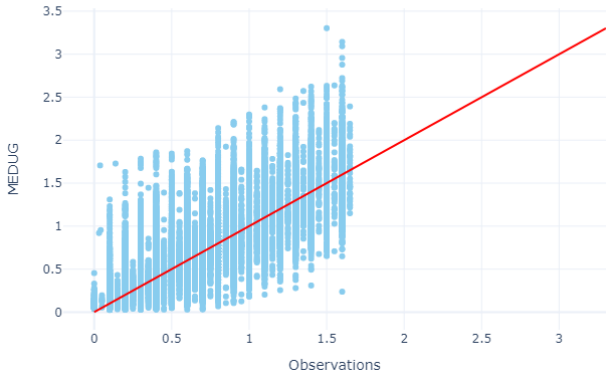

MED4 - n

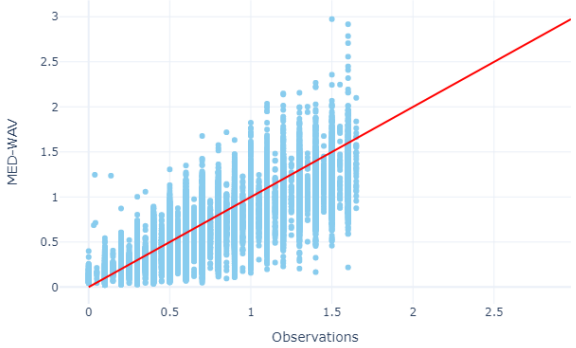

2.2 Water Levels

BOULOGNE-SUR-MER - n

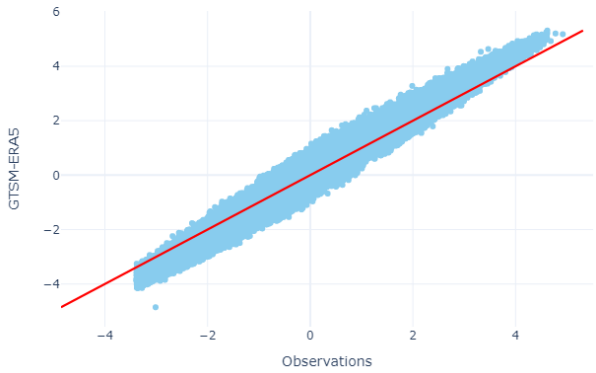

BOULOGNE-SUR-MER - n

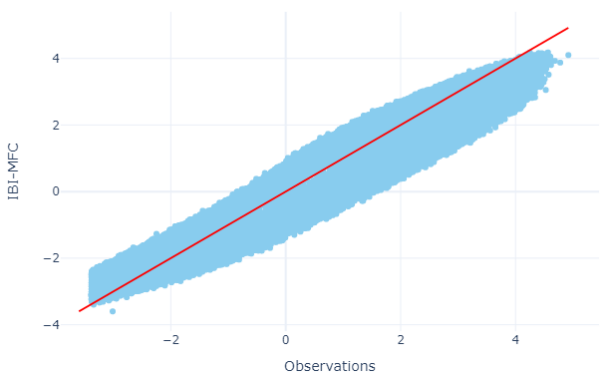

CALAIS - n

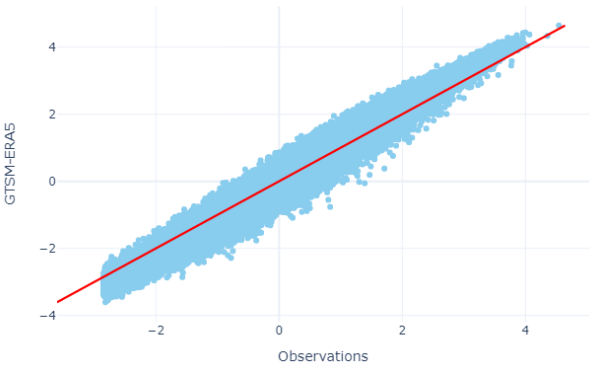

CALAIS - n

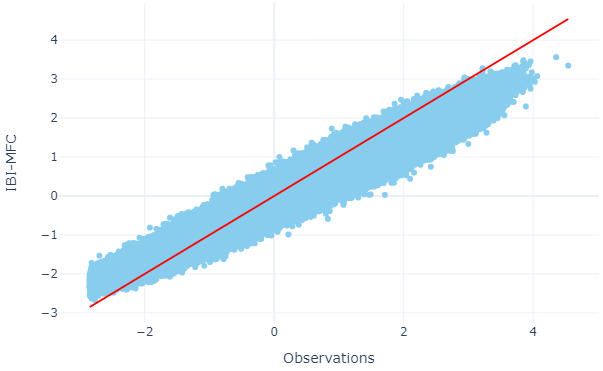

CHERBOURG - n

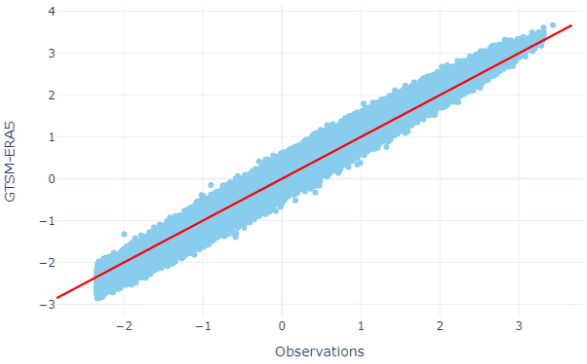

CHERBOURG - n

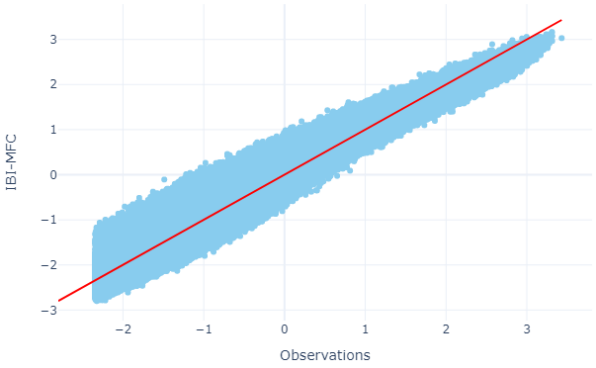

DIEPPE - n

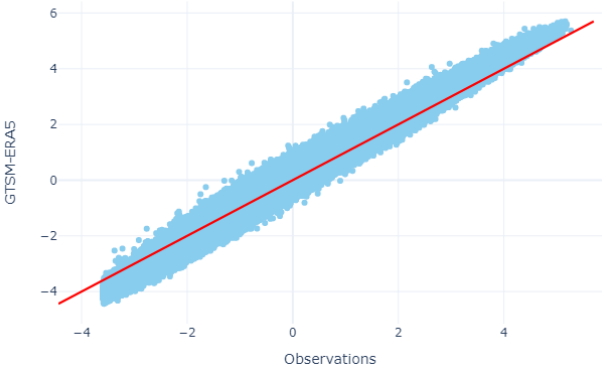

DIEPPE - n

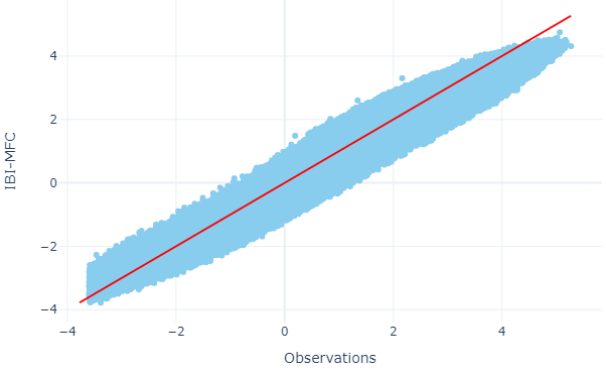

DUNKERQUE - n

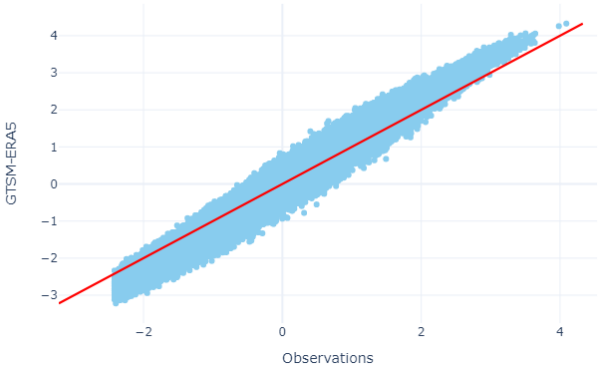

DUNKERQUE - n

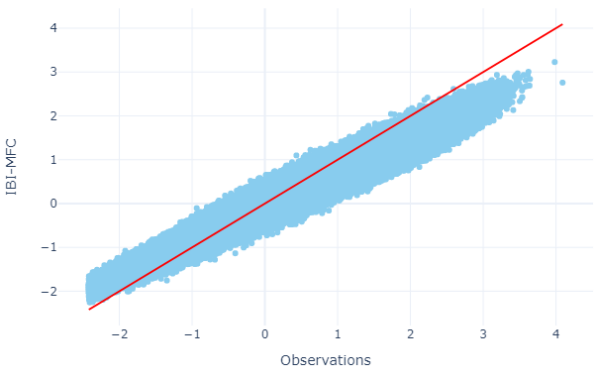

LE_HAVRE - n

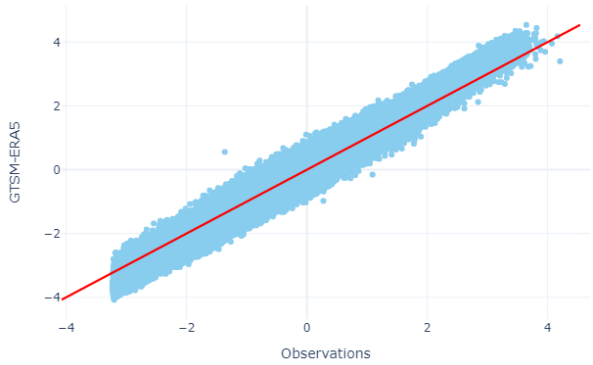

LE_HAVRE - n

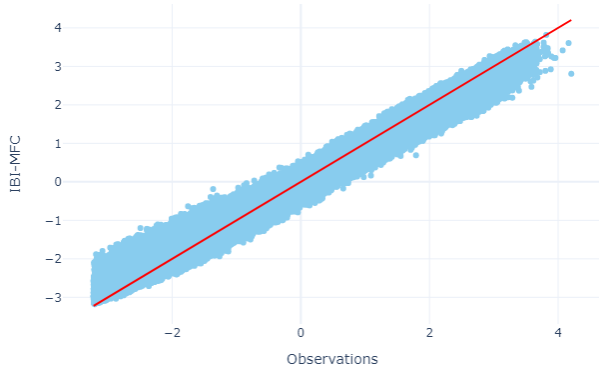

ROSCOFF - n

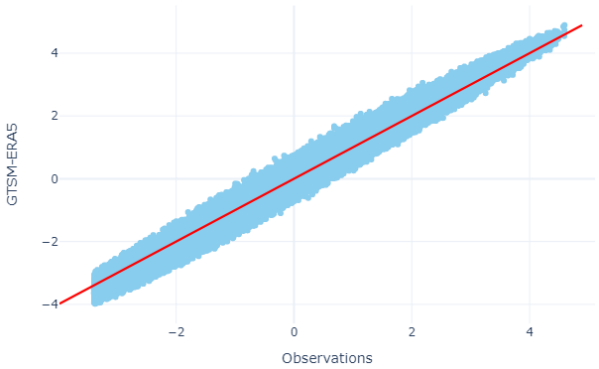

ROSCOFF - n

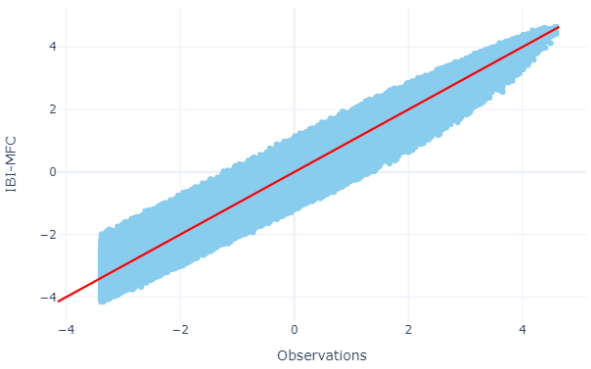

SAINT-MALO - n

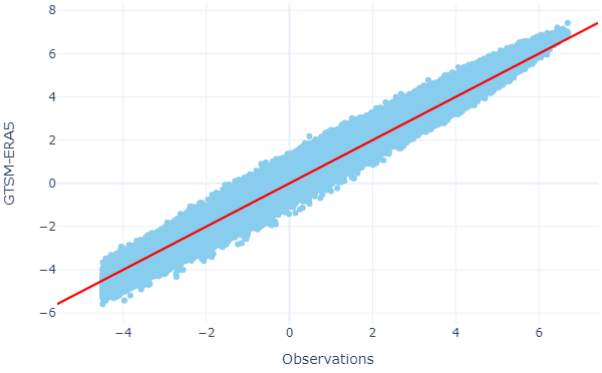

SAINT-MALO - n

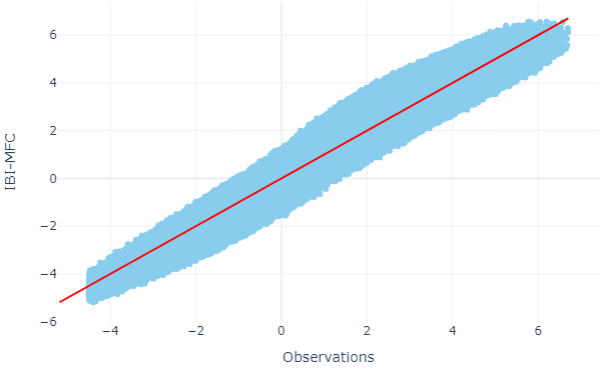

ARCACHON_EYRAC - n

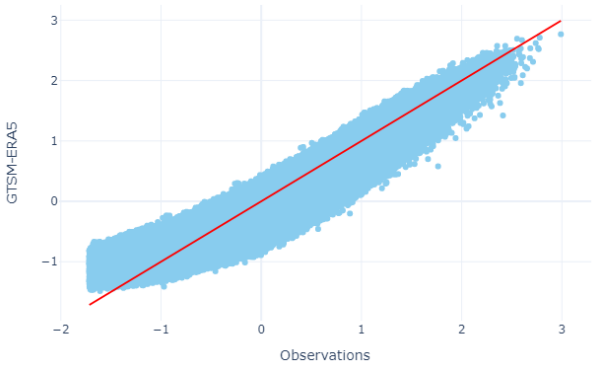

ARCACHON_EYRAC - n

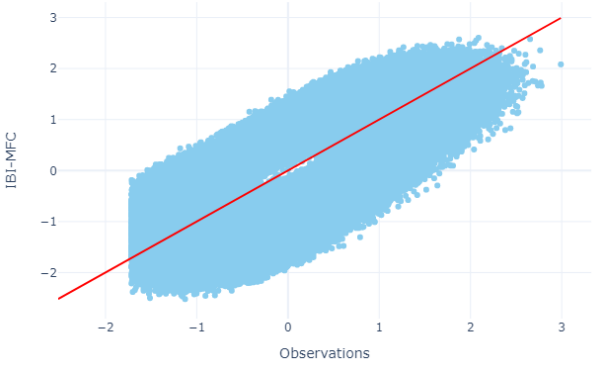

BAYONNE_BOUCAU - n

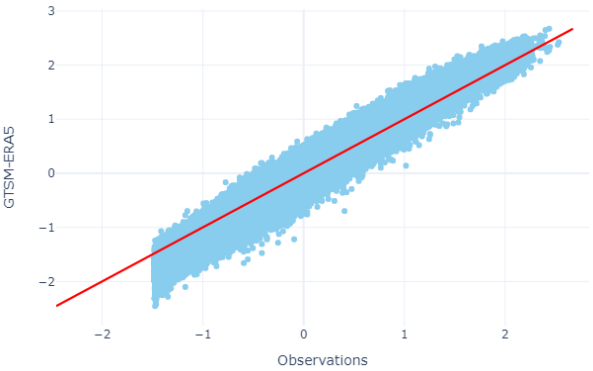

BAYONNE_BOUCAU - n

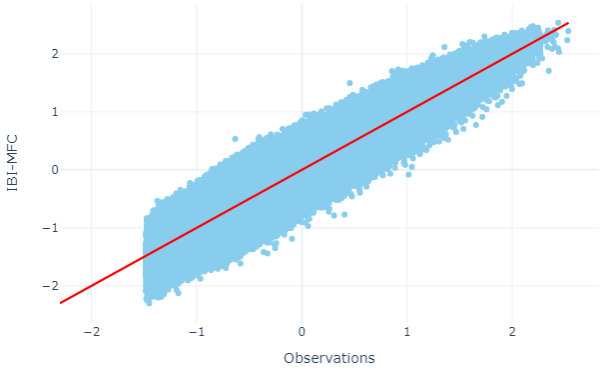

BREST - n

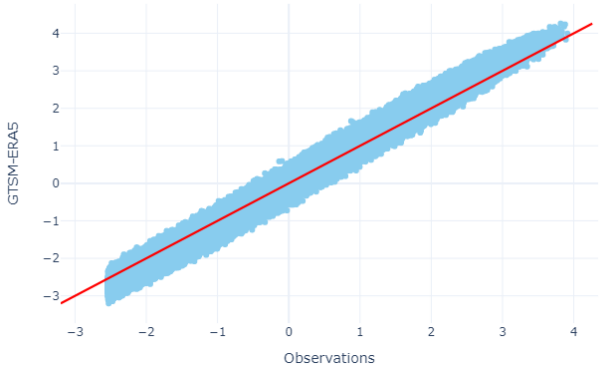

BREST - n

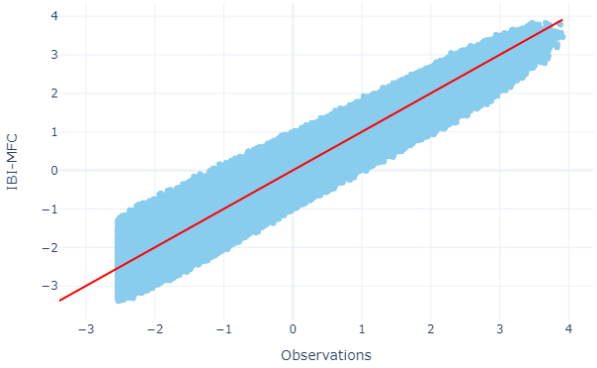

CONCARNEAU - n

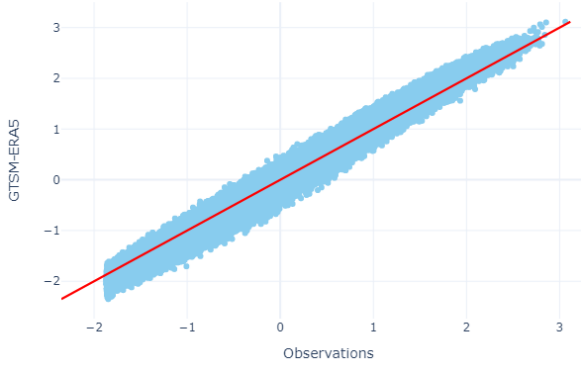

CONCARNEAU - n

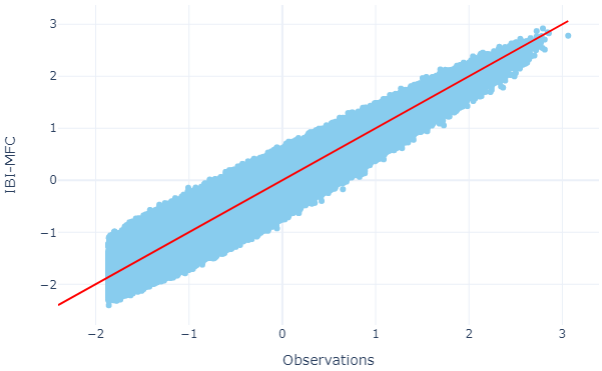

ILE_D_AIX - n

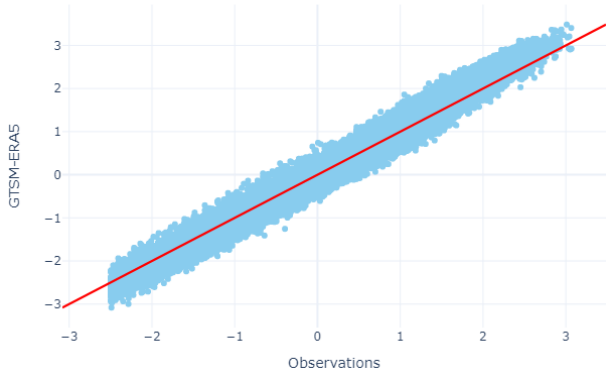

ILE_D_AIX - n

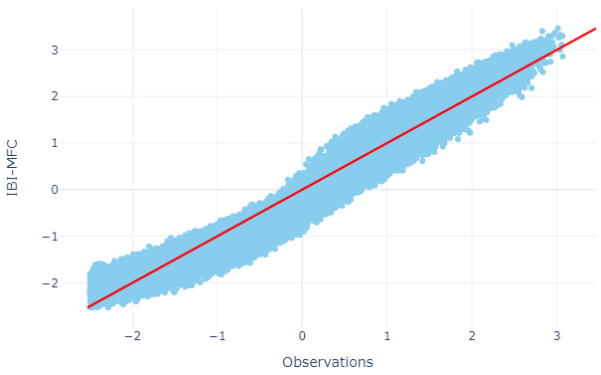

LA_ROCHELLE_LA_PALLICE - n

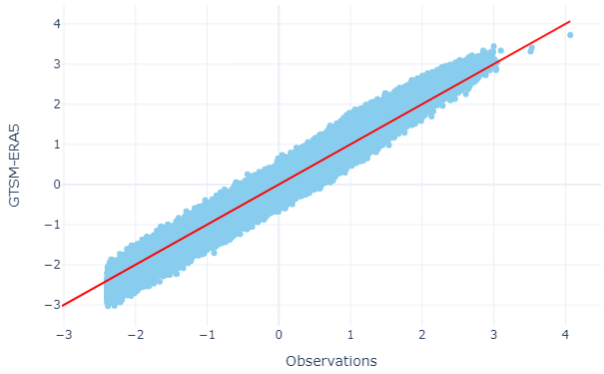

LA_ROCHELLE_LA_PALLICE - n

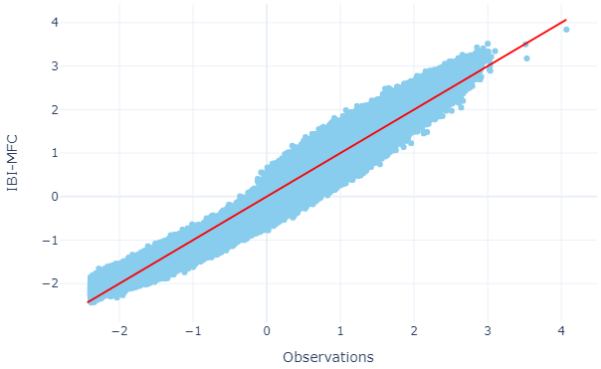

LE_CONQUET - n

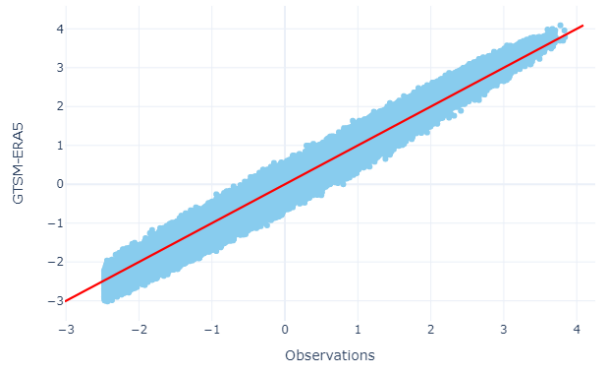

LE_CONQUET - n

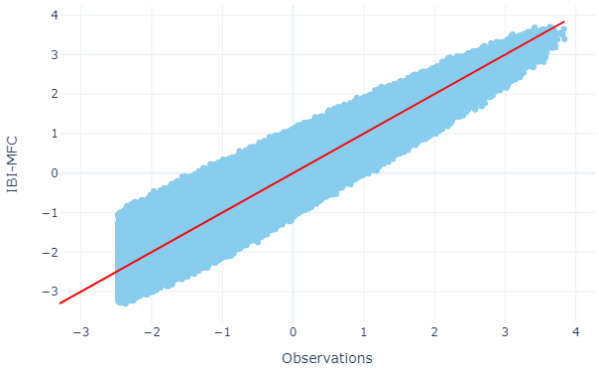

LES_SABLES_D_OLONNE - n

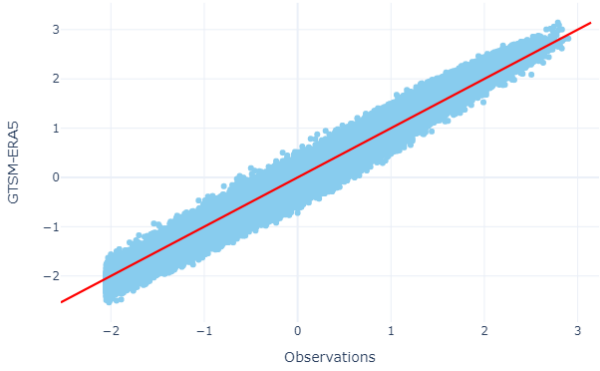

LES_SABLES_D_OLONNE - n

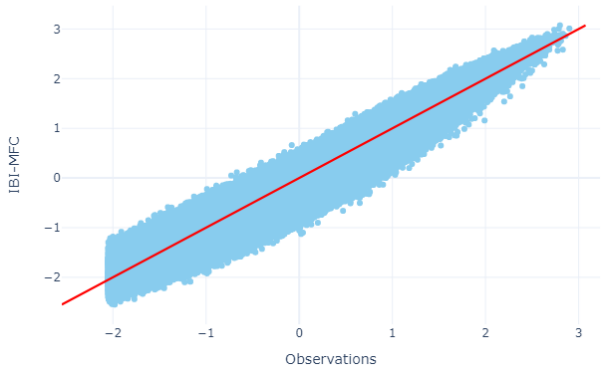

PORT-BLOC - n

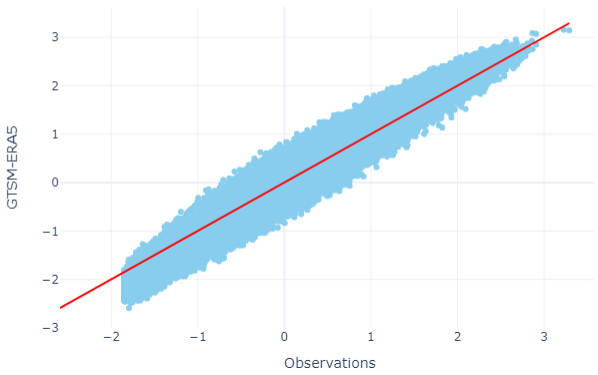

PORT-BLOC - n

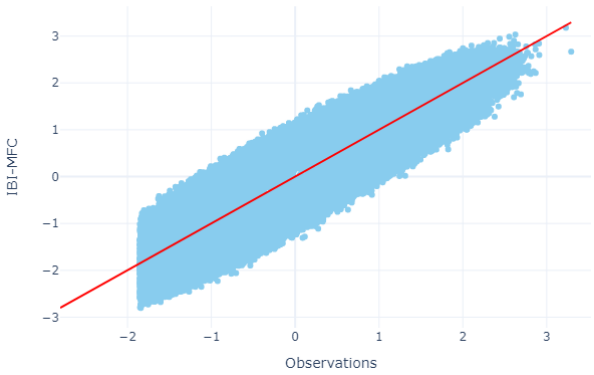

PORT-TUDY - n

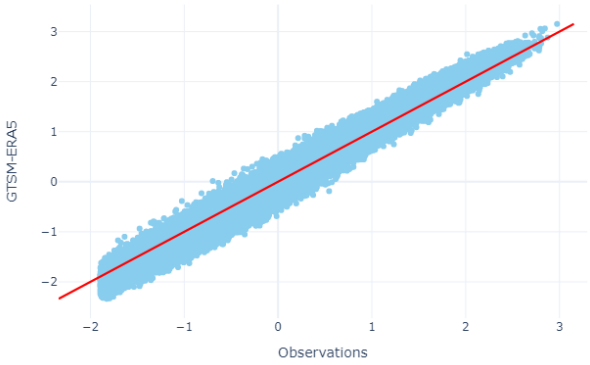

PORT-TUDY - n

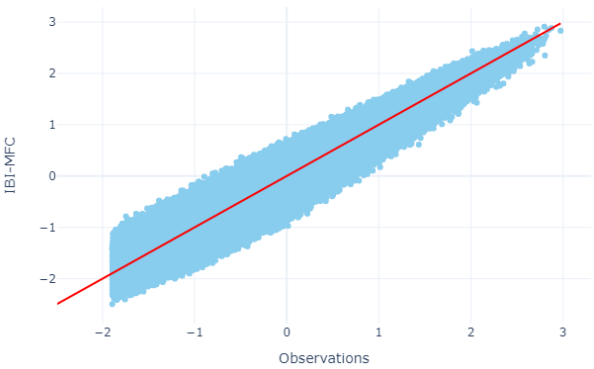

SAINT-GILDAS - n

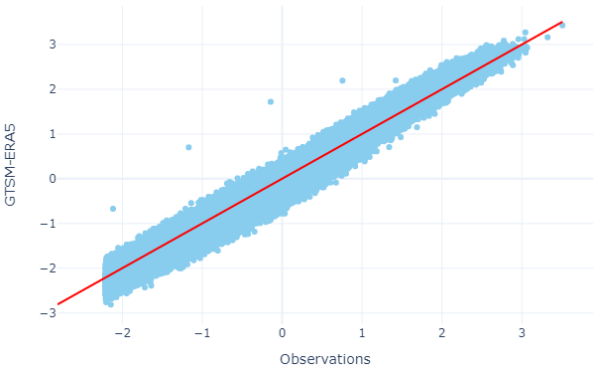

SAINT-GILDAS - n

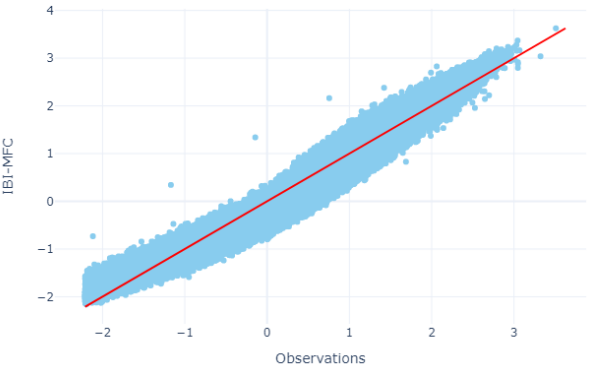

SAINT-JEAN-DE-LUZ_SOCOA - n

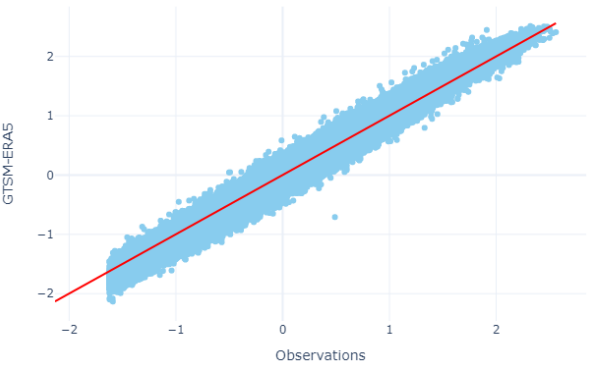

SAINT-JEAN-DE-LUZ_SOCOA - n

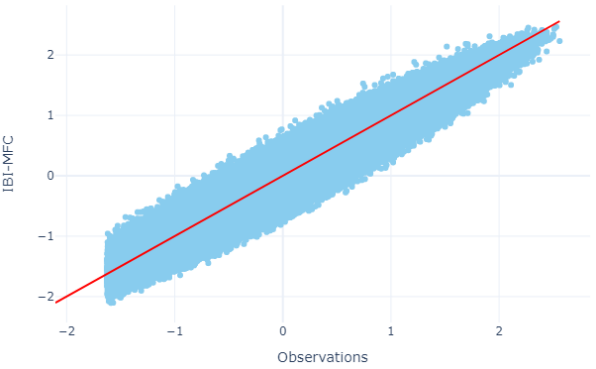

SAINT-NAZAIRE - n

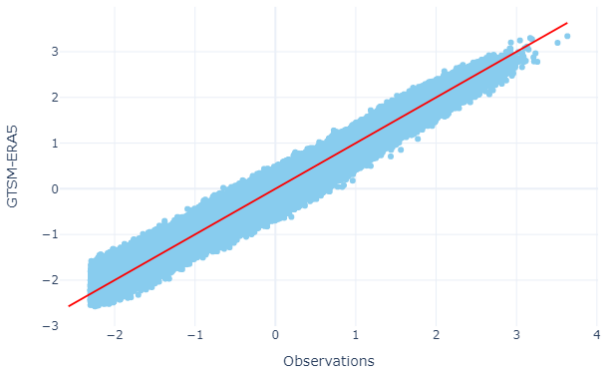

SAINT-NAZAIRE - n

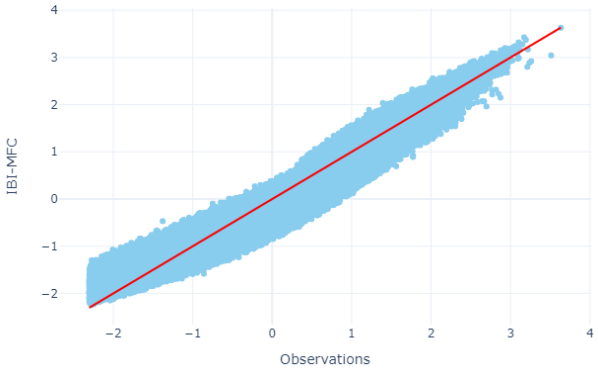

FOS-SUR-MER - n

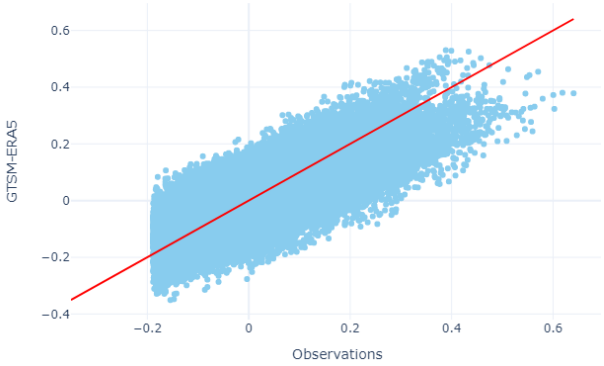

FOS-SUR-MER - n

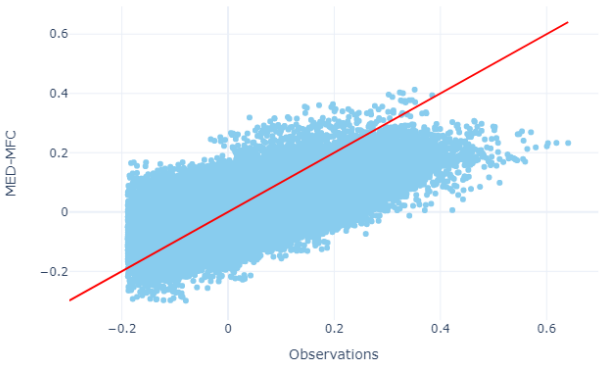

MARSEILLE - n

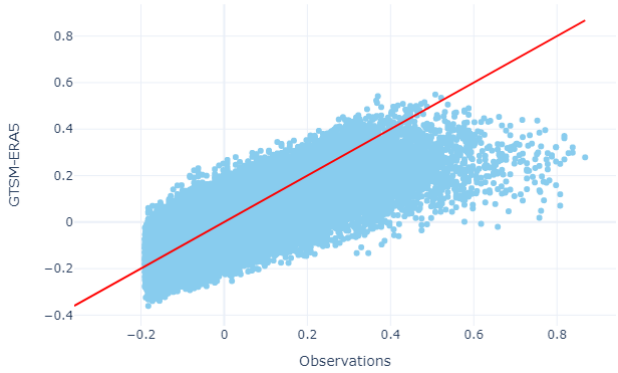

MARSEILLE - n

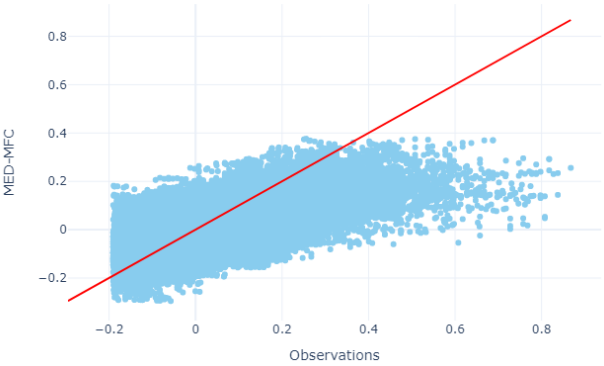

MONACO_FONTVIEILLE - n

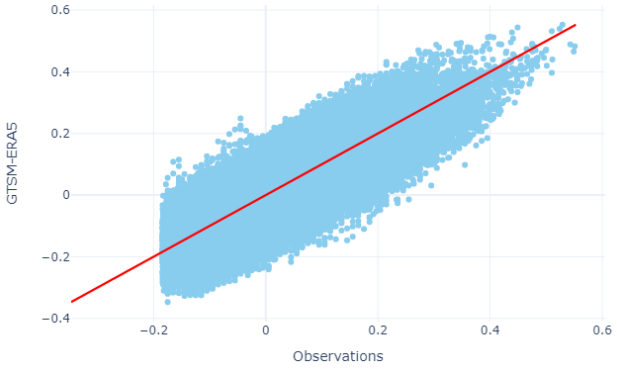

MONACO_FONTVIEILLE - n

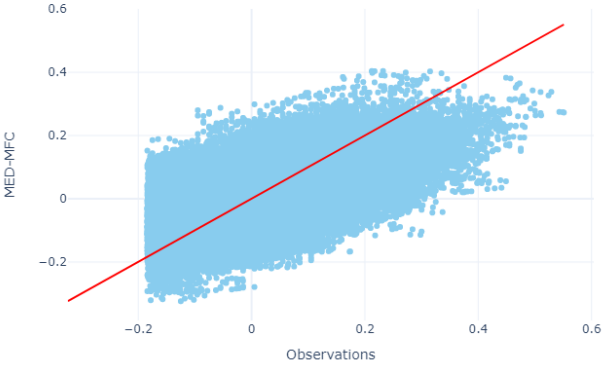

NICE - n

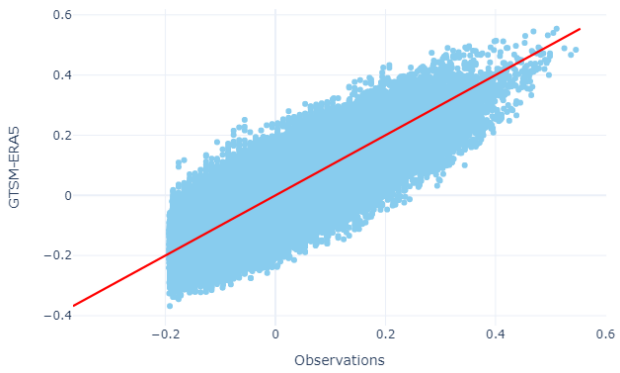

NICE - n

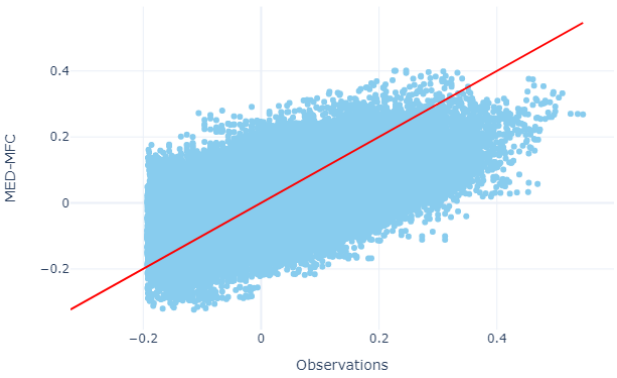

PORT-VENDRES - n

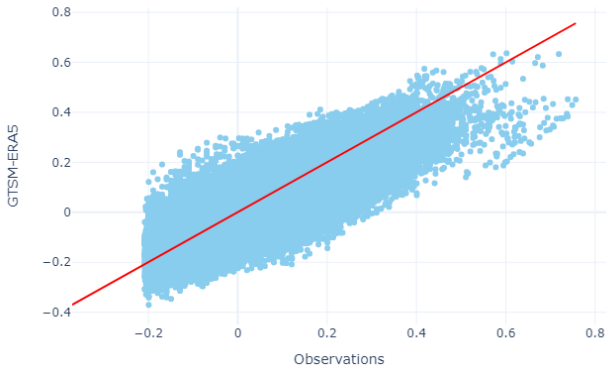

PORT-VENDRES - n

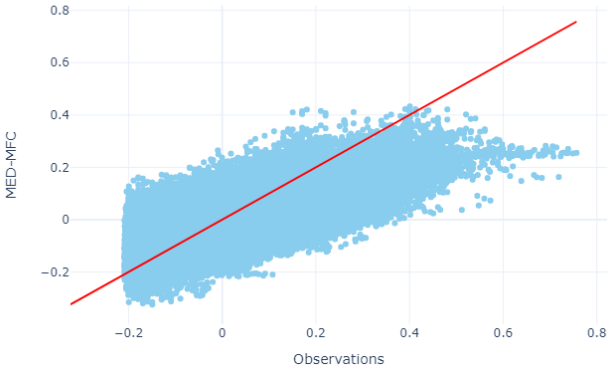

SETE - n

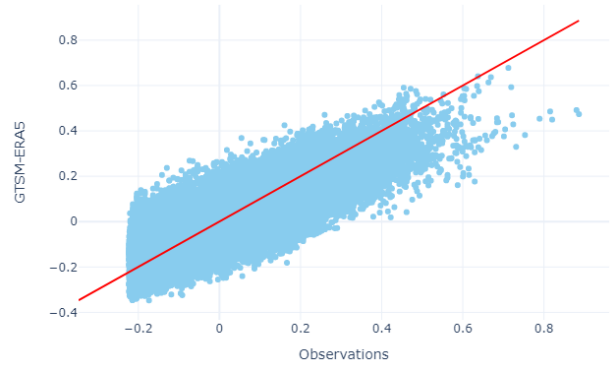

SETE - n

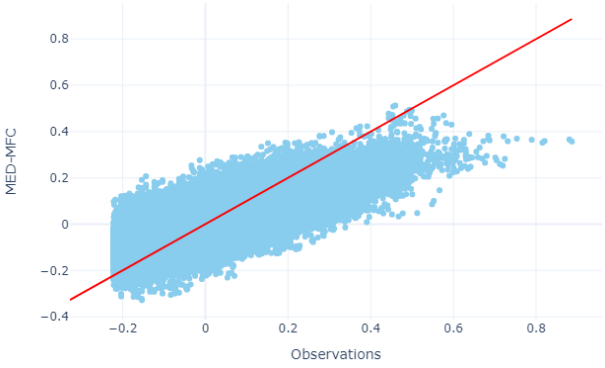

TOULON - n

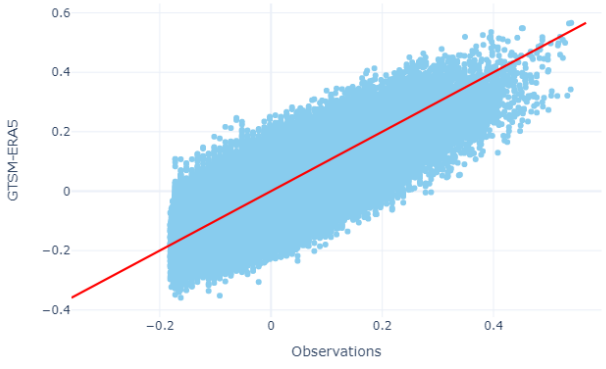

TOULON - n

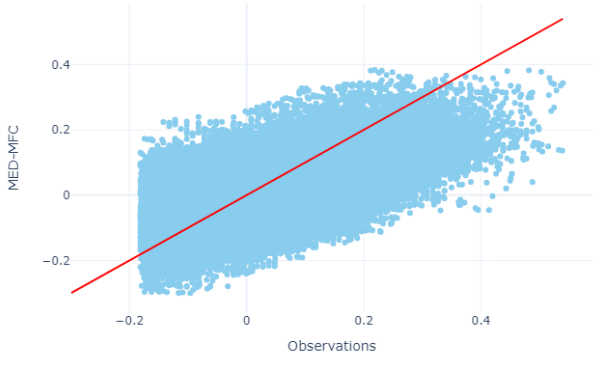

3 Appendix 3: Taylor Diagrams

3.1 Waves

Atlantic Ocean (1994-2019) - P95

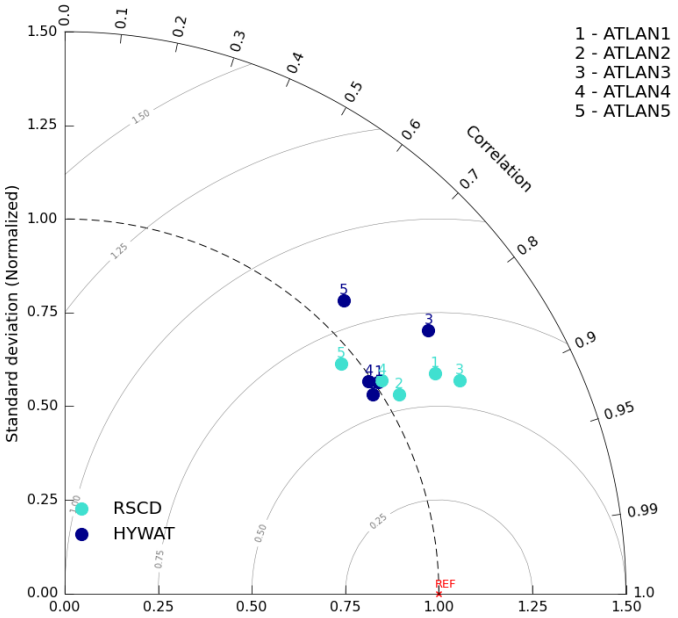

Atlantic Ocean (1994-2019) - P50

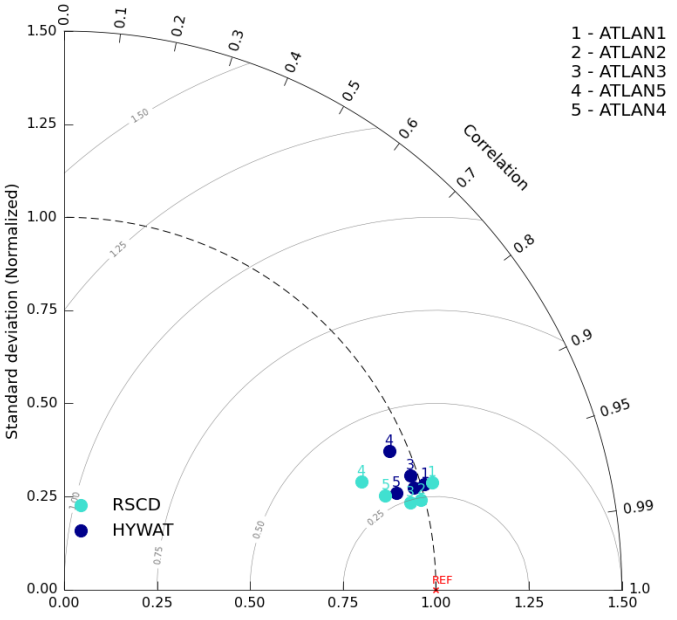

English Channel (1994-2019) - P95

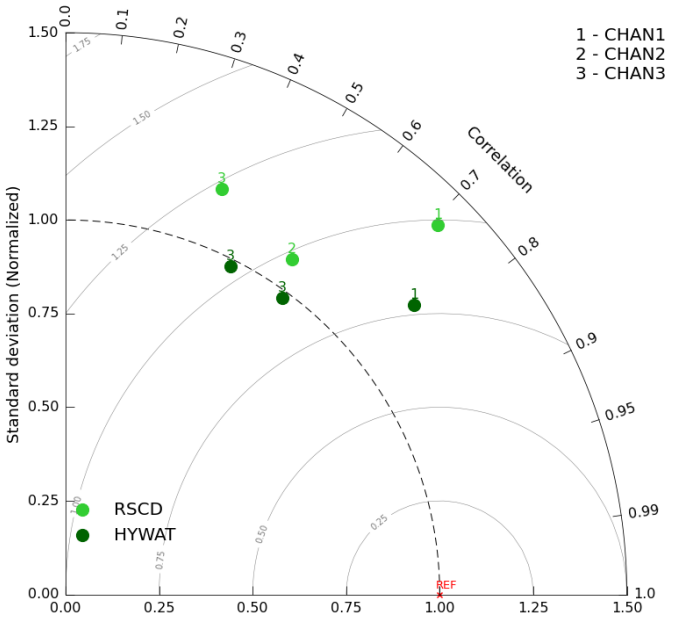

English Channel (1994-2019) - P50

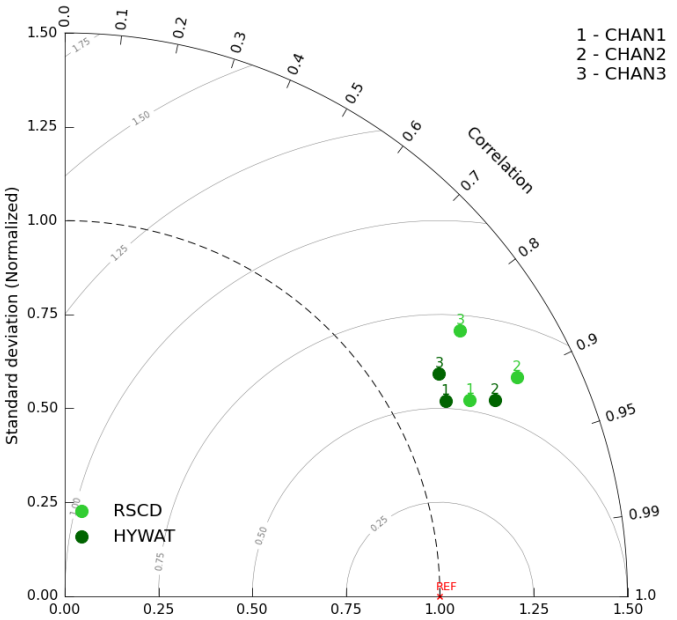

Mediterranean Sea (1994-2019) - P95

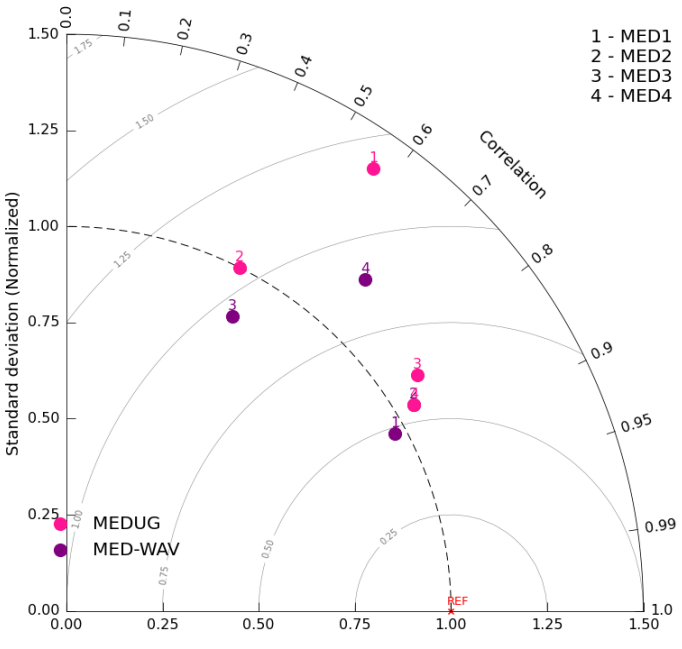

Mediterranean Sea (1994-2019) - P50

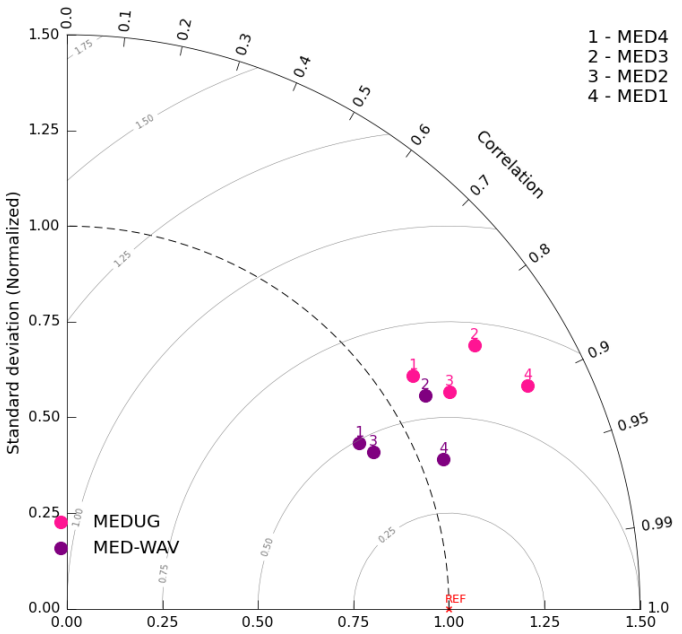

3.2 Water Levels

Extreme total water level - Atlantic Ocean

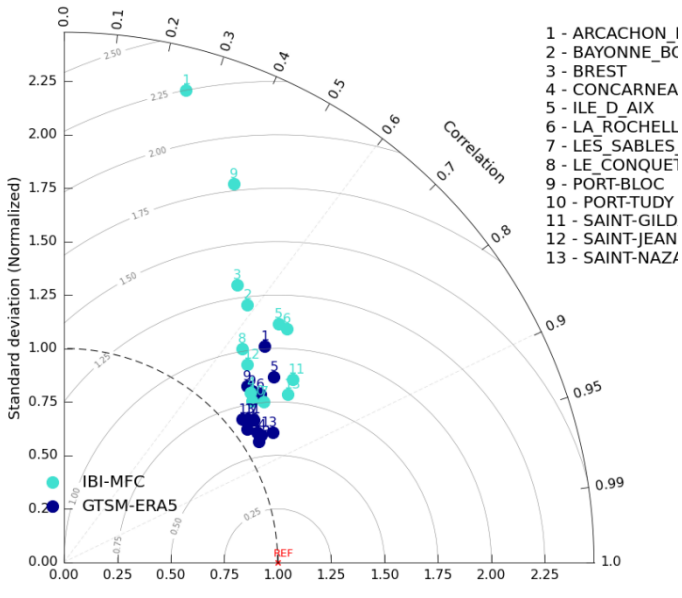

Mean total water level - Atlantic Ocean

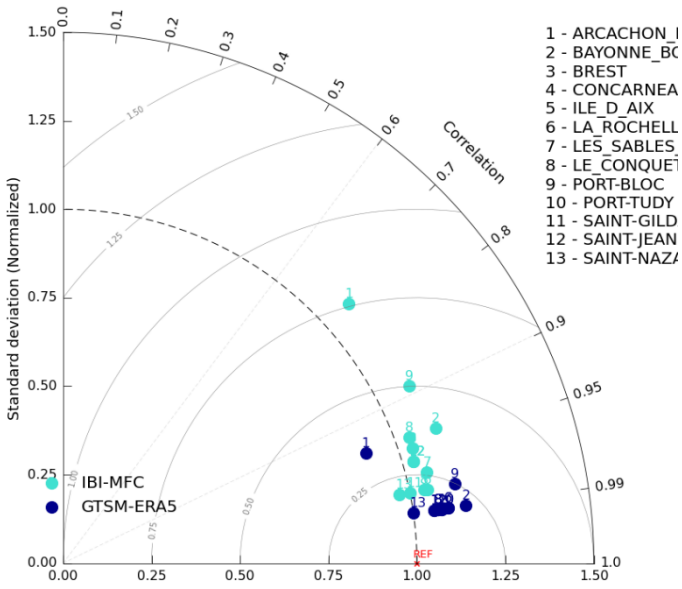

Extreme total water level - English Channel

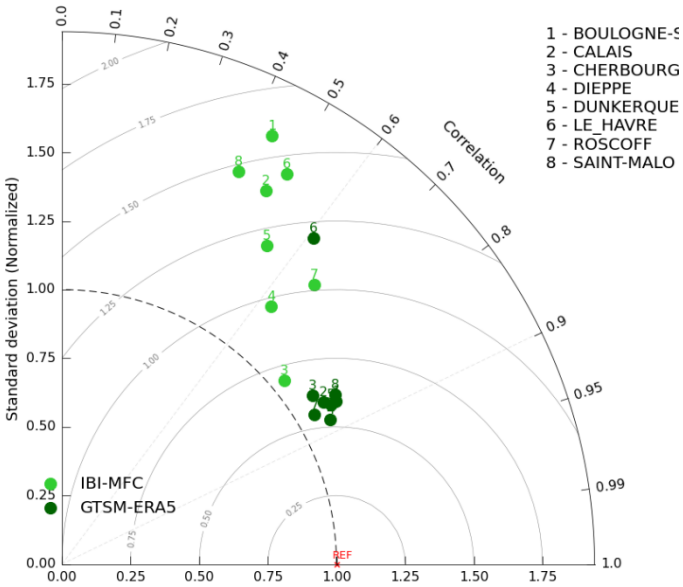

Mean total water level - English Channel

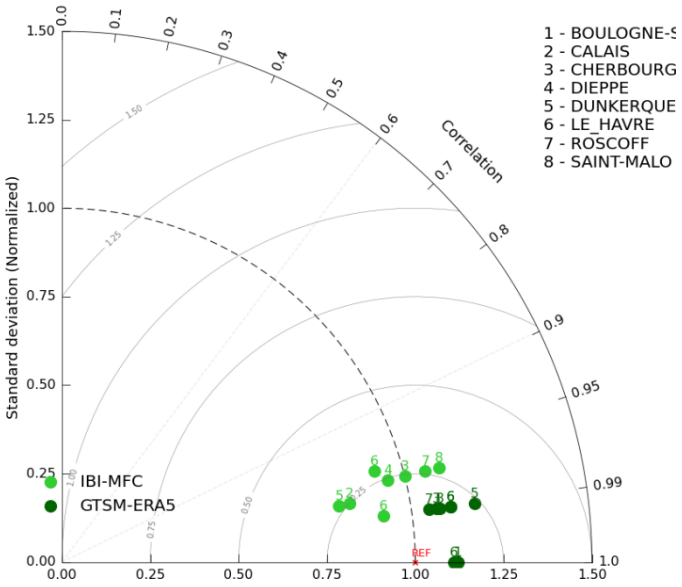

Extreme total water level - Mediterranean Sea

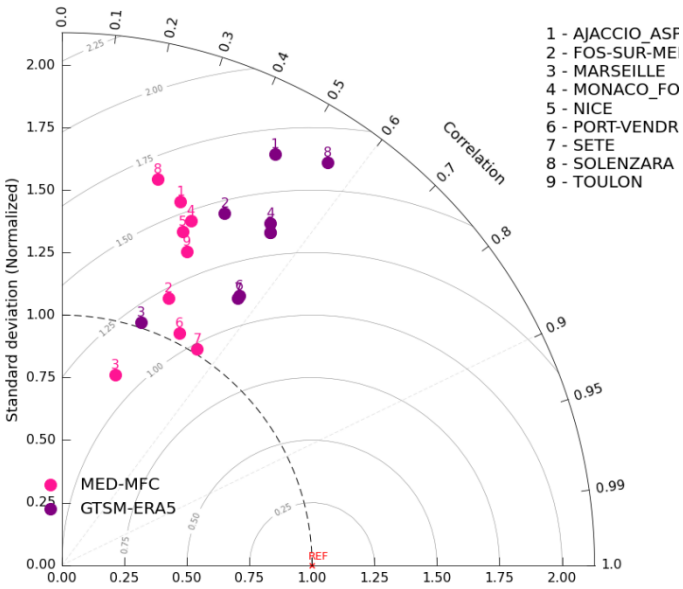

Mean total water level - Mediterranean Sea

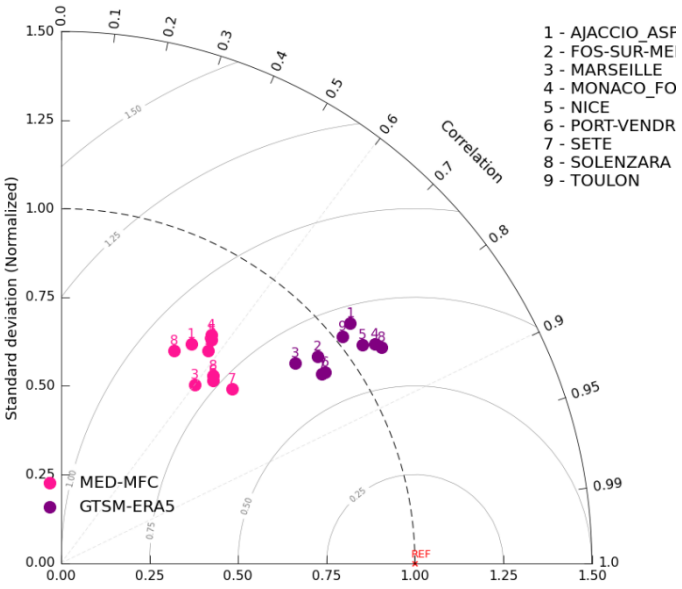

4 Appendix 4: Table of representativity of available wave observations data

STATION NAME	% available wave data over 2014-2024
CHAN1	50
CHAN2	90
CHAN3	95
ATLAN1	98
ATLAN2	65
ATLAN3	91
ATLAN4	51
ATLAN5	50
MED1	70
MED2	52
MED3	52
MED4	50